ATMOSPHERE-VEGETATION INTERACTIONS OVER SOUTH AFRICA

DEBBIE SHANNON BSc(Hons)

Thesis submitted in partial fulfillment of the Master of Science degree in the Department of Environmental and Geographical Science at the University of Cape Town

February 1997

ABSTRACT

This study examines the sensitivity of the atmospheric circulation to vegetation change over South Africa in the context of the portended global warming. This is achieved using a vegetation model driven by climate change information and subsequently incorporated within a general circulation model (GCM). The stand-alone vegetation model is driven using precipitation, temperature and relative humidity derived from downscaling using artificial neural networks. The vegetation model is then run with perturbed precipitation, temperature and relative humidity from downscaled model data from $1xCO_2$ and $2xCO_2$ GCM simulations. The resultant vegetation perturbation response to climate change is then examined and incorporated into the GCM in order to ascertain the atmospheric sensitivity to vegetation changes.

The off-line results of the vegetation model indicate a moderate degree of sensitivity of the vegetation to perturbations in precipitation, temperature and relative humidity. The general trend in response to the CO_2 climate is a westwards and altitudinal shift of lowland vegetation over the eastern part of the country, and a southwards and eastwards shift of the more dryland vegetation in the west. These shifts are in accordance with expected responses, since lowland vegetation responds more to temperature changes and the dryland vegetation to precipitation changes. Nonetheless, the use of the model provides a physically justifiable scenario on which to base the GCM studies, and at a finer resolution than otherwise available.

A GCM simulation with the perturbed vegetation was then performed using sea surface temperature boundary conditions for 1980 and compared to an identical GCM run without the perturbation. 1980 was chosen since this year does not represent either a strong El Niño or La Niña year. The atmospheric sensitivity to the vegetation perturbation has been examined in terms of climatic variables such as temperature, precipitation, pressure, specific humidity, horizontal divergence, and sensible and latent heat fluxes. The results show that the atmosphere is quite sensitive to relatively small vegetation changes.

Atmospheric response to vegetation perturbations indicates greater sensitivity over the NW and SE regions of southern Africa. The perturbation indicates a reduction in precipitation over the SE interior, related to less moisture feeding in over the interior from the SE Indian Ocean. Wind speed changes over the adjacent ocean were also evident, and are probably related to the changes in the South Atlantic and Indian high pressures. A southwards extension of the Hadley Cell was also suggested, as well as changes in sensible and latent heat fluxes, relating to precipitation and temperature changes. It is suggested that changes may be in response to the general drying out of the country and the associated increase in aridity.

This research forms the preliminary investigation for further work incorporating the atmospheric perturbation response back into driving the vegetation model in order to examine the direction of the feedback -- whether this is positive or negative in the longer term.

Thus, this study has demonstrated that the atmosphere is significantly sensitive to vegetation changes over South Africa and reinforces the need for improved land surface parameterization schemes and vegetation models in general circulation models.

TABLE OF CONTENTS

LIST OF FIGURES

LIST OF TABLES

ACKNOWLEDGMENTS

I would like to thank Mr Jon Bergengren at the National Center for Atmospheric Research (NCAR) in Boulder, Colorado, for providing me with access to the vegetation model. I would also like to extend my gratitude to him for the time and effort he spent in answering my numerous questions, and for helping me to successfully customise the vegetation model for the purposes of my study.

I am grateful to the Earth Systems Science Center (ESSC) at the Pennsylvania State University for provision of facilities and access to their Cray supercomputer. In particular, I wish to thank Mr Bill Peterson, the systems administrator, who provided technical expertise needed in performing the general circulation model runs. The Computer Centre for Water Research (CCWR) in Pietermaritzburg is also gratefully acknowledged for provision of the fine resolution station archive temperature and precipitation data for southern Africa.

Dr Mike O'Callaghan at the National Botanical Institute in Kirstenbosch, Cape Town, and Mr Henry Mulenga from the Department of Oceanography at the University of Cape Town, are both acknowledged for some useful discussions. Mrs Susan Sayers from the Department of Environmental and Geographical Science at the University of Cape Town, is thanked for drawing the map of South Africa. My colleagues, Mrs Debbie Hudson and Mr Jeremy Main, are thanked for their valuable assistance with various aspects of my thesis.

The generous funding provided by the Foundation for Research (FRD) and the Electricity Supply Commission (ESKOM) is much appreciated.

Finally, I am indebted to my supervisor, Dr Bruce Hewitson, for his guidance, support and advice throughout my thesis, and for the numerous opportunities he has given me during this time.

CHAPTER 1

INTRODUCTION

CHAPTER 1

INTRODUCTION

The processes which occur at the atmosphere-land interface are perhaps one of the most important reasons for studying the climate, since the livelihood of humankind is largely dependent on these interactions (Henderson-Sellers *et al.*, 1993a). However, the climate modelling community had given minimal recognition to these processes until the last decade or so (Sato *et al.*, 1989). It is therefore essential that we gain a better understanding of the sensitivity of the land surface to changes in the climate system, coupled by an understanding of the sensitivity of the climate to perturbations in land surface processes (Henderson-Sellers *et al.*, 1993a).

The exchanges of sensible and latent heat, and momentum between the atmosphere and surface are important for the absorption of solar radiation and emission of infra-red radiation, and thus the physical characteristics of vegetation and soil are a vital consideration (Henderson-Sellers, 1990). Radiation, momentum, and sensible and latent heat fluxes between the atmosphere and surface may likely have an effect on atmospheric dynamics, temperature, precipitation and humidity fields (Sato *et al.*, 1989). These may subsequently feed back into the land surface processes as part of a cyclical system.

In this work, a preliminary investigation of the interactions between vegetation and the atmosphere over the South African region (fig. 1) is performed. South Africa has a vulnerable climate which shows a high degree of both spatial and temporal variability. There are regions characterised by summer, winter and all-year-round rainfall regimes, with considerable spatial and temporal variability within these regions. There are quasi-periodic oscillations such as the 18-year cycle (Tyson, 1987 and Preston-Whyte and Tyson, 1988), the 10-11 year cycle (Currie, 1993), the semi-annual oscillation (SAO) (Hurrel and van Loon, 1994) and the quasi-biennial oscillation (QBO) (Mason

and Lindesay, 1993) which have an influence on rainfall. The 18-year oscillation, for example, has been associated with periodic wet and dry spells (largely in the summer rainfall regions) and their associated floods or droughts respectively. Droughts are characteristic of large portions of South Africa and often exacerbate desertification. They are also linked, in part, to the El Niño Southern Oscillation (e.g. in the 1982/83 El Niño during which South Africa experienced widespread, severe droughts).

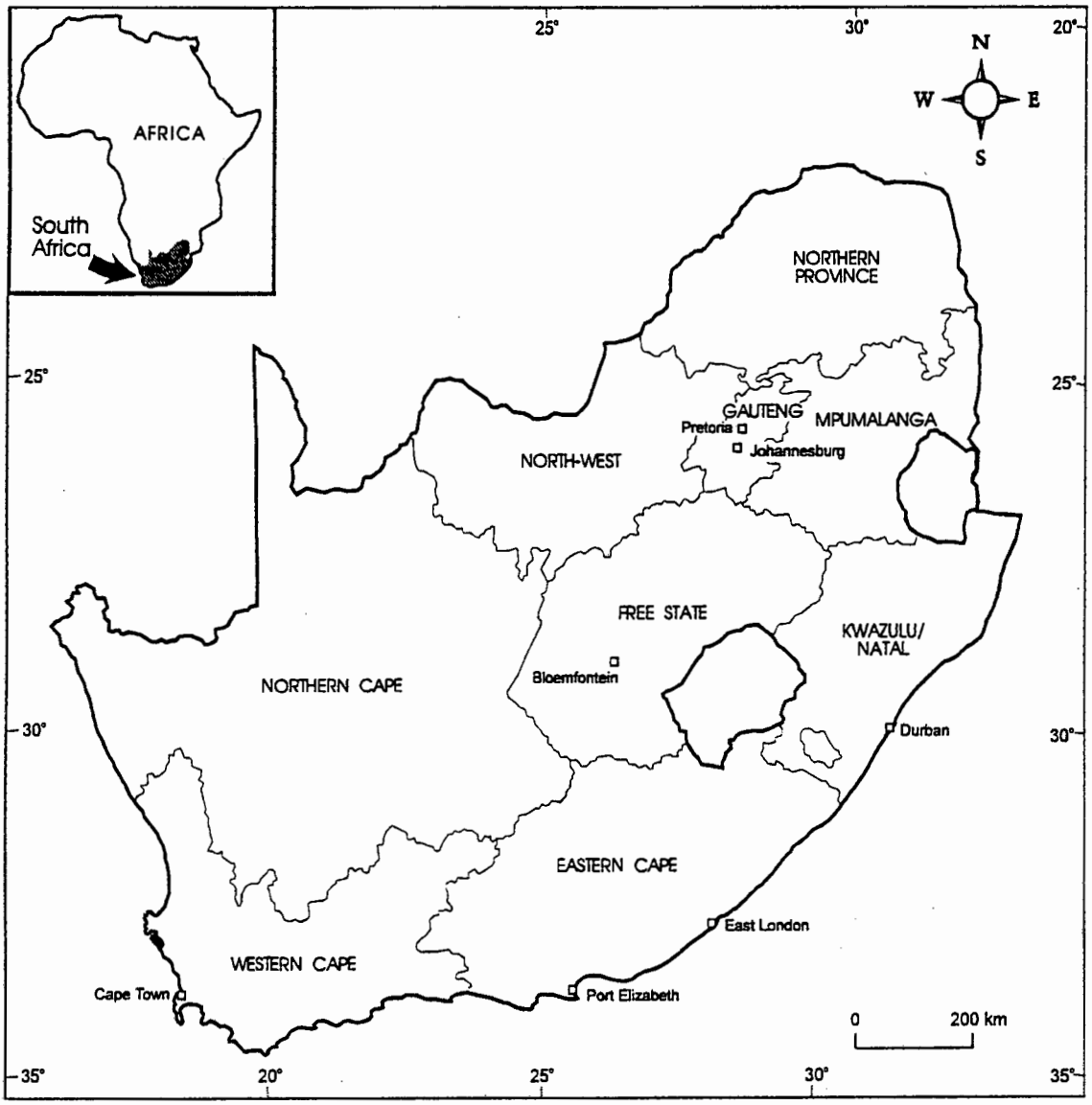

Figure 1: Map of South Africa showing major cities and provincial boundaries

The country also demonstrates steep gradients in terms of vegetation with a broad range of vegetation types adapted to suit the variable climate. Adaptations range from drought tolerance to the ability to thrive in an all-year-round rainfall regime. Approximately 9% of the country is cultivated (crops include maize, wheat, sugar cane and fruit) and 59% is natural pasture (for cattle and sheep farming predominantly) (Reader's Digest, 1984). Given the diversity of land use in South Africa, the country is one of contrast and difference and is therefore an interesting and unusual area to study.

A current global issue which has become a concern in South Africa is the significant impact humans have had on the global environment over the last century, through industrial expansion, land-use changes, agriculture and the burning of fossil fuels. This appears to be the cause of the enhancement of the greenhouse effect primarily through the emission of greenhouse gases such as Carbon Dioxide (CO_2), Methane (CH_4) and Nitrogen Oxide (N_2O). Atmospheric CO_2 values in the early 1980s were in the range of 335-340 ppm, which is substantially more than in pre-industrial times, where values were of the order of 280-300 ppm. Most of this increase can be ascribed to the burning of fossil fuels (Hansen *et al.*, 1981). If this trend continues at the present levels, there would be an almost steady increase in concentrations for a minimum of two centuries, with an estimate of 500 ppm by the end of the 21st century (IPCC, 1995).

Greenhouse gases such as CO_2 and N_2O remain in the atmosphere for extended periods of time ranging from decades to centuries (IPCC, 1995) and thus there is cause for concern. At present there is not complete acceptance of the discernible influence of humans on the global climate by all of the scientific community. There is, however, the support of the influential Intergovernmental Panel on Climate Change (IPCC), as evidenced by their most recent report (IPCC, 1995). The validity of this report, and particularly chapter 8 ("Detection of Climate Change and Attribution of Causes"), has been questioned by some and the details of this controversy are outlined in Feder (1996). However, despite the debate, it is clear that the impacts of an increase of such greenhouse gases could be far-reaching, and require examination at

both global and regional scales, in order for appropriate planning policies to be implemented.

This study is therefore placed in the context of the portended global climate change and makes use of a general circulation model (GCM) and a vegetation model in order to examine the interactions between vegetation and the atmosphere over South Africa. Past studies over the country have investigated the effect of climate change on biomes over South Africa (e.g. Ellery *et al.* (1991) and Midgley and O'Callaghan (1993)), but with a primary focus on individual plant species. There has been little emphasis on the sensitivity of the atmosphere to broad scale vegetation changes.

In this study, a vegetation model is driven in conjunction with a GCM in order to investigate atmospheric sensitivity to vegetation changes. The vegetation model is initially driven in stand-alone mode and uses climatic variables of temperature, precipitation and relative humidity to predict life form percentage coverage for each 1° grid cell in the study domain. In this work, station data are area-averaged to the appropriate 1° resolution to provide an observed data set. A functional relationship between these data and atmospheric circulation is then derived through downscaling[1]. Subsequently these relationships are used with observed and GCM circulation data to generate comparable input data sets for driving the vegetation model.

Thereafter, the modelled observed vegetation coverage can be determined and the response of model vegetation to climate change over South Africa can be examined. Although the vegetation model produces percentage coverage at the life form level, it also allows for a larger biome level response to be considered, and it is this level of vegetation description which is used in this work. The study therefore examines the initial broad scale vegetation-atmosphere response to perturbations in the climate as a result of CO_2 forcing (i.e. from a $1xCO_2$ to $2xCO_2$ scenario).

[1] Downscaling, or translation across scales, involves finding a functional relationship between large scale resolved features (atmospheric variables of specific humidity and pressure in this case) and local or regional parameters (precipitation or temperature in this case) (Hewitson and Crane, 1996). Detail on this is found in chapters 2 and 3.

The vegetation perturbation in response to $2xCO_2$ forcing is then incorporated into a control simulation of a GCM in order to isolate the atmospheric sensitivity to vegetation changes. The response to the vegetation change of atmospheric fields such as sea level pressure, heights of the 500 hPa surface, wind fields, and moisture and heat fluxes are then examined in terms of seasonal mean and variance changes. This work therefore provides an initial understanding of the atmospheric first order response to changed vegetation, and whether the vegetation feedback is negative or positive in nature. A greater understanding of atmospheric sensitivity to perturbations in vegetation is therefore achieved in this study.

The subsequent sections are constructed as follows: Chapter 2 will provide more details on GCMs and their use in regional prediction, and a brief description of vegetation in South Africa and some potential changes which have been predicted. This will be accompanied by an examination of land surface parameterizations in GCMs. The GENESIS GCM, used in this study, will then be described, and some background information relevant to the present study will be provided. Chapter 3 introduces the vegetation model used and details some of its specifics. It also illustrates its operation and presents the methods and results of the model driven in stand-alone mode. Chapter 4 provides a validation of the Atmospheric Model Intercomparison Project (AMIP) configured run (described in more detail in the chapter) of the GENESIS control simulation GCM, which is used as the control for the vegetation perturbation study. Following this, in chapter 5, the details and specifics of the vegetation perturbation simulation with the GCM, taking into account changes in vegetation induced by doubling of CO_2 (as predicted by the vegetation model), will be analysed and discussed. This chapter therefore sheds some light on the potential atmospheric sensitivity to changes in vegetation induced by global climate change within South Africa. A study such as this will inevitably have a number of constraints and these, along with some overall comments and suggestions for further studies, will be presented in chapter 6.

CHAPTER 2

BACKGROUND

CHAPTER 2

BACKGROUND

This chapter affords some details on the use of general circulation models for regional studies. Subsequently, the vegetation characterising South Africa is described, in order to provide the necessary background to the study. The chapter also presents a summary of some of the potential changes which could be anticipated at a biome level. This is followed by a brief description of some of the land-surface parameterization schemes found in GCMs, after which the GENESIS GCM, used in this analysis, will be described.

2.1 General circulation models and regional prediction

GCMs have been used and designed historically for short term weather prediction (Henderson-Sellers and McGuffie, 1987). The first of the generation of atmospheric GCMs was that of Phillips (1956), and models have grown substantially since this time. There have been improvements in computational facilities and capabilities and therefore spatial and temporal resolution has increased considerably over the last few decades (Peixoto and Oort, 1992).

GCMs have been used through the years to gain a better understanding of the climate system, and validation and improvements of parameterizations have been a major focus (Henderson-Sellers and McGuffie, 1987). There has also been a shift over the last decade or so to using GCMs for projections of a possible future climate. This has been in response to the portended climate change as a result of anthropogenic influences. A climate model is used in such studies to determine whether or not a perturbation of certain parameters in the model has a significant effect on the climate (Henderson-Sellers and McGuffie, 1987).

CHAPTER 2

BACKGROUND

This chapter affords some details on the use of general circulation models for regional studies. Subsequently, the vegetation characterising South Africa is described, in order to provide the necessary background to the study. The chapter also presents a summary of some of the potential changes which could be anticipated at a biome level. This is followed by a brief description of some of the land-surface parameterization schemes found in GCMs, after which the GENESIS GCM, used in this analysis, will be described.

2.1 General circulation models and regional prediction

GCMs have been used and designed historically for short term weather prediction (Henderson-Sellers and McGuffie, 1987). The first of the generation of atmospheric GCMs was that of Phillips (1956), and models have grown substantially since this time. There have been improvements in computational facilities and capabilities and therefore spatial and temporal resolution has increased considerably over the last few decades (Peixoto and Oort, 1992).

GCMs have been used through the years to gain a better understanding of the climate system, and validation and improvements of parameterizations have been a major focus (Henderson-Sellers and McGuffie, 1987). There has also been a shift over the last decade or so to using GCMs for projections of a possible future climate. This has been in response to the portended climate change as a result of anthropogenic influences. A climate model is used in such studies to determine whether or not a perturbation of certain parameters in the model has a significant effect on the climate (Henderson-Sellers and McGuffie, 1987).

Global climate change modelling studies in the past commonly have focused on aspects such as sea surface temperatures (e.g. Rind (1987), Mitchell and Lupton (1984) and Kumar *et al.* (1994)) or ice related studies (e.g. Ingram *et al.* (1989) and Rind *et al.* (1995), Miller and de Vernal (1992)). However, until recently, relatively little attention has been placed on the interaction between the vegetation components and the atmosphere (Verseghy, 1991), besides studies such as those conducted on the Amazon Forest (e.g. Henderson-Sellers and Gornitz (1984) and Henderson-Sellers (1987)). Despite this, there does appear to be consensus that surface processes are one of the more imperative factors affecting climate (Henderson-Sellers and McGuffie, 1987).

One of the inherent problems in GCMs is the fact that they need to generalise sub-grid scale features such as the land surface, and this leads to a high degree of over simplification in some regions. Much of these data with regard to land-use and vegetation have, in the past, been generalised from basic map sources, and more recently, derived from satellite imagery. Although there are inaccuracies in these data, a more pressing problem is how best to average land-surface characteristics successfully to a suitable resolution for input into GCMs (Henderson-Sellers and McGuffie, 1987). Furthermore, vegetation is usually prescribed, implying that there is not an interactive relationship between the vegetation and the atmosphere within GCMs. A number of studies are now being done in order to examine these potential problems, and to gain deeper insight into how the land surface and the atmosphere respond to each other. Ojima *et al.* (1991), for example, investigated some of the important issues which need to be addressed in order to understand the effects of climate change on terrestrial ecosystems. Franchito and Rao (1992) performed a number experiments (e.g. deforestation and desertification) and examined the climatic changes as a result of these alterations, while Henderson-Sellers (1993b) examined the dynamic linking of vegetation to a global climate model.

Current GCMs present a reasonable simulation at the global, continental or hemispheric scales, but are still restricted in their usefulness at the finer scales as a consequence of their limited spatial resolution (Carter, 1994, Hewitson and Crane,

1996). Unfortunately, it is this regional level which is most useful and in which society's interest primarily lies, and this forms the scale of concern for the present study. Therefore, there is a necessity for translation across scales, or 'downscaling', in order to translate larger scale features resolved by GCMs to local or regional parameters in order to evaluate vegetation response to the atmospheric forcing.

The term 'downscaling' has only recently gained widespread use in climate related applications, despite the fact that the concept has been within the discipline in some form for a number of years (Hewitson and Crane, 1996). This is apparent in the historical categorisation of atmospheric dynamics into a number of groups (referred to as synoptic climatology), thereby attempting to understand the relationship between individual or collective weather elements and atmospheric circulation (Barry and Perry, 1973, in Hewitson and Crane, 1996). Hewitson and Crane (1996) thus describe downscaling as a sensible extension or progression of synoptic climatology.

There are two approaches to model downscaling for regional prediction, namely, process based (e.g. nested modelling) or empirically based (e.g. atmosphere-surface transfer function downscaling) techniques. In the empirical model a relationship is derived between large-scale features (resolvable by GCMs) and a local parameter in question using observed data. The relationships may then be used with other atmospheric input data (e.g. from GCMs) to derive local climate response. The advantages of using this method are the relative ease with which computers can process the data, it is interpretable, and it is easy to apply over large areas. There are, nonetheless, some problems such as the assumption that GCM large scale features are correct, that a relationship exists when one may in fact not and that the relationship holds in a doubled CO_2 climate. The last of these assumptions is not as easily justified as the first two assumptions. Nonetheless, it is reasonable to assume that the laws governing atmospheric dynamics will not change. In other words, changes one could anticipate are likely to be modifications in intensity, frequency and persistence of synoptic-scale circulation features rather than their characteristics (Hewitson and Crane, 1996). The downscaling techniques therefore do not account for the direct radiative forcing impact of the instantaneous doubling of CO_2. Furthermore, there may

be some uncertainty in the circulation-precipitation relationship with the large scale changes in water vapour (Hewitson and Crane, 1996). These assumptions can, however, largely be justified.

The approach of nested models involves a high resolution model being placed within a GCM over the area of concern with the GCM large scale features being used to drive the high resolution model (Giorgi and Bates, 1989). Examples of this approach in the literature can be found in Dickinson *et al.* (1989), Giorgi and Bates (1989) and Giorgi (1990). Some of the problems with this are that GCM grid cell values (which may be highly erroneous) are used to set the boundary conditions (Dickinson *et al.*, 1989), the approach is computer intensive and there are also inconsistencies between the nested model and the GCM in terms of physics. The nested model is nevertheless perhaps the more accurate approach to take in the long term, but solutions are required now and thus empirical downscaling currently forms a common approach, and it is this approach which is used in the context of this study.

2.2 Vegetation Description of South Africa

South Africa has a broad range of vegetation types adapted to suit the variable climate. Vegetation ranges from plant species able to withstand long periods of drought to species tolerant of plentiful rainfall. There is a need to group these variations in vegetation into vegetation units which are manageable and representative (Acocks, 1988) and which give a fair representation and descriptive understanding of the observed vegetation distribution. The classification of vegetation into different groups is an unenviable task and will be dependent on the needs of the classifier and the resolution to be considered. As is true of almost any classification system, a vegetation classification system is only a means of summarising an infinitely more complex system into units which can be handled more easily. Different levels of classification are important for varying objectives and a number of schemes have been used historically in South Africa.

Early vegetation maps of South Africa include those of Pole Evans (1936), Adamson (1938) and Pentz (1945). These classification systems were followed by the division of vegetation into veld (Afrikaans word for "field" or "plain") types in the 1950s, to which Acocks (1953) is attributed. A veld type, as defined by Acocks (1953), is a vegetation unit which is sufficiently small in variation to allow it in its entirety to have the same potential for farming. Acocks identified 70 different veld types in South Africa and the particulars of this classification system can be found in Acocks (1988).

More recently, Rutherford and Westfall (1986) have classified southern African vegetation more broadly, in terms of biomes, and it is this level of classification which is appropriate for this study. A biome can be defined as a large ecological unit, extending over a broad natural area, and it is the largest land unit recognisable on a continental or sub-continental scale. Each biome differs from others predominantly in terms of governing life forms in stable systems and is mappable at a scale of 1:10 000 000, at maximum. Climatic features are a secondary distinction (Rutherford and Westfall, 1986). The seven biomes distinguished by Rutherford and Westfall (1986) comprise desert, forest, fynbos, grassland, nama-Karoo, savanna and succulent Karoo and are described briefly below. Figure 2 shows the location of these biomes.

- The *desert* biome is characterised climatically by summer rainfall, which ranges from 13 mm per annum on the western margin to 70 mm or 85 mm on the eastern margin. The region is arid and minimum temperatures do not usually fall below 0°C. Species diversity within this biome is low. This biome falls just outside of the borders of South Africa.
- The term *forest* biome in South Africa is generally used to describe the woody vegetation with continuous vegetation canopy cover. Vegetation is primarily evergreen and multi-layered. This biome is the smallest in South Africa.
- *Fynbos* (meaning "fine-leafed bush") is similar to vegetation described in other areas of the world as Macchia, and is characteristic of a Mediterranean climate. The fynbos biome is restricted to areas of winter or even rainfall. Mean annual rainfall is variable, ranging from 210 mm to an excess of 3000 mm. Vegetation in this biome is low in height (usually less than 3 m), grassy, dwarf shrubby and

shrub/woodland, and has a very high diversity. Fire and fire frequency is a crucial factor in this biome. Fires in this biome were formerly of natural origin (i.e. as a result of lightning), although human habitation has resulted in anthropogenically induced fires as well. Fynbos in fact relies on fires for survival, but at a frequency of approximately 10-15 years. Alien invasives have constituted a problem, more so in this biome than any other.

- The *grassland* biome is found in summer rainfall regions where mean annual rainfall is between 400 mm and 2000 mm. Hail frequency in this biome is high. Frost is a common occurrence, and minimum temperatures are generally below 1°C in the coldest month. Vegetation conforms to the rainfall gradient which accords with the relative contribution of 'sweet' and 'sour' grasses.
- The *nama-Karoo* biome is restricted to summer and even rainfall areas and includes regions with an annual rainfall variability of 100 mm to 520 mm. Minimum temperatures in winter can be low, reaching below 0°C or even as low as -9°C in some cases. Plants in this biome are drought tolerant. Much of this biome is presently used for grazing purposes.
- The *savanna* biome, which is the largest in South Africa, consists of grasses interspersed with woody vegetation. Woody plants can be fairly dispersed or can have as much as 75% canopy coverage, where these areas are often referred to as woodland. The savanna biome falls mainly within the summer rainfall areas, with some degree of rainfall variability. This biome also has the greatest variability in minimum temperatures.
- The *succulent Karoo* biome is perhaps the most difficult to describe or determine, since in other biomes either geography or distinct vegetation can successfully delimit it from others. Most plants, yet not all, are characteristically succulent and the biome falls within the winter rainfall regime. A strong summer aridity is characteristic.

2.3 Biome response to climate change

Studies have been done on the effect of global climate change on biomes and more often, individual species, but without much consideration of the atmospheric response to vegetation changes. Midgley and O'Callaghan (1993) have reviewed some of the potential changes which could be anticipated for biomes, and these warrant some attention here. Their predictions are based on a number of assumptions made by the Interdepartmental Co-ordinating Committee for Global Climate Change (ICC) (unpublished). The ICC, which is no longer operational, was established in 1991 by the Director General of the Department of Environmental Affairs in South Africa. The primary function of this committee was to formulate a national policy and strategy on affairs related to environmental change (ICC, unpublished). The more relevant of the assumptions made by the ICC, in the context of the portended changes suggested by Midgley and O'Callaghan (1993) are the following:

- An increase of 1° - 2°C in ambient temperatures. This increase will be greater in winter rainfall regions and greater for minimum than maximum temperatures.
- Summer rainfall increase of 0% to 10% and more temporal variability. In winter rainfall regions a change of between -5% to +5%.
- Atmospheric CO_2 will increase from 350$\mu l.l^{-1}$ to a value of 560$\mu l.l^{-1}$ by between 2030 and 2050.

Table 1 summarises each biome's primary threats and the associated vegetation responses, outlined in Midgley and O'Callaghan (1993).

This approach, although useful, is based on a number of broad assumptions about the climate response and therefore there is the need for an approach with a stronger physical foundation. This work therefore makes use of a GCM. Given the problem of determining regional climate information from GCMs, in particular with regards to the hydrological cycle, there remains some uncertainty about the regional specifics of the vegetation response. In this regard, this study also uses downscaling to derive data of possible vegetation change. Therefore the approach used in this work accounts for a

variable magnitude of response to climate in different regions, and is not based on broad climate change assumptions.

Biome	*Primary Threats*	*Vegetation Responses*
Desert	- Atmospheric vapour pressure deficit increase - Increasing plant thermal stress	- Possible extinction of some specialised species
Nama- Karoo	- Atmospheric vapour pressure deficit increase - Increasing thermal stress - shrubs favoured above grasses due to CO_2 increase - Soil aridification	- Vegetation composition change (C_3 shrubs favoured above C_4 grasses)
Savanna	- Increasing vapour pressure deficit - Increasing thermal stress - Soil aridification - Trees favoured above grasses due to CO_2 increase	- Woody vegetation will replace grasses
Grassland	- Soil aridification - Increasing vapour pressure deficit - Increasing thermal stress - Reduced competitivity of dominant C_4 plants against C_3 plants	- Invasion of shrubs and trees from Nama-Karoo and Savanna Biomes - Reduced fire frequency
Succulent Karoo	- Primary changes in southern parts - Convective rainfall increase inducing increased erosive force and destructive hailstorms - Increasing thermal stress	- major loss of leaf-succulent species - C_4 grasses having competitive advantage (because of increased summer rainfall); increased CO_2 will favour C_3 grass and non-succulent shrubs - Increased risk of fire
Fynbos	- Changing seasonality of rainfall and predictability; changed fire regime - Increasing thermal stress - Increasing vapour pressure deficit - Nutrient cycling disruptions - Threat of invasive alien woody plants increased	- Loss of specialist species - Grasses will experience greater success in lowland areas
Forest	- Fragmentation overshadows effects of climate change - Soil desiccation	- Greater forest fragmentation - Slow-growing species will become extinct

Table 1: Vegetation changes predicted for each biome (Midgley and O'Callaghan, 1993)

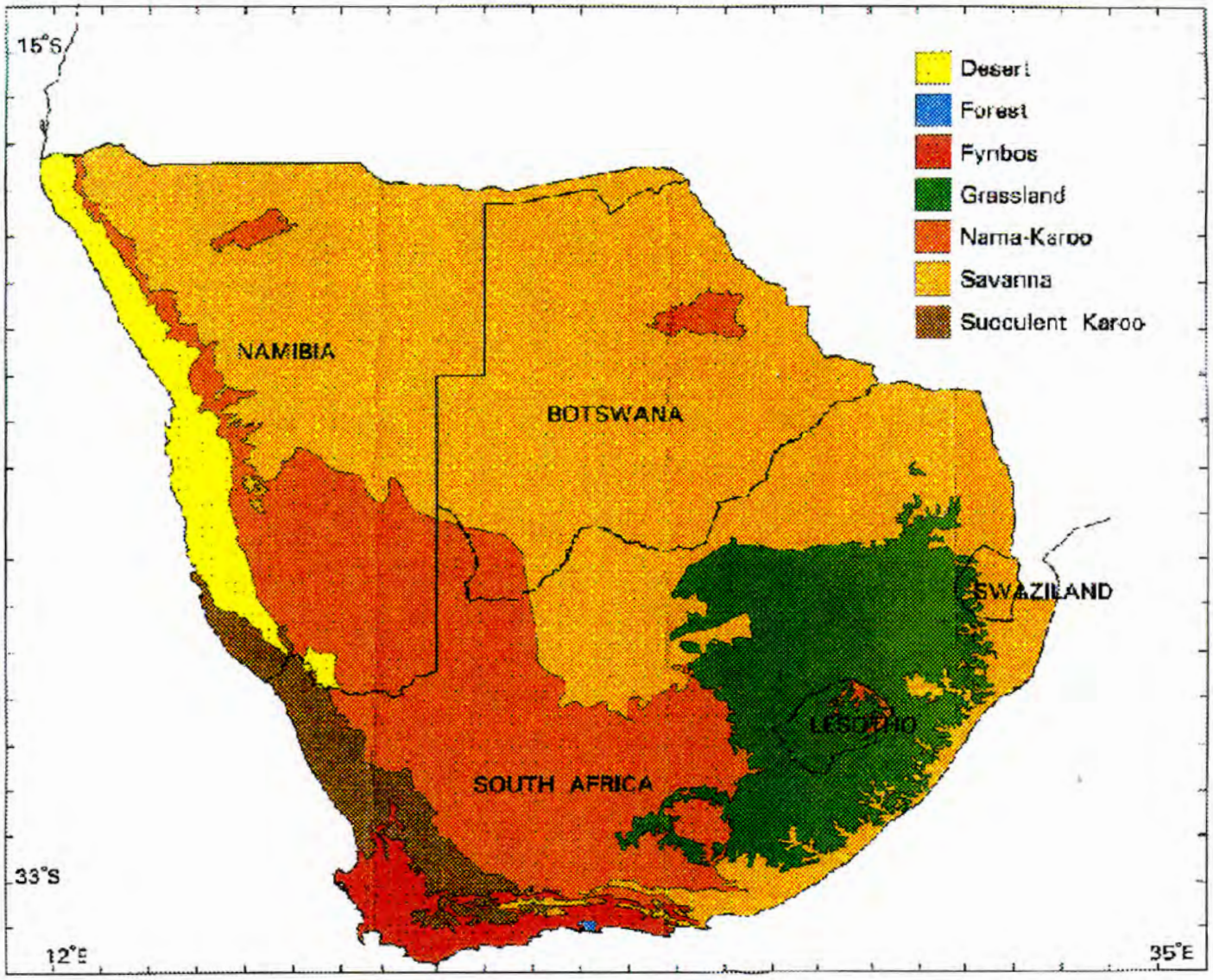

Figure 2: Biome map of southern Africa (after Cowling and Richardson, 1997)

2.4 Land-surface parameterization schemes in GCMs

The need for representation of the land surface was recognised in early GCMs, since surface processes are one of the most crucial aspects of the climate system (Henderson-Sellers and McGuffie, 1987). The surface absorbs more than 70% of the energy absorbed within the climate system and models have demonstrated the sensitivity of the climate system to surface hydrology (Henderson-Sellers and McGuffie, 1987). Historically, land surface hydrology has been incorporated conventionally using very simple parameterizations and there are a number of such land surface parameterization schemes that have been incorporated into different GCMs through time, all having their varying advantages and disadvantages. Figure 3 illustrates the variables which would be likely to be taken into account in a land-surface parameterization scheme.

Before the 1980s, and specifically the work of Dickinson (1984), the general method for representing land surface processes in GCMs was to define the relationship between evaporation and soil moisture by prescribing albedo, land surface roughness length and using the Budyko hydrological "bucket" model (Dorman and Sellers, 1989). The "bucket" model parameterization of the land surface hydrology considers the soil to be a bucket of fixed or maximum depth. Excess water will run-off once the "bucket" is full (i.e. once precipitation exceeds evaporation) (Henderson-Sellers and McGuffie, 1987). There are a number of schemes that have been developed since this somewhat simplistic approach and the details of a few of the more well known of these will be highlighted, in order to illustrate the variety of approaches which can be taken to successfully account for land surface variations.

The Biosphere-Atmosphere Transfer Scheme (BATS) is first described by Dickinson (1984) followed by Dickinson *et al.* (1986). There have been several versions of this scheme, with the most recent scheme (BATS1E) described in Dickinson *et al.* (1992). Henderson-Sellers (1993b) has provided a useful summary of some of its essentials in her paper, from which the information presented here is drawn. The model includes a single canopy vegetation layer, multi-layer soil scheme and allows for snow cover to be represented on the land surface. Each grid point has a seasonally defined fraction of

the surface cover which is vegetated, the remainder of which is assumed to be bare soil. When coupled to the National Center for Atmospheric Research (NCAR) Community Climate Model (CCM1) there are 18 defined vegetation types, representative of both naturally and agriculturally defined vegetation. This vegetation was generated by using the data sets of Matthews (1985), Wilson and Henderson-Sellers (1985) and Olson *et al.* (1983). Each of the 18 vegetation classes has 16 parameters associated with it, two examples being vegetation roughness length and short wavelength albedos.

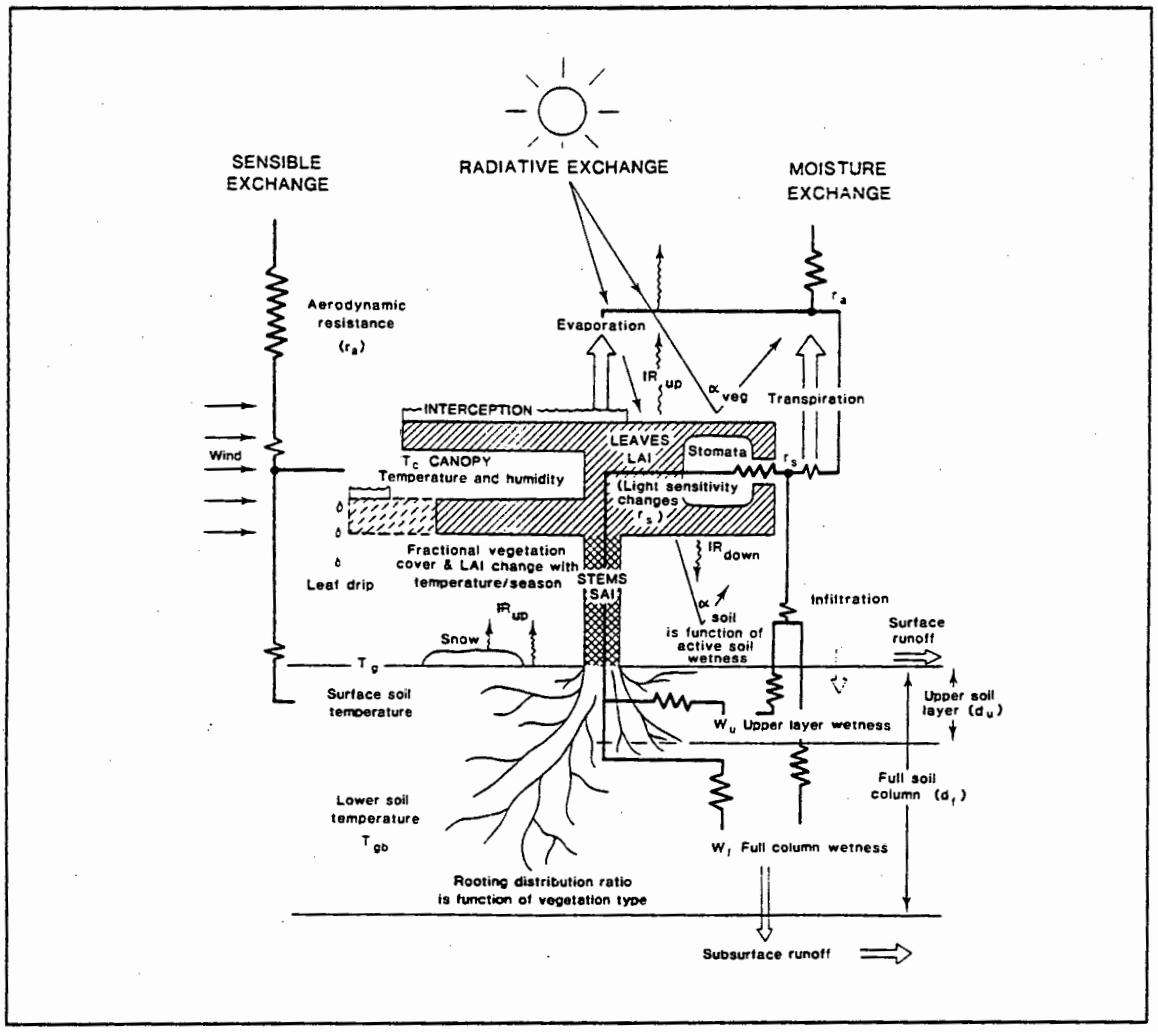

Figure 3: Schematic representation of some of the variables to be taken into account in land-surface parameterization schemes (after Henderson-Sellers and McGuffie, 1987)

Another model is the Simple Biosphere Model (SiB) of Sellers *et al.* (1986), summarised in Dorman and Sellers (1989), with some of the salient features given here. SiB has many of the fundamental principles of Dickinson's (1984) model, but differs in detail. SiB attempts to assemble information on the mean morphological, physical and physiological state of a given vegetation type as it varies on a seasonal basis. The vegetation canopy can have up to two layers, with the model using this together with details of the atmospheric boundary conditions to compute heat, momentum, radiation and water vapour fluxes between the terrestrial surface and the atmosphere; these computations essentially characterise the vegetation/atmosphere interactions. In essence, SiB consists of three submodels describing radiative transfer, turbulent transport and biophysical control of evapotranspiration. Each of these three submodels functions with a set of vegetation parameters suitable for a particular vegetation type. The radiative transfer generates the time series of associated albedo, the turbulent transport, the roughness length and the biophysical control of evapotranspiration. One of the aims of SiB was to reduce the number of world vegetation types into a manageable number for incorporation into GCMs and the data sets of Kuchler (1983) and Matthews (1985) were used in the generation of the resultant 12 major classes or biomes.

A new version of SiB, SiB2 has recently been developed (Sellers *et al.* 1996a, 1996b) and it has a number of improvements over the original. Some of these refinements are a more representative canopy photosynthesis-conductance model, use of satellite data to specify vegetation phenology, modifications of the hydrology submodel and a more realistic snow melt treatment (Sellers *et al.* 1996a). Due to some of these changes, it was necessary to reduce the vegetation canopy structure to one layer.

In order to reduce the computational requirements of SiB, a Simplified Biosphere Model (SSiB), a derivative of the former, was developed by Xue *et al.* (1991). Three primary alterations were made to SiB in order to reduce its complexity. Diurnal variations in the surface albedo were simplified, root zone soil moisture effects on stomatal resistance were approximated, and surface stress and heat and moisture fluxes between the top of the vegetation canopy and atmosphere were parameterized,

substantially reducing the computational requirements by roughly 55% (Xue *et al.*, 1991).

The Canadian Land Surface Scheme (CLASS), developed by the Canadian Climate Centre (CCC) is described in Verseghy (1991, 1993). This scheme includes 3 soil layers, and therefore differs from schemes such as SiB, where emphasis is placed primarily on canopy processes (Verseghy, 1991). Soil models in the remaining schemes are usually of two types. The first (e.g. McCumber and Pielke (1981) and Camillo *et al.* (1983)) assumes that the change in temperature with height in the soil to be linear within each soil layer and thus requires multiple soil layers in order to represent the temperature profile, making this type of scheme computationally intensive (Verseghy, 1991). The second type uses the force-restore method to model the temperature (e.g. Dickinson *et al.* (1986) and Noilhan and Planton (1989)), whereby there is a restoring sub-surface layer and a thin surface layer (Verseghy, 1991). Modification of snow-covered or inhomogeneous soils is therefore necessary. CLASS seeks to address some of the deficiencies, such as the soil models, in GCM land surface schemes.

The Bare Essentials of Surface Transfer (BEST) land-surface scheme is described in detail in Pitman *et al.* (1991) and Yang (1992). Yang (1995) has provided a brief overview of the essentials of the BEST scheme and figure 1 in his paper provides a good schematic overview of the land-surface processes operating. Although physically more simplistic than SiB or BATS, BEST does provide an improvement on the "bucket" models. Wilson and Henderson-Sellers' (1985) soil and vegetation data are used to designate the 12 vegetation and 2 soil parameters in the model.

A further land surface scheme is the ISBA (Interactions between Soil Biosphere Atmosphere) described in detail by Noilhan and Planton (1989) and Mahfouf *et al.* (1995). ISBA is simpler than either BATS or SiB, but this can be explained by the fact that it was not only developed for climate modelling applications, but also for operational forecasting. The developers of this model argue that more sophisticated

treatments do not have the necessary knowledge of input parameters on a global scale, needed to capture the diversity of world ecosystems.

In the early 1990s it was realised that there is the necessity for a project with the primary goal of acquiring a better understanding of the current and new land surface schemes in atmospheric models, thereby potentially enabling improvement of the parameterizations of the terrestrial land surface. In response to this need, a Project for Intercomparison of Land-Surface Parameterization Schemes (PILPS) was launched in 1992 in agreement between the World Meteorological Organisation (WMO)-Commission for Atmospheric Sciences (CAS) Working Group on Numerical Experimentation (WGNE) and the GEWEX Continental-Scale International Project (GCIP) science panel, and it is envisaged to span a 7 year period (Henderson-Sellers *et al.*, 1993a, Henderson-Sellers *et al.*, 1995). More detail on the phases and progress thus far can be found in Henderson-Sellers *et al.* (1995).

In addition to and associated with PILPS, is a joint PILPS-AMIP (Atmospheric Model Intercomparison Project) venture, the AMIP diagnostic subproject "Land-surface Processes and Parameterizations". This subproject is under the leadership of Ann Henderson-Sellers of the Climatic Impacts Centre, Macquarie University, Australia, and has two primary objectives. The first is to examine the performance of PILPS models included in AMIP GCMs and the second, to compute atmospheric forcing from the AMIP GCMs to perform an off-line examination of a number of the PILPS models (Phillips, 1996).

2.5 The GENESIS GCM

The GENESIS (Global Environmental and Ecological Simulation of Interactive Systems) GCM was developed at the National Center for Atmospheric Research (NCAR) in Boulder, Colorado, and is also installed on the Cray at the Pennsylvania State University through which necessary access to run the model was gained. The model comprises coupled global models of the atmosphere, ocean, vegetation, snow, soil, sea ice and ice sheets. The three-dimensional atmospheric general circulation

model (the atmospheric component) is coupled to the models of the land surface through a Land-Surface Transfer Scheme (LSX).

A new version of the GENESIS GCM (version 2.0a) has recently been released and is used in this study. Version 2.0a of the model shows substantial improvements, most notably in the increased horizontal and vertical resolutions, the new prognostic cloud scheme and alterations to the convective plume scheme (Thompson and Pollard, 1997). No documentation on the physics of the model has as yet been released, besides the Release Notes for GENESIS 2.0a (henceforth referred to as version 2) and Thompson and Pollard (1997), on which the following description is based.

The new model version has a standard spectral resolution of T31 (3.75° latitude by 3.75° longitude) and 18 levels in the vertical. The cloud scheme in version 2, as mentioned, is quite different from that of version 1.02 (henceforth referred to as version 1). In version 1, cloud parameterization similar to that of Slingo and Slingo (1991) has been used to predict three possible cloud types (viz., anvil cirrus, convective and stratus). In contrast, version 2 uses a prognostic three-dimensional water cloud amounts scheme (e.g. as in Smith (1990)) to predict clouds. The cloud fields are separate for anvil cirrus, convective and stratus clouds. The scheme includes evaporation from clouds, conversion to precipitation and its aggregation during falling, re-evaporation of falling precipitation as well as turbulent deposition of cloud particles in the lowest layers.

Version 2 uses a hybrid co-ordinate system, tending from sigma co-ordinates near ground level to pressure co-ordinates at the upper level of the atmosphere (Simmons *et al.*, 1989, in Thompson and Pollard (1997)). The model has a diurnal cycle and calculations of solar radiation are performed every 1.5 hours. As for version 1, the atmospheric GCM (AGCM) horizontal grid is not dependent on the surface grid used for any of the surface models. Bilinear interpolation allows for field transferral between the AGCM and the surface and area-averaging for transferral between the surface and AGCM (Thompson and Pollard, 1997).

A number of palaeoclimate studies have been done using GENESIS version 1 (e.g. Barron *et. al.* (1993), Crowley and Baum (1994), Foley *et al.* (1994) and Pollard and Schulz (1994)), as well as some present-day applications including sensitivity to CO_2 (e.g. Bonan *et al.* (1992) and Pollard and Thompson (1994)). Analyses using version 2 are only presently being undertaken, owing to the fact that the model became wholly operational at the beginning of 1996.

Some analyses which have been done using version 2 over southern Africa include those of Hudson and Hewitson (1997) and Hudson (1997). Hudson and Hewitson (1997) compare midlatitude cyclones south of Africa in the two versions of the GENESIS model. The aim of their work was to evaluate the capabilities of the two versions of the GCM and to establish whether version 2 of the model is a notable improvement of its predecessor (version 1). Their results show a substantial improvement of the model climate with regards to midlatitude cyclones, and these improvements are likely to be related, in part, to the improvement of the model resolution (Hudson and Hewitson, 1997). Hudson (1997) has examined the equilibrium response to a doubling of CO_2 over southern Africa and the adjacent oceans. She has shown that the GENESIS model performs well under present climatic conditions, except possibly with respect to precipitation. The $2xCO_2$ equilibrium response indicated, amongst other things, an increase in temperatures over southern Africa by 2°C to 3°C, and an increase in sea level pressure south of Africa in the midlatitudes (related to the weakened westerly circulation in this region).

The GENESIS land surface transfer scheme, LSX, which is 2° x 2° at the standard resolution, is comparable to BATS and SiB (although it is mathematically simpler than SiB), and takes vegetation into account when calculating momentum, thermal energy and water mass exchanges between the atmosphere and the surface. Details of the model can be found in Pollard and Thompson (1995a, 1995b) and Thompson and Pollard (1995, 1997). A few of the key characteristics, based on the above papers, are outlined here.

LSX has, at maximum, two vegetation layers defined for each grid point, namely, the upper layer ("trees") and the lower layer ("grass"). Shrubs will be included in either of these two, depending on the real vegetation mix. Upper-layer leaves, upper-layer stems, and lower-layer leaves and stems combined have separate predicted temperatures. Turbulent and radiative fluxes through the two vegetation layers to the soil or snow surface are computed. Vegetation can intercept snow or rain, which blows or drips off. The primary equations of LSX use the AGCM, soil and snow conditions to predict vegetation and canopy-air temperatures, and specific humidities. Each land surface grid cell has a specified fractional amount of open water (representing coastal water or lakes) and separate calculations of surface-AGCM fluxes for the open water and land fractions are made. Vegetation characteristics such as leaf area index, fractional cover, leaf orientation, canopy heights and stomatal resistance are prescribed using one of the three global model options described below.

The first option is the data set described in Dorman and Sellers (1989), which is the vegetation prescribed for GENESIS version 1. The data file is a 4° by 5° biome map with 12 different biomes being used to describe world vegetation. A description of these biomes is provided in Dorman and Sellers (1989). The second vegetation prescription option is referred to as the "Wisconsin" Vegetation Categories and was developed by Jon Foley and his group from the University of Wisconsin (Pollard and Thompson, 1995c). Their data set aims not at capturing biome or species contrasts, but rather the climatically important distinctions, with vegetation being described by cover type, climate zone, phenology and C_3 or C_4 understorey (Pollard and Thompson, 1995c). The third option (which is used in this study) was developed by Jon Bergengren from the National Center for Atmospheric Research (NCAR) in Boulder, Colorado, and is called the Equilibrium Vegetation Ecology model (EVE). The following chapter will provide some details on this vegetation model.

CHAPTER 3

THE EQUILIBRIUM VEGETATION ECOLOGY MODEL AND OFF-LINE RESULTS

CHAPTER 3

THE EQUILIBRIUM VEGETATION ECOLOGY MODEL AND OFF-LINE RESULTS

3.1 Description of the Equilibrium Vegetation Ecology model

Detailed information on the Equilibrium Vegetation Ecology Model (EVE) can be found in Bergengren and Thompson (1997a, 1997b) and some of the essentials of these papers are presented here. EVE uses basic ecological principles to predict the equilibrium state of natural terrestrial plant community structure as determined by climate. The model allows examination of the climate predicted distribution and abundance of vegetation life forms, as well as the mechanisms involved. While many other vegetation models exist, some with high degrees of complexity, EVE is particularly suited to this project as it is designed to be coupled to a GCM and has the specific requirements of the physical parameters of a GCM. Thus, in the context of GCM studies, EVE provides the most viable solution for developing a vegetation perturbation to drive the GCM.

It should be noted that EVE is designed such that it predicts and simulates natural vegetation only. Therefore the model cannot account for anthropogenic influences on natural vegetation, as it generates natural vegetation in areas which may now be used for agricultural purposes. Thus, the model may for example produce grasslands or savanna in regions which are currently being used for grazing purposes or crop production.

The EVE model divides the natural vegetation into 110 life forms (see Appendix A). A life form is considered to be a group of species having comparable biophysical, physiognomic and ecological characteristics (Bergengren, 1995). The advantage of this method of classification as an alternative to biomes, is that whereas life forms are heterogeneous within biomes, EVE allows for a more homogeneous spatial

parameterization of the terrestrial surface (Bergengren, 1995). From the life forms, the accumulated phenology and physical characteristics of the vegetation for each grid cell are resolved and passed to the Land-Surface Transfer Model (LSX) of the GENESIS GCM (Pollard and Thompson, 1995c).

EVE has two submodels, the Life-Form Model (LFM) and the Plant Community Model (PCM). The LFM is a small component of EVE, and is based on E.O. Box's (1981a and 1981b) Potential Vegetation Model (PVM). Monthly temperature and precipitation values are used to predict a list of plant life forms adapted to a particular climate in Box's (1981a, 1981b) model. In addition to precipitation and temperature data, relative humidity data are used in EVE, distinguishing the LFM from Box's PVM.

Box (1981a) notes that water availability, ambient temperature and incident solar radiation seem to be the critical climatic elements affecting plants and he explains the use of precipitation and temperature in classifying and predicting plants structural types. Water availability and its relationship to plant types is complex and conditions such as rainy season length, the reliability of the rainy season and morphological adaptations need to be considered in a classification system. Temperature controls the type and size of plants, predominantly on the colder end of the spectrum. An example of this can be found in the polar regions where there is not the necessary warmth for wood production at height (Box, 1981a).

Average monthly temperature and precipitation (mm/month) data used in EVE are derived from the combining of two 0.5° by 0.5° data sets (Legates and Willmott, (1990a, 1990b), and Leemans and Cramer (1990) respectively). Corrections have been made for a small area over central Siberia and for an area over the Tibetan Plateau. Average monthly relative humidity is derived through interpolation of a 5° x 5° data set forming part of the Rand Climatology (Schutz and Gates, 1971-1974). The spatial resolution of these relative humidity data is therefore poor. However, the influence of relative humidity in determining life form percentage coverage over South Africa is negligible (discussed in more detail later).

In order to transform life forms into community structure it is necessary to determine how effectively each life form is adapted to the site's climatic conditions. In doing this, Bergengren and Thompson (1997a) assumed that the relative competitive ability is highest at the centre of the life form's tolerance range and diminishes slowly to zero at the edges. In view of this, 7 "adaptive index" (AI) components are assigned by the model to each life form for each site. The Adaptive Index (AI) calculated is used by the PCM, which itself calculates plant community structure. Twelve monthly values of precipitation, temperature and relative humidity, constituting 36 climatic variables, are converted into 7 ecoclimatic predictors. These 7 predictors effectively capture the important annual and seasonal characteristics of a site's climate, from an ecological perspective. The life form best adapted to a particular climate is recorded and therefore the model can be seen as operating on a class exclusion principle.

The Plant Community Model (PCM) produces a quantitative description of community structure based on the total vegetation and fractional cover of component life forms. Five light layers are distinguished and the model can operate on a global scale or for a specific location (i.e. the model can be driven using globally gridded climatological data or using site specific data). Furthermore, the PCM discards any life forms predicted by the LFM which have never been known to exist on a particular site's continent. This is followed by the construction of the 5 canopy layers of the model. Plant community structure is predicted in the undisturbed community, followed by the successional mosaic community.

A global biome model developed by Prentice *et al.* (1992) shows some similarity to EVE, in that this model is also based on the categorisation done by Box (1981a, 1981b). Biomes in Box's (1981a, 1981b) model are not taken as given (i.e. they are not fixed), but originate or evolve through the interaction between component plants (Prentice *et al.*, 1992). The Quaternary plant record clearly shows that plants respond to climate change as individual taxa; it is possible for an entire biome to form or disappear within one Milankovich cycle (Huntley and Webb (1988) and Prentice (1992) in Prentice *et al.* (1992)). Therefore, in order to examine the response of global vegetation patterns to climate change, it is important to start with climate tolerances of

different plants, rather than distributions of biomes that are apparent today (Prentice *et al*, 1992). A model such as that of Box (and therefore EVE) is therefore useful in any contemporary system in a climate change context, since it meets these requirements.

3.2 The operation of the Equilibrium Vegetation Ecology model

EVE can be run in a stand-alone mode, or coupled to a GCM. This chapter considers the former and chapter 5 the latter. The stand-alone mode was made available by J. Bergengren from the National Center for Atmospheric Research (NCAR) in Boulder, Colorado. It allows vegetation to be predicted at a 1° x 1° or 2° x 2° grid cell resolution, centred on the half degrees of a latitude/longitude grid. The model produces output of the percentage coverage of each life form in a particular grid cell, which can in turn be summarised into a number of classes, in order to aid interpretation.

The model classes defined can be modified and extended to better reflect the observed classes in the study area concerned. This was necessary for this study of the South African region, where the classes existing in EVE were not ideal, since the model was tailored more to vegetation class description on a global rather than regional scale. Regional scale vegetation classification was therefore not optimal and thus the vegetation classes defined were modified to capture more suitably the observed class distribution over South Africa. The classes were derived through consultation with the National Botanical Institute (NBI) in Cape Town, an examination of Acocks' (1988) Veld Types, and Rutherford and Westfall (1986) and Cowling and Richarson's (1997) biomes of southern Africa maps. In this regard, the individual life forms in EVE were reclassified into suitable classes for differentiating vegetation boundaries over South Africa. The reclassification process was experimentally determined, and the class system derived here represents the system which was deemed the most appropriate. The sum of the fractional covers at one particular grid point location will vary from 0% to 300%, since life forms compete in three light layers. The list of classes specified is shown in table 2.

1. Evergreen Broadleaf Trees
2. Summergreen Broadleaf Trees
3. Evergreen Needleleaf Trees
4. Summergreen Needleleaf Trees
5. Savanna
6. Evergreen Shrubs (non-arborescent)
7. Summergreen Shrubs (non-arborescent)
8. Stem Succulents
9. Grassland
10. Dry or Desert
11. Fynbos
12. Forbs, Herbs, Vines, Epiphytes or Ferns
13. Other (all those life forms not classified into the above classes)

Table 2: Vegetation classes specified in EVE

The list of classes in table 2 represents obvious differentiations, all of which may not occur in significant quantities in South Africa. The classification is a fair representation of the observed biome distribution as described by Rutherford and Westfall (1986). However, it must be realised that there are invariably difficulties in a model based vegetation classification system with regards to representing the observed biome distribution. Biomes in South Africa do not display distinct boundaries in some areas, but rather they represent a gradational change. Thus, a model will have difficulty in capturing gradational and indistinct boundaries. EVE was not able to successfully distinguish vegetation biomes on the drier end of the spectrum. The observed biomes of desert, succulent Karoo and parts of the nama-Karoo are therefore represented in EVE as a single class (dry or desert). In addition, the nama-Karoo biome is represented in the stem succulents class. Tree classes in EVE are also incorporated within broader biomes. Life forms in EVE which could not successfully be placed into any one of the other 12 classes distinguished were termed

'other' and therefore represent a range of observed biomes. Further detail on observed distributions of the classes follows in section 3.4 of this chapter.

3.2.1 Modification to better represent the observed vegetation

The model is designed such that the prescribed climatic variables (precipitation, temperature and relative humidity) can be replaced with values derived from alternative sources. This study makes use of GCM data (from control and doubled CO_2 runs) in order to capture the CO_2 forcing on vegetation. GCM data have poor spatial resolution and therefore downscaling is necessary in order to represent an appropriate finer scale for analysis.

In the downscaling procedure observed data are initially used to define the downscaling relationship which is subsequently applied to the lower resolution GCM atmospheric data. The existing 1° x 1° precipitation and temperature data in EVE for the southern African region are therefore replaced with downscaled data derived from observed and GCM atmospheric circulation. It is necessary to use data downscaled from observed circulation, as opposed to the actual observed surface data, in order to be consistent with the downscaled GCM data.

3.2.1.1 Downscaling and artificial neural networks

Downscaling, as established earlier, involves finding a relationship between large scale features and local parameter(s), and is described in detail in Hewitson and Crane (1996). A range of methodologies are available, but all involve some technique to derive a quantitative function relating data sets, usually involving a spatial scale translation as well.

For this application, the downscaling procedure was performed using artificial neural networks (ANNs) in order to derive the function relating circulation to the target local variables (precipitation and temperature in this case). ANNs can be seen as performing brain-like functions and essentially learn by association (Donlin and Child, 1992). They have an advantage over techniques such as regression, because they are not linearly constrained or subject to prescribed non-linearities. Typical earth

science applications in the past have varied from prediction of snowfalls (McGinnis, 1994) to classification of satellite imagery (Key, 1994). Details on ANNs may be found in a wide range of literature (e.g. Wasserman (1989), Donlin and Child (1992), Hewitson and Crane (1992, 1994, 1996)).

In general, an ANN consists of several layers, each of which has one or more nodes or processors (analogous to a neuron in the brain) connected by weighted links. Each input to the network is multiplied by a corresponding weight, all of which are summed, giving an individual node in a layer a non-linear weighted input. The data are passed from one layer to the following in the network. A node in one particular layer will receive data from every node in the previous layer. It will also transmit data to every node in the following layer, until the output layer node is reached. Therefore, there is typically an input layer, one or more hidden layers and an output layer, each of which has one or more nodes. Figure 4a) shows an example of a neural node and a neural network's construction.

A neural network is initially 'untrained' where the weighted links are randomly initialised, and the network consequently represents a random function. Thus, the first step in neural network computation involves training the network with some sample of the data, so that the weights are trained to represent the relationship between the input and output data. In this process the ANN is presented with a set of inputs with known target outputs, and the weights are adaptively modified to minimise the error between the ANN output and the target output. For example, in the context of this project the inputs would be represented by characterisation of the atmospheric circulation, while precipitation or temperature would form the output. Training would be accomplished using observed circulation, precipitation and temperature data.

3.2.1.2 Applying the downscaling techniques to observed data

The downscaling data used in this project were generated as part of a project for the South African Water Research Commission (WRC), and were made available for this work. A general description is provided here, and further details may be found in Hewitson (1995) and Hewitson (1996).

Daily observed rainfall and minimum/maximum temperatures were obtained from the Computer Centre for Water Research's (CCWR) station archive in Pietermaritzburg. These data are station data and are available for South Africa, including parts of southern Africa (viz. the southern parts of Botswana, Namibia and Zimbabwe). The station data were area averaged to a 2° square grid, and downscaling was performed at this resolution. Subsequently, downscaled data were reinterpolated to a 1° square grid. Downscaling was done at the 2° resolution rather than 1°, since the relationship for this grid proved to be less erroneous than the 1° grid.

The input data for the ANN were obtained from the Goddard Space Flight Center (GSFC) observed circulation data (heights of the 500 hPa and 700 hPa pressure surfaces, specific humidity at 2m above ground level, and specific humidity at the 500 hPa and 700 hPa levels) for a grid extending from 16°S to 38°S and 12.5°E to 37.5°E. The GSFC data were made available through the Goddard Distributed Active Archive Center (DAAC). These data produced are an assimilation of global meteorological observations using a GCM. Where there are missing observed data for a particular time and grid cell, the GCM data are used (Simmon, 1997). The resultant data therefore represent the best estimate of observed atmospheric state at a particular time and grid cell (Simmon, 1997). The resolution for these data is 2° x 2.5°.

A separate ANN is trained for each target grid cell and target variable over South Africa. The atmospheric window extends between 5 and 10° beyond the precipitation or temperature fields, and therefore enables the major synoptic features to be captured (Hewitson and Crane, 1996). The inputs comprise 9 geopotential height grid points (at each of 500 hPa and 700 hPa levels) above each grid location and the atmospheric column specific humidity (2m above ground surface, 500 hPa level and 700 hPa level) for each grid location (figure 4b)). These are then lagged over 3 days in order to capture the antecedent characteristics of synoptic forcing. The data are then subdivided seasonally and separate relationships derived for each season. 25% of the data are removed prior to training for testing the relationship determined by the ANN. Downscaling of both temperature and precipitation was subsequently considered

accurate with typical monthly mean errors of less than 5% for precipitation and 1°C for temperature.

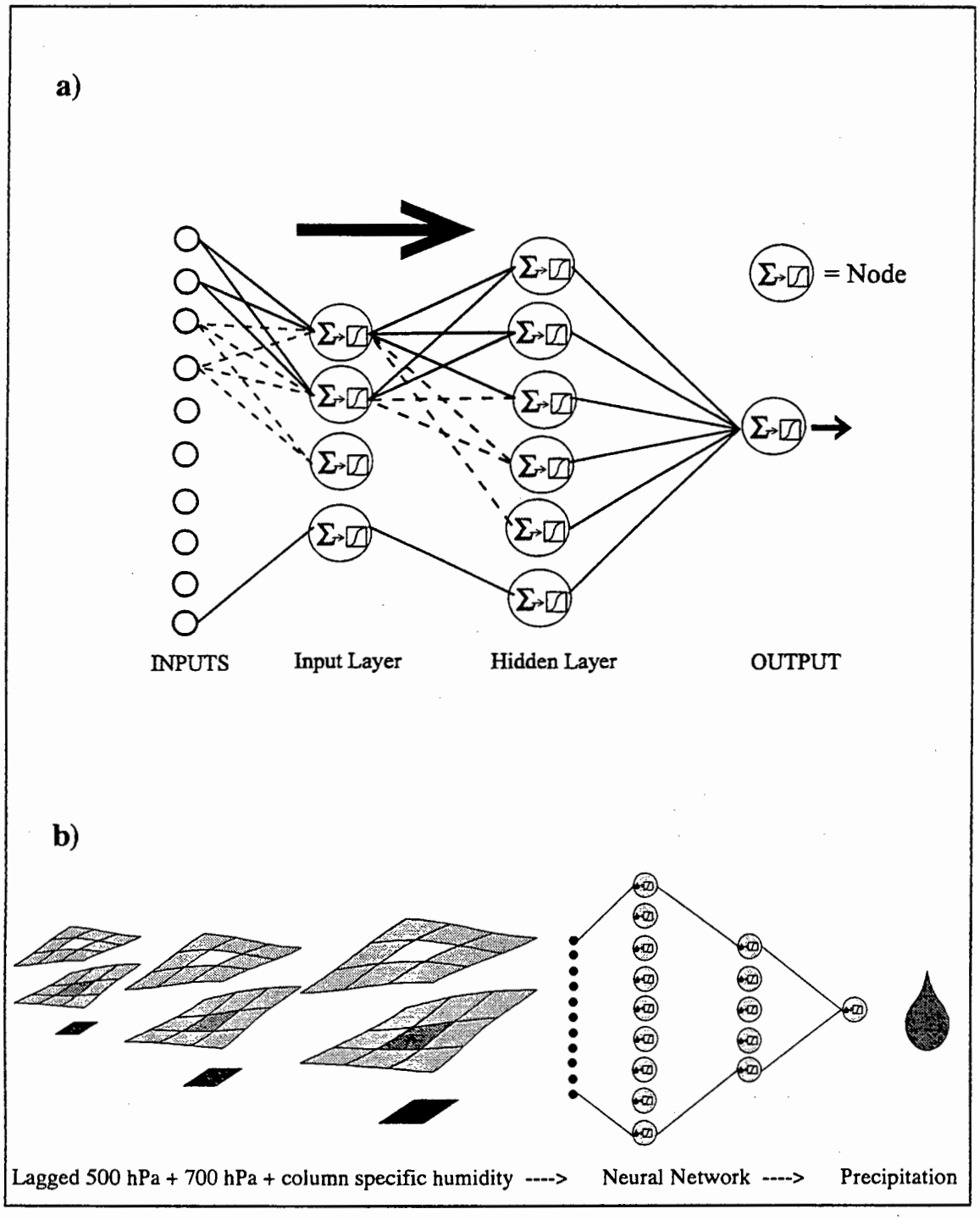

Figure 4: a) Construction of a simple artificial neural network (after Hewitson and Crane, 1994) and b) downscaling procedure (after Hewitson, 1996)

3.2.1.3 Applying the downscaling techniques to general circulation model data

The resultant functional relationships derived between the atmospheric geopotential height fields and specific humidity fields, and the observed temperature and precipitation fields were applied to the GENESIS GCM data. The GENESIS GCM data used in this application are that of the $1xCO_2$ and $2xCO_2$ mixed layer model runs (5 years each) which have been performed at NCAR.

Thus, the functional relationship derived from the observed data is applied to the geopotential heights and specific humidity fields of both the $1xCO_2$ and $2xCO_2$ GCM runs. The coarse resolution GCM control run precipitation and temperature data prior to downscaling were unacceptable for this study, but the downscaled control run data are a significant improvement. These results will be discussed further at a later stage.

3.2.1.4 Relative humidity data

Since the precipitation and temperature data sets used in EVE (see section 3.1 for a detail on these data sets) were replaced, it was necessary, for consistency, to replace the relative humidity data used in driving EVE as well. In order to test whether or not the vegetation over South Africa shows much response to variations in relative humidity, these data in EVE were replaced with values which were either considerably higher or lower than observed. However, the influence of relative humidity on determining life forms in South Africa was found to be minimal compared to the influences of temperature and precipitation. It therefore appears that temperature and precipitation are the two primary forcing factors determining the life form distribution in this region.

Observed values for specific humidity were available for the GSFC data (regridded onto a 1° square grid), from which relative humidity (equation 1 in table 3) can be derived using the following equations:

$e_s = 6.1078 * 10\exp(T*A/(T+B))$

(where T is in ºC)

(see Palmer, 1996)

$q_s = 0.622e_s/(P-0.378e_s)$

$RH = (q/q_s)*100$

Thus, $RH = q*100/(0.622e_s/(P-0.378e_s))$ ..... (1)

where:

e_s = saturation vapour pressure	q = specific humidity
T = temperature (surface)	q_s = saturated specific humidity
A = 7.5	P = surface pressure
B = 237.3	RH = relative humidity

Table 3: Derivation of relative humidity

Observed surface pressure and temperature data used in the above equation (1) are derived from the GSFC data sets, regridded onto a 1° grid.

The daily data for observed and GENESIS GCM precipitation, temperature and relative humidity were converted into twelve monthly means, in accordance with the requirements of running EVE.

3.3 Evaluation of downscaled temperature and precipitation data

Since precipitation and temperature are the primary factors driving EVE and determining the corresponding life form output, the data from the observed, $1xCO_2$ and $2xCO_2$ downscaling warrant further examination. It should be noted that the five years of GCM control run data do not represent an observed time period and therefore this could account for some of the dissimilarities between the modelled and observed precipitation and temperature.

3.3.1 Temperature

From an examination of figures 5 a) and 6 a), which show the downscaled observed (referred to as "observed" here) and GENESIS $1xCO_2$ downscaled mean temperatures (referred to as GENESIS $1xCO_2$ mean temperatures) over South Africa during summer (December, January, February - DJF), it is evident that the general pattern is similar. The lowest temperature observed (21°C) is over the escarpment regions around 28°S and 28°E. In the $1xCO_2$ simulation, temperatures are slightly lower, with a minimum of approximately 19°C over the coastal areas. The highest observed temperatures are over the NW regions of the country, with values of up to 28°C. The $1xCO_2$ scenario is comparable, but with a maximum of 27°C.

In winter (June, July, August - JJA), the lowest temperatures observed (figure 5 b)) are over the interior and escarpment regions, where temperatures are 9°C. The GENESIS control simulation temperatures (figure 6 b)) show a comparable pattern, but the lowest temperatures are found slightly further north. In addition, coastal areas around Cape Town are approximately 1°C lower. Maximum temperatures in the north are on average 1°C warmer.

It is evident that there are some differences in temperatures between the observed and the $1xCO_2$ GENESIS simulation. However, temperatures are on average comparable and the patterns are quite alike. Therefore, in the context of this study, the control simulation is deemed acceptable.

The $2xCO_2$ mean temperatures are displayed in figure 7 a) and b) for summer and winter respectively. The highest temperatures in summer are 29°C to the extreme west and the lowest are found over the coastal regions. In winter the lowest mean temperature is 11°C (over the central interior) and coastal areas are on average 14°C to 15ºC.

Figure 8 a) and b) are anomaly maps showing the difference between the $1xCO_2$ and $2xCO_2$ mean temperatures in summer and winter, respectively. It is apparent from figure 8 a) that summer temperatures are generally 2°C warmer in the doubled CO_2

scenario. Temperatures over the Western Cape and extreme NE are up to 2.4°C warmer, but only 1.8°C warmer in the NW. In winter there is more extensive warming than was observed for summer, with temperature increases of up to 3°C in the north. Most of the interior shows a warming of between 2.1°C and 2.6°C.

Thus, it is evident that mean temperatures are likely to increase more in winter than in summer. Although not displayed here, there is also slightly more variability in the transition seasons.

3.3.2 Precipitation

The observed precipitation in summer (figure 9 a)) is at a maximum (140 mm/month) in the eastern part of the country where summer rainfall is experienced. Minimum values are found in the west where values are of the order of 20 mm/month. In the control simulation (figure 10 a)) the maximum precipitation is 200 mm/month, but with a precipitation pattern similar to the observed. The minimum precipitation, found in the winter rainfall areas on the west coast, is 20 mm/month and is therefore comparable to the observed.

In winter, the observed precipitation (figure 9 b)) is highest over the coastal regions, e.g. in Cape Town, where it is 45 mm/month. There is a steady decrease in rainfall moving northwards. The 1xCO_2 precipitation in winter (figure 10 b)) is effectively reflecting the observed in terms of both the pattern and amount.

Thus, the overall pattern of precipitation in summer and winter is comparable, with the most noticeable difference between the observed and the control simulation precipitation being the amount in summer.

In the doubled CO_2 simulation, the pattern of precipitation in summer (figure 11 a)) and winter (figure 11 b)) is similar to the control simulation, but there is a general decrease in the precipitation amount in the peak regions and an increase to the west of the peak. It is evident from the anomaly maps (figures 12 a) and b)) that there is a decrease of up to 25 mm/month over the eastern regions in summer, and an increase

by up to 25 mm/month to the west of this. There is also a decrease in precipitation in winter over most of the country, with a decrease of up to 14 mm/month over the winter rainfall region of the Western Cape.

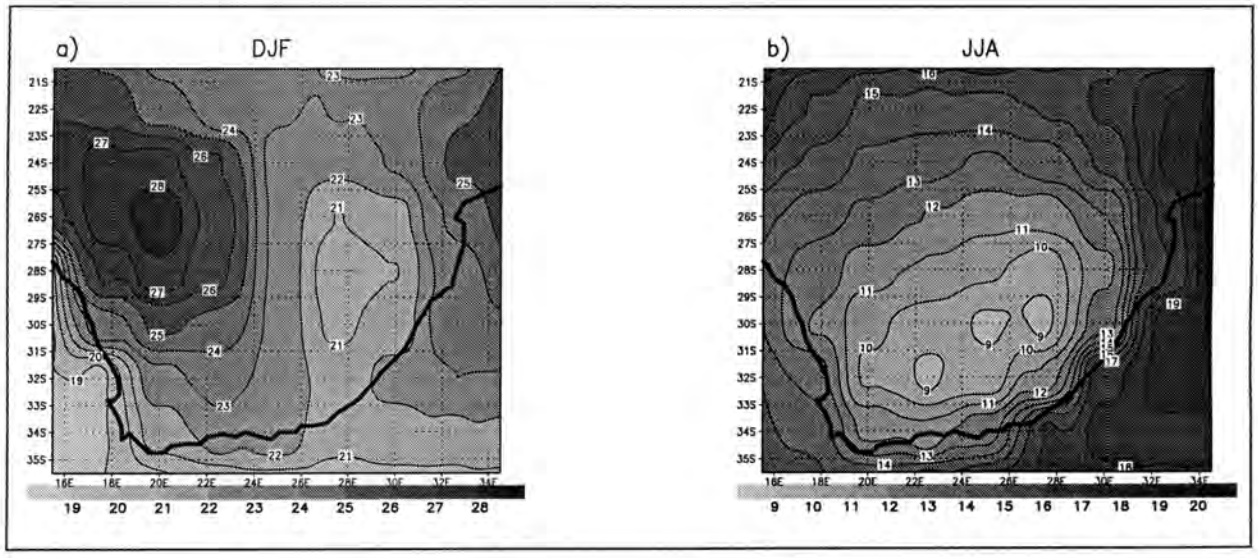

Figure 5: **Downscaled observed mean temperature distribution (degrees C) for a) summer (DJF) and b) winter (JJA)**

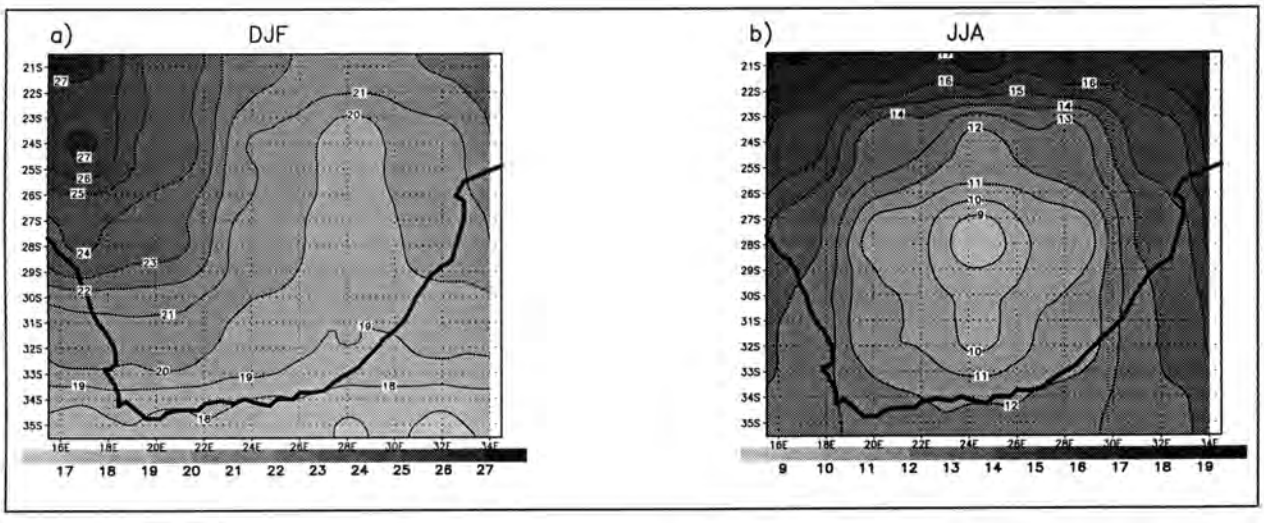

Figure 6: **GENESIS 1xCO_2 mean temperature distribution (degrees C) for a) summer (DJF) and b) winter (JJA)**

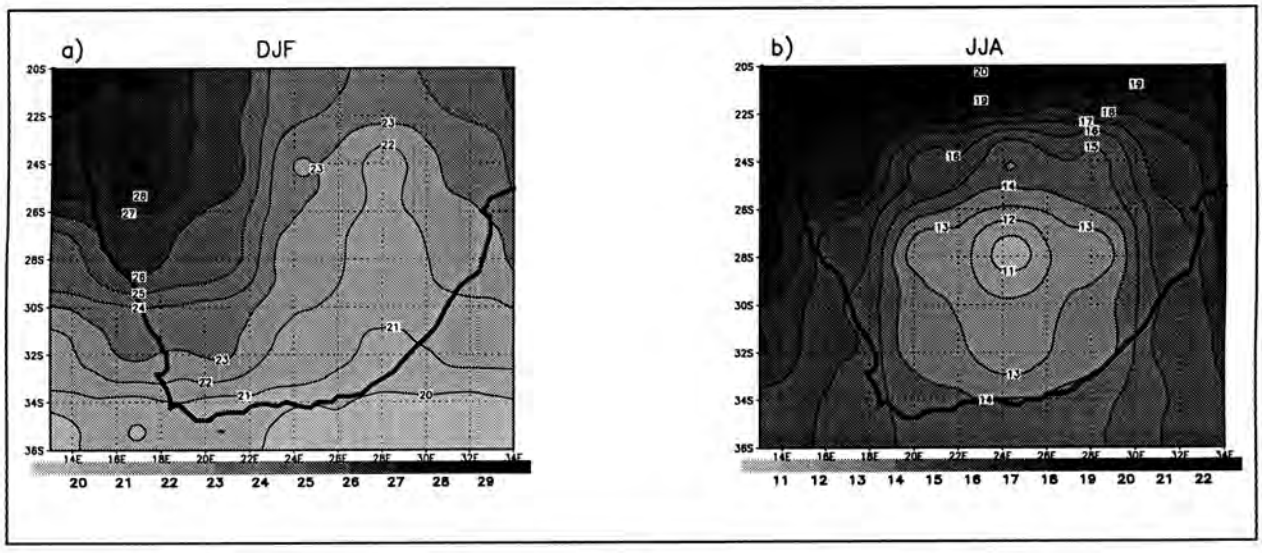

Figure 7: **GENESIS $2xCO_2$ mean temperature distribution (degrees C) for a) summer (DJF) and b) winter (JJA)**

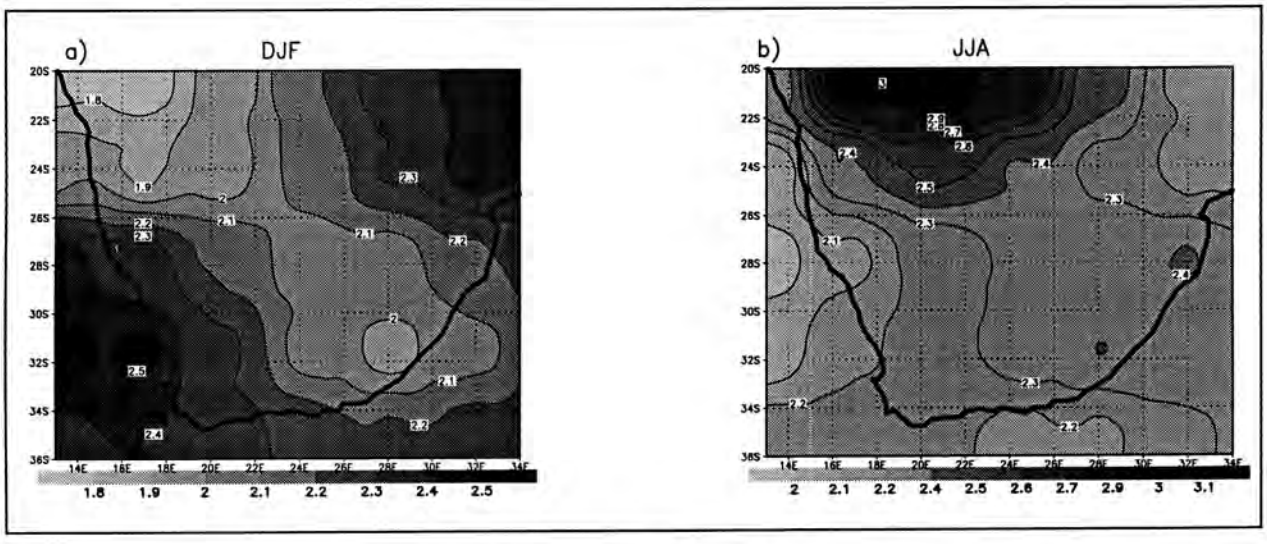

Figure 8: **Anomaly map showing GENESIS $2xCO_2$ -$1xCO_2$ mean temperature differences (degrees C) for a) summer (DJF) and b) winter (JJA)**

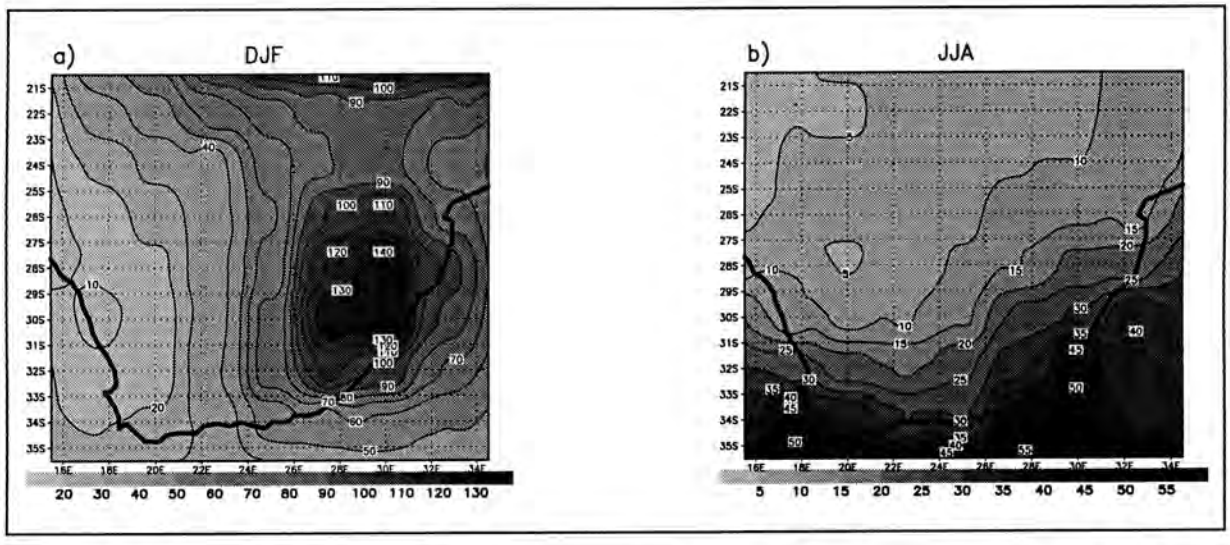

Figure 9: Downscaled observed precipitation (mm/month) for a) summer (DJF) and b) winter (JJA)

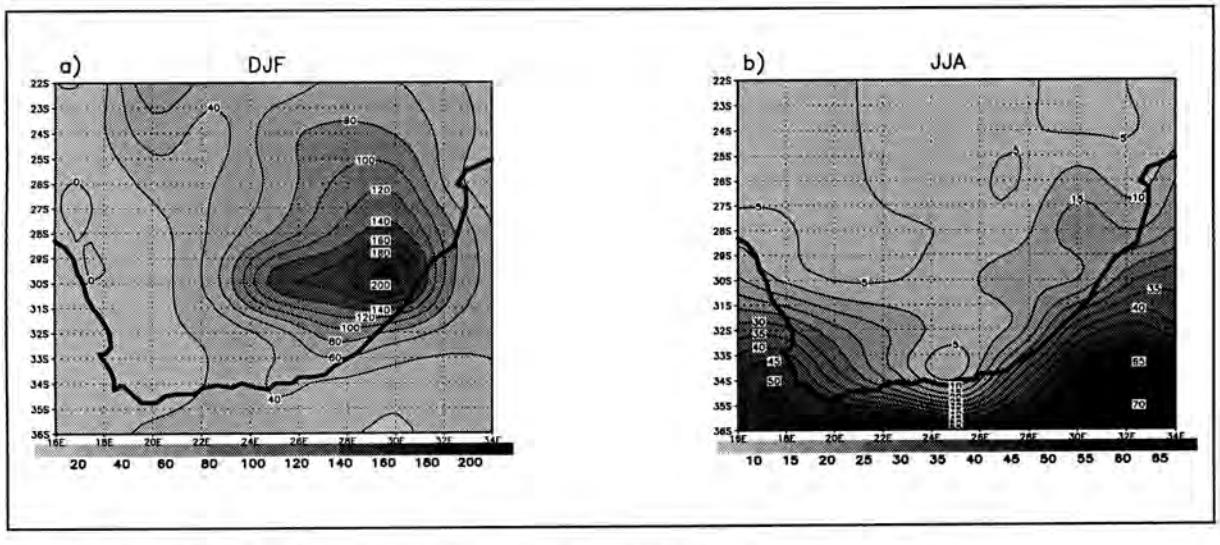

Figure 10: GENESIS downscaled 1xCO_2 precipitation (mm/month) for a) summer (DJF) and b) winter (JJA)

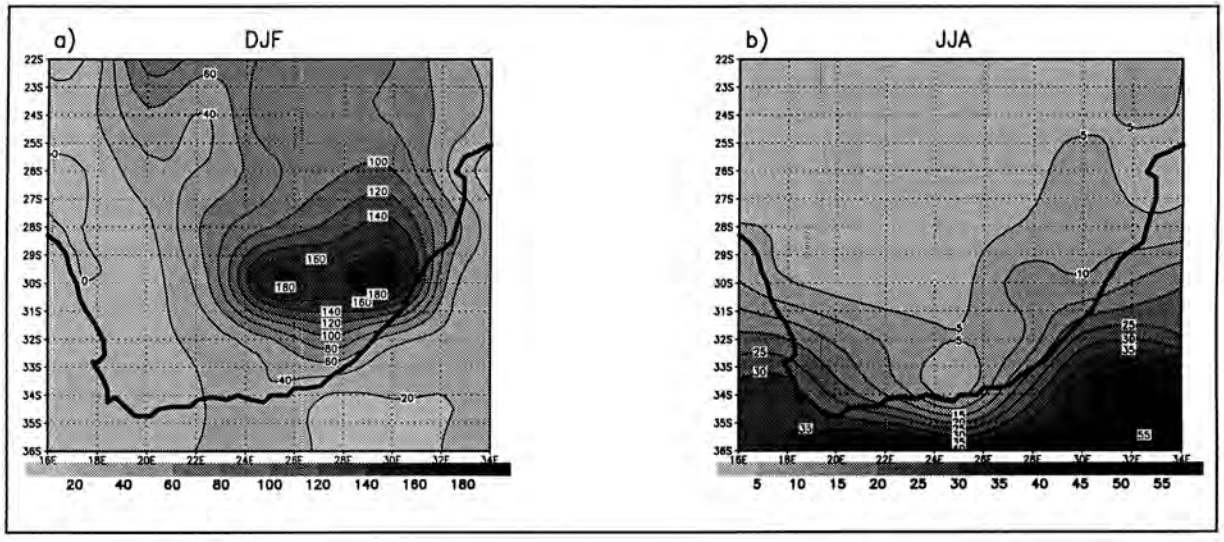

Figure 11: **GENESIS downscaled 2xCO_2 precipitation (mm/month) for a) summer (DJF) and b) winter (JJA)**

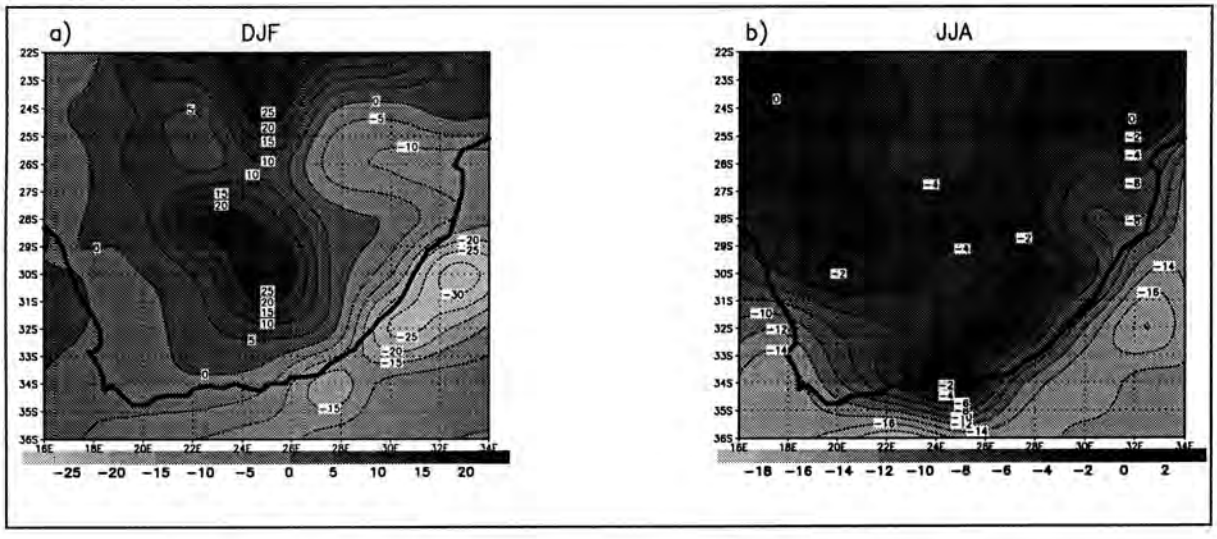

Figure 12: **Anomaly map of GENESIS precipitation (2x-1xCO_2) (mm/month) for a) summer (DJF) and b) winter (JJA)**

3.4 Comparison of vegetation classes

It is necessary to emphasise at this point that EVE is purely a model and therefore the vegetation which it produces represents a simulation and approximation of reality. In any model scenario, it is difficult to represent the observed wholly. It must be cautioned that the subjectivity of the classification system used must be taken into account in evaluating the validity of the results. However, a model such as this is a useful starting point in analysing the sensitivity of vegetation to climatic variables. It should also be stressed that since large portions of the country are used for agricultural purposes, the results need to be viewed within this context as well.

The class classification system described in section 3.2 identified thirteen classes (see table 2), eleven of which are observed in South Africa. Summergreen needleleaf and evergreen shrubs (non-arborescent) are, as would be anticipated, absent. Of the remaining eleven, the first three classes (evergreen broadleaf trees, summergreen broadleaf trees and evergreen needleleaf trees) are not representative of a particular biome and do not occur in isolation (as will be illustrated by the low percentage coverage in a few areas) but are, rather, included within other biomes. Class 12 (forbs, herbs, vines, epiphytes or ferns) is likewise, and seems to capture part of the nama-Karoo and fynbos biomes. The forest biome identified by Rutherford and Westfall (1986) is not represented by any of the classes, but since it is in such a limited area, it would be difficult for a modelling based classification scheme to represent or capture such a small spatial extent.

In the figures and text which follow the terms 'observed vegetation', 'downscaled observed vegetation' (DOV) and 'downscaled GCM vegetation' (DGV) have been used. These refer to, respectively, the observed vegetation using EVE's climatic variables in driving the model, the vegetation produced by EVE using downscaled observed precipitation and temperature climatic variables, and the vegetation produced by EVE using the downscaled GENESIS GCM climatic variables of temperature and precipitation.

Figures 13 - 23 a) and 13 - 23 b) display EVE's observed and the DOV respectively for each biome class. In order to evaluate the skill of the DOV versus EVE's observed vegetation (see figure 2), the observed biome distribution of Cowling and Richardson (1997) was used as a basis for comparison, since this is the most recent map of biome distributions over South Africa.

It can be seen that in EVE's observed vegetation savanna extends too far to the west (figure 16 a)), and this is corrected for in the DOV (figure 16 b)). The DOV also captures the intensity in the extreme east more successfully. Grassland and fynbos in the DOV are likewise more comparable to figure 2 than EVE's observed vegetation. The stem succulents class, which represents part of the nama-Karoo biome is misrepresented in EVE's observed vegetation, and is more realistic in the DOV. Therefore, in comparing EVE's vegetation and the DOV with the observed biome distribution of Cowling and Richardson (1997), it is apparent that the DOV equates better than EVE's observed vegetation.

Due to the overprediction of precipitation in the downscaled $1xCO_2$ GENESIS simulation, it would be unrealistic to apply these precipitation changes to EVE in determining the response of vegetation to climate change, since EVE relies heavily on precipitation amount in determining life forms and therefore vegetation classes. Instead EVE is run taking into account the magnitude of change induced from the $1xCO_2$ to $2xCO_2$ simulation. This is accomplished by subtracting of the $1xCO_2$ precipitation from the $2xCO_2$ and adding the monthly anomaly pattern to the observed downscaled precipitation. The same is applied, for consistency, to temperature and relative humidity data.

Thus, comparisons of the changes between the DOV and the change implied from the CO_2 forcing (DGV) can be made. Figures 13 - 23 c) show the results of the perturbation and figures 24 a) - k) show the anomaly fields. Each class will be discussed individually and in the context of the following description the 'DOV' will be referred to as the 'observed' vegetation and the 'change from $1xCO_2$ to $2xCO_2$' as the 'perturbation'. Note that the percentage coverage increases and decreases referred

to in the text relate to absolute change of the percentage coverage in a grid cell (i.e. a change from 10% to 12% coverage is mapped as a change of 2%).

In the perturbation, isolated patches of evergreen broadleaf trees show an increase (from approximately 5-10% up to 50%), with a small concentrated increase to the west of the observed coverage. Summergreen broadleaf trees also show a general minor increase, although their occurrence is still limited. Evergreen needleleaf trees have completely disappeared. Evergreen broadleaf trees in fact show an increase in a portion of the region formerly covered by evergreen needleleaf trees.

Savanna has maintained a similar pattern, although there appears to be a slight decrease in the percentage coverage overall in the NW (15%) and central regions (20%). This can be seen fairly clearly in the tongue of vegetation extending southwards from the high concentrations to the north. There is also an increase to the east of the tongue of vegetation extending southwards, by as much as 25%. In contrast, evergreen shrubs, while still constituting a very small percentage coverage, have shifted their concentration, with the peak now south of the former peak concentration.

Stem succulents, which constitute part of the nama-Karoo, exhibit an increase in percentage concentration, by as much as three times the percentage coverage in the observed and an overall percentage coverage increase of 10%. The peak which seems to have been misrepresented in the observed has reduced to almost no noticeable occurrence in the perturbation.

Grassland has generally reduced in extent (e.g. in the extreme eastern areas around 22°S and 34°E), but has increased substantially (up to 40%) in an area east of this. The general pattern has, nonetheless, remained the same, but with a general reduction of the percentage coverage in the peak concentration areas.

Dry and desert areas which are found on the western side of the sub-continent, indicate a general small reduction in the intensity of coverage in a few isolated areas.

The general trend is, however, an increase in percentage coverage in the extreme south, associated with the slight increase in the southwards extent. A region in the NE (a potential misrepresentation of the observed) also exhibits a substantial increase (up to 35%) in coverage.

Fynbos shows a slight reduction in the northern extent and a minimal decrease in percentage coverage. Forbs, herbs, vines, epiphytes or ferns also show a general reduction in percentage coverage. Some of this class may be indicative of parts of the fynbos or nama-Karoo biomes and this would therefore imply a reduction in the percentage coverage of these two biomes. The number of plants which could not be classified into any of the other 12 classes of vegetation has reduced substantially in percentage coverage in the perturbation.

Two primary deductions can be made from the changes in vegetation distribution predicted as a result of the CO_2 forcing. The first is, for the eastern portion of the region, that there is a general westward shift of lowland plants, coupled with an upwards (altitudinal) movement. It is therefore evident that these plants are responding most significantly to the temperature changes in the model. Evergreen broadleaf trees, for example, have moved westwards and altitudinally, in adaption to the increase in temperature. The westwards altitudinal movement involves a movement into areas previously occupied by evergreen needleleaf trees. These trees, which are cold-loving and therefore occur at the higher latitudes, have disappeared completely in consequence to the temperature increase.

The second observation that can be made is that the more dryland classes (e.g. dry or desert, savanna, grassland, stem succulents and fynbos) have moved southwards and eastwards. The eastwards migration of these plants has been predicted by Acocks (1953), but the additional southwards movement is interesting. Thus, the movement of these classes seems to be more in response to precipitation changes. Fynbos has reduced its coverage completely, since with a southwards migration of dryland plants, fynbos will be likely to disappear almost completely.

It must at this stage be highlighted that the general westwards movement of lowland plants, and southwards and eastwards movement of more dryland plants is what would be expected given generalised precipitation and temperature increases over the sub-continent. Thus, these findings are not necessarily a new observation, but rather they demonstrate the ability of EVE in predicting vegetation. They are therefore most useful in the context of the atmospheric sensitivity to vegetation changes.

Ellery *et al.* (1991) have considered an approach to predicting the sensitivity of the grassland biome of South Africa to climate change. This warrants some consideration, since this is one of the few studies which lends itself to comparison with this work, as it also considers the biome level and relates the biomes deterministically to precipitation and temperature. Ellery *et al.* (1991) used a biome model with a pre-determined temperature increase of 2°C and precipitation decrease of 15%, although this was purely to illustrate the use of their model. They found in their study that the grassland biome would be invaded by the savanna, and the savanna of the eastern Cape would be invaded by the nama-Karoo. They also found an increase in the extent of the succulent Karoo at the expense of fynbos (although topography would limit the horizontal displacement). They also noted the high correlation between climate and biome distribution, which is an important finding in the context of the present study, which is reliant on the strength of this relationship. Ellery *et al.* (1991) point out a limitation of their study, which holds true for the current study too, that being the fact that the direction of change may be predicted, but consideration cannot be given to the rate of change.

Ellery *et al.*'s (1991) results do not reflect all the changes found using EVE, although there is some agreement. The grassland invasion by savanna is partially represented, but the Eastern Cape invasion by nama-Karoo is not apparent in EVE. However, the increase in the succulent Karoo (falls within the class of dry or desert in EVE) at the expense of fynbos does seem comparable; EVE shows a reduction in the percentage coverage of dry or desert areas in the south, but with an increase in the southwards extent and also reflects a decrease in fynbos coverage.

The differences apparent can be explained by two important factors. The first is the fact that EVE's results are derived from modelled vegetation boundaries whereas Ellery *et al.*'s (1991) results are based on observed vegetation boundaries. Secondly, EVE has one distinct advantage over the model used by Ellery *et al.* (1991), since the percentage changes for precipitation and temperature can vary from one grid point to the next and are therefore not limited to a fixed change in these climatic variables. The latter factor is particularly important, as studies often tend to rely heavily on change scenarios of a set magnitude over an entire region. It is more realistic to consider the precipitation and temperature changes as a result of CO_2 forcing to vary from one grid point to the next, and these results are likely to be more useful in the development of regional scale scenarios.

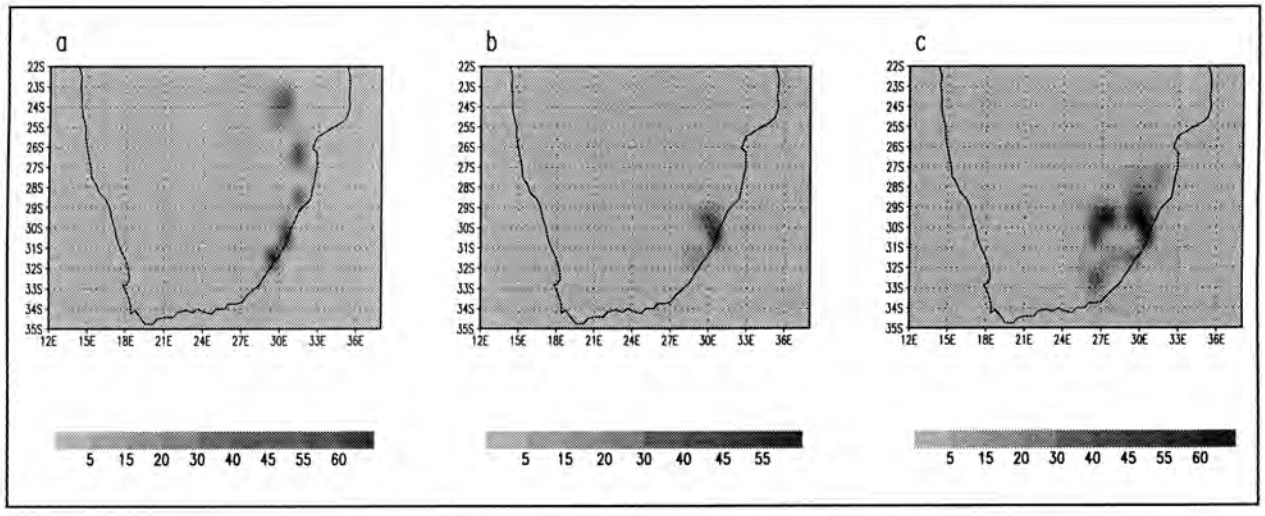

Figure 13 : Evergreen Broadleaf Trees (% coverage) for a) EVE observed, b) downscaled observed and c) perturbation ($2xCO_2$) situations

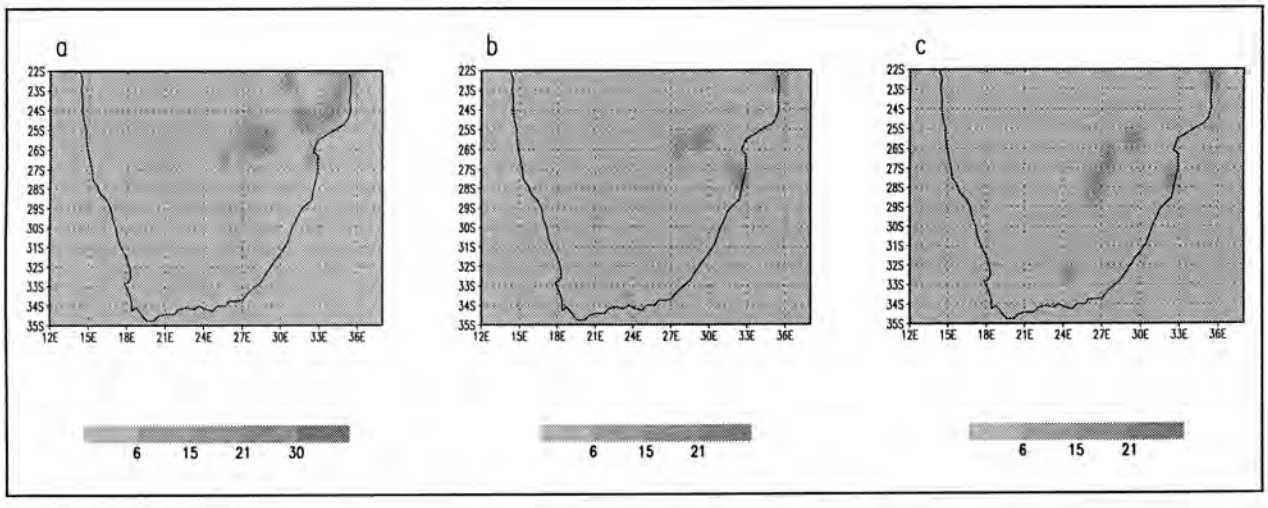

Figure 14: Summergreen Broadleaf Trees (% coverage) for a) EVE observed, b) downscaled observed and c) perturbation ($2xCO_2$) situations

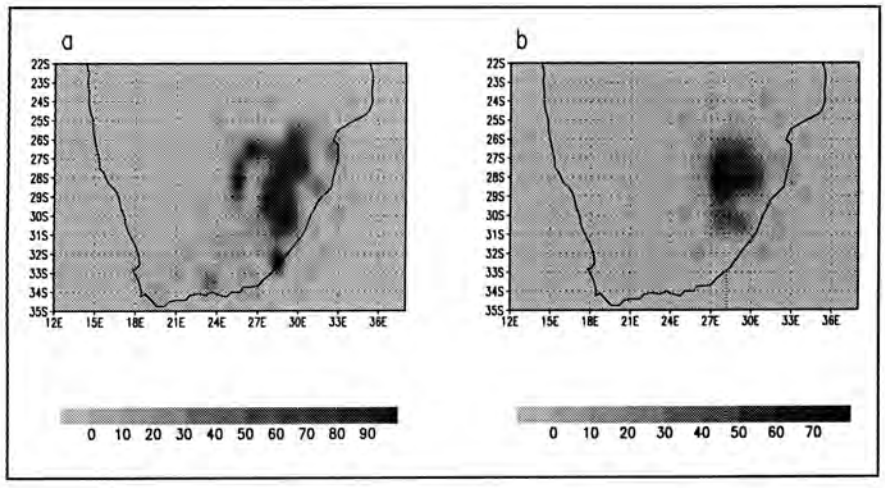

Figure 15: Evergreen Needleleaf Trees (% coverage) for a) EVE observed and b) downscaled observed situations

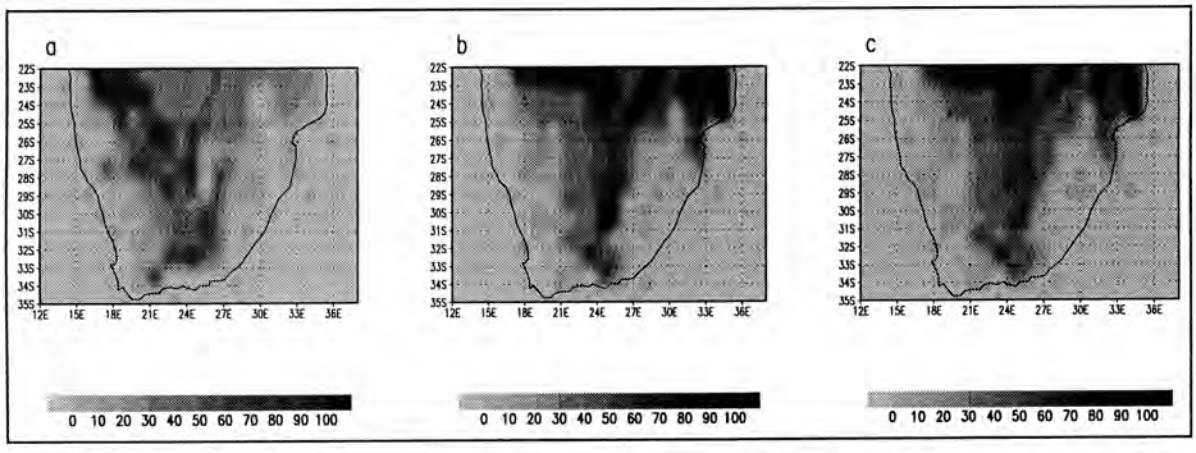

Figure 16: Savanna (% coverage) for a) EVE observed, b) downscaled observed and c) perturbation ($2xCO_2$) situations

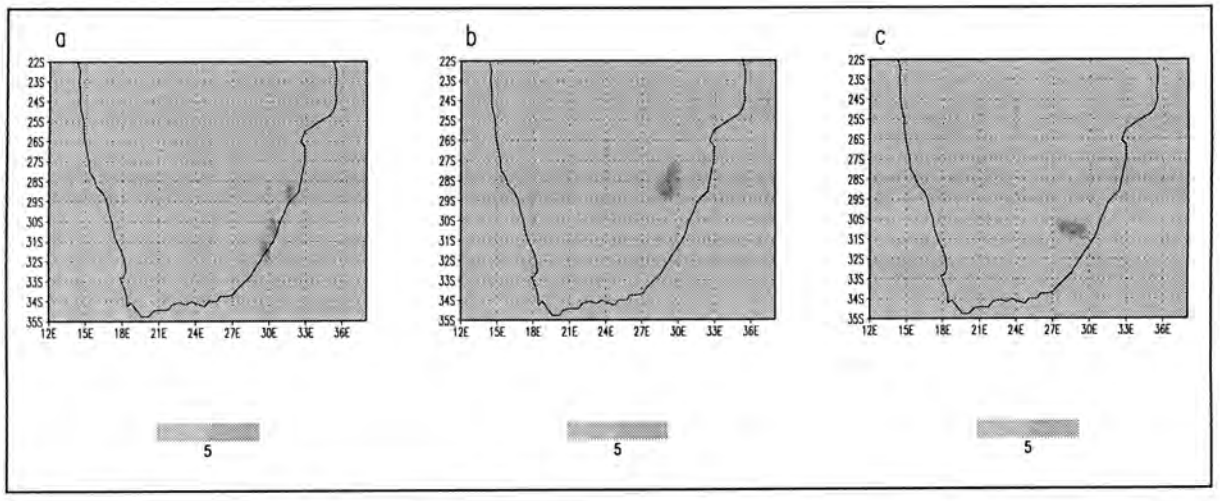

Figure 17: Summergreen Shrubs (non-arborescent) (% coverage) for a) EVE observed, b) downscaled observed and c) perturbation ($2xCO_2$) situations

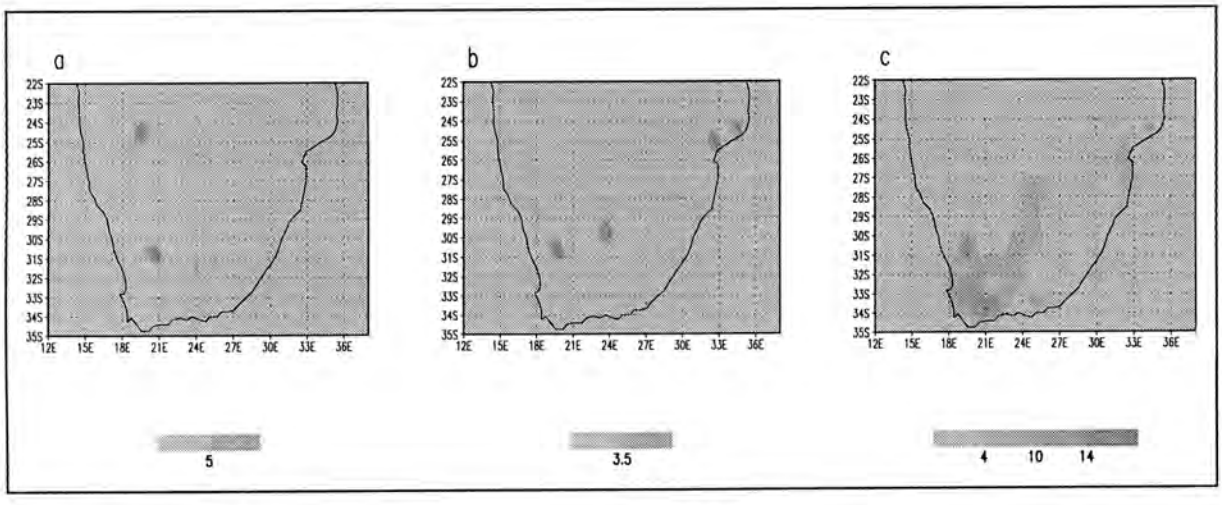

Figure 18: Stem Succulents (% coverage) for a) EVE observed, b) downscaled observed and c) perturbation ($2xCO_2$) situations

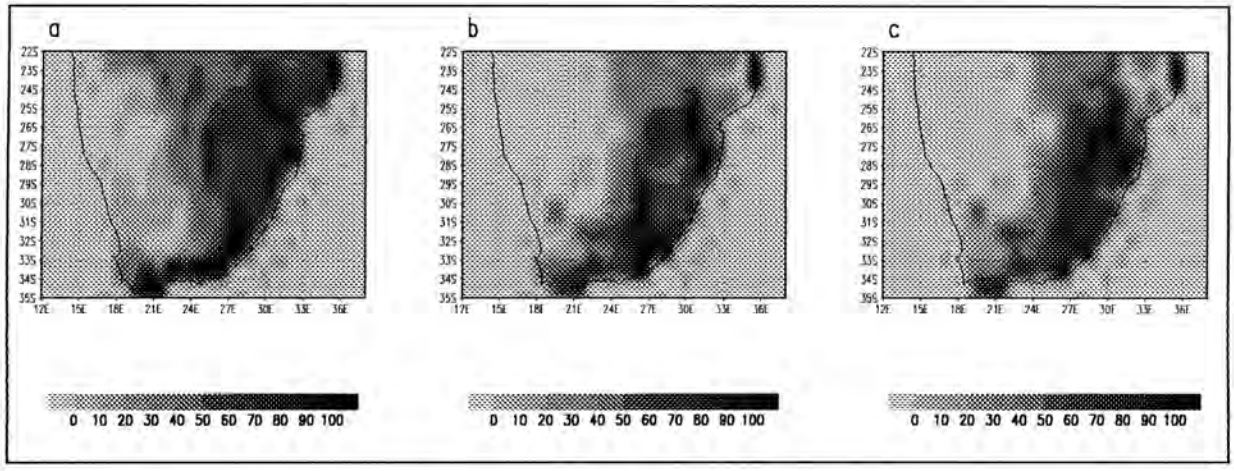

Figure 19: Grassland (% coverage) for a) EVE observed, b) downscaled observed and c) perturbation ($2xCO_2$) scenarios

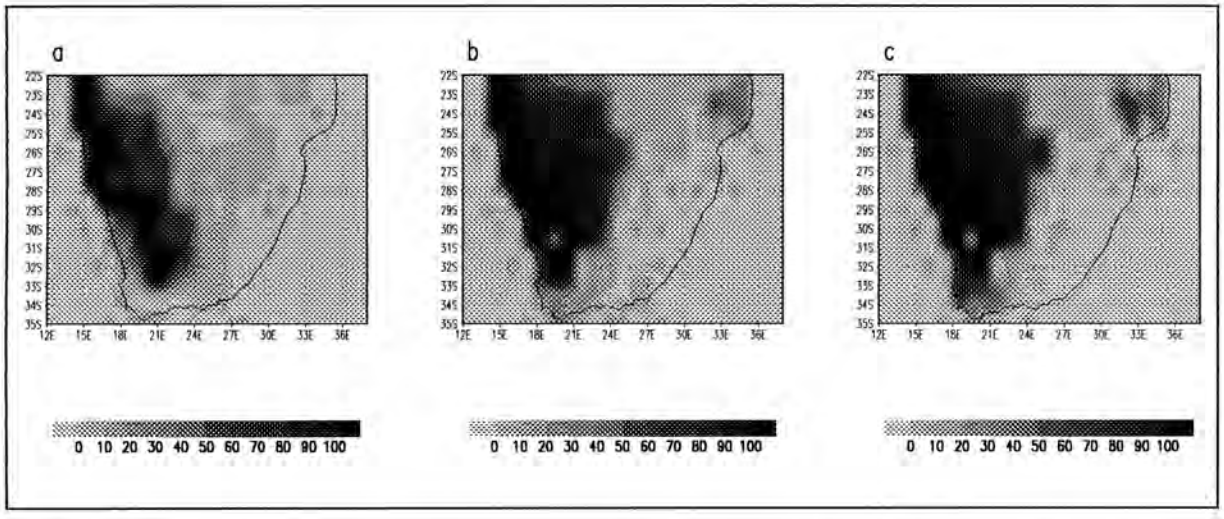

Figure 20: Dry or Desert (% coverage) for a) EVE observed, b) downscaled observed and c) perturbation ($2xCO_2$) scenarios

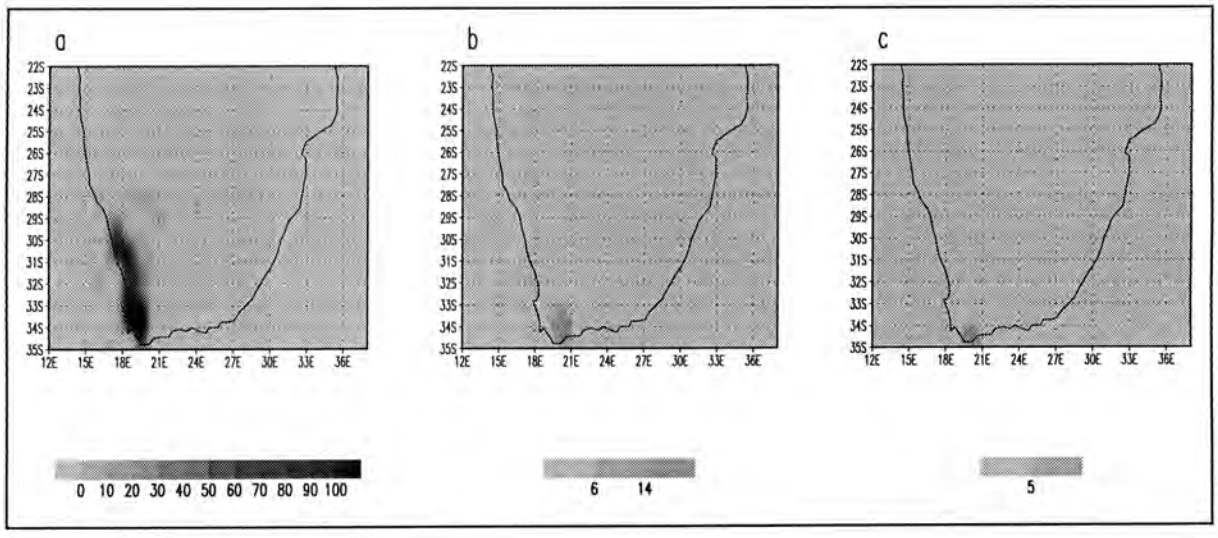

Figure 21: **Fynbos (% coverage) for a) EVE observed, b) downscaled observed and c) perturbation ($2xCO_2$) situations**

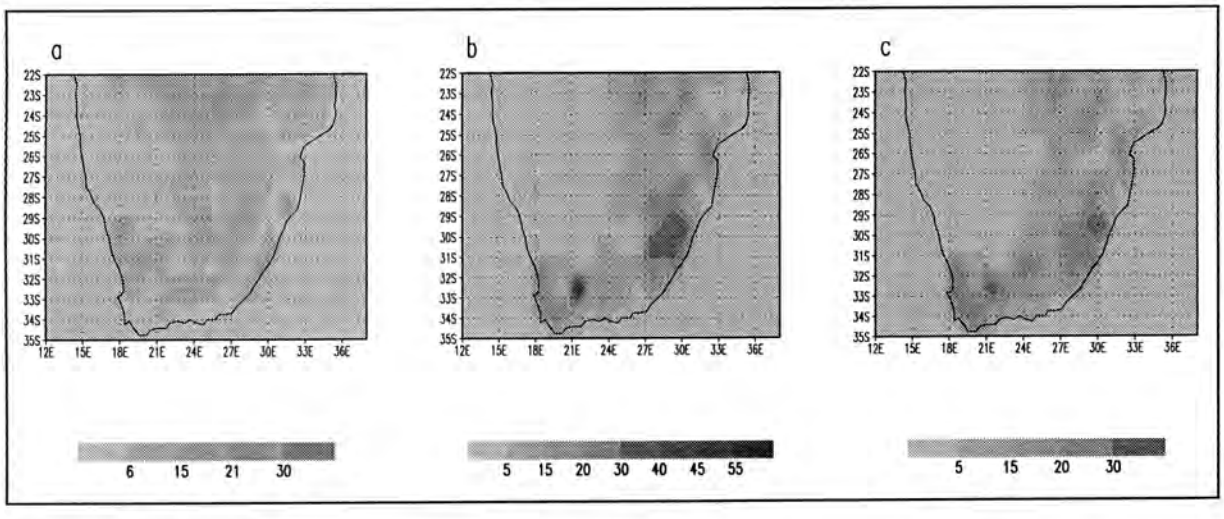

Figure 22: **Forbs, Herbs, Vines, Epiphytes or Ferns (% coverage) for a) EVE observed, b) downscaled observed and c) perturbation ($2xCO_2$) situations**

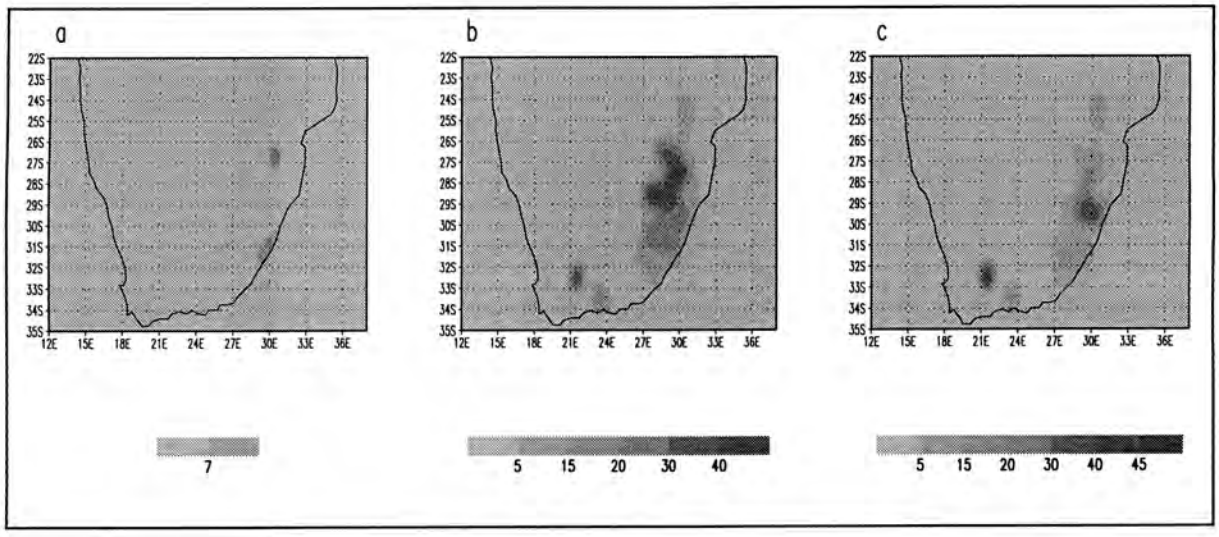

Figure 23: Other (% coverage) for a) EVE observed, b) downscaled observed and c) perturbation ($2xCO_2$) situation

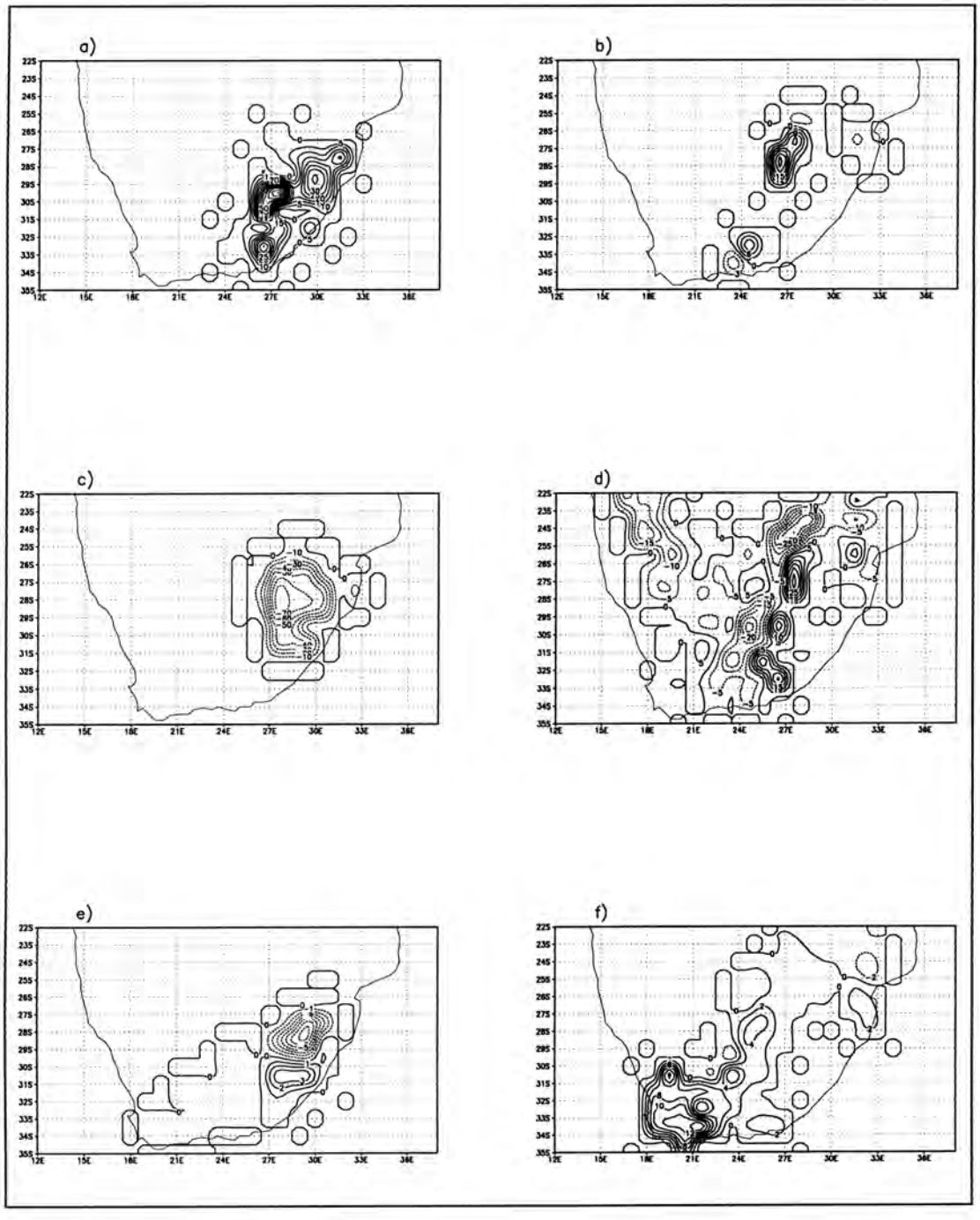

Figure 24: **Vegetation class percentage cover anomalies (perturbation - observed) for a) Evergreen broadleaf trees, b) Summergreen broadleaf trees, c) evergreen needleleaf trees, d) Savanna, e) Evergreen shrubs (non-arborescent) and f) stem succulents**

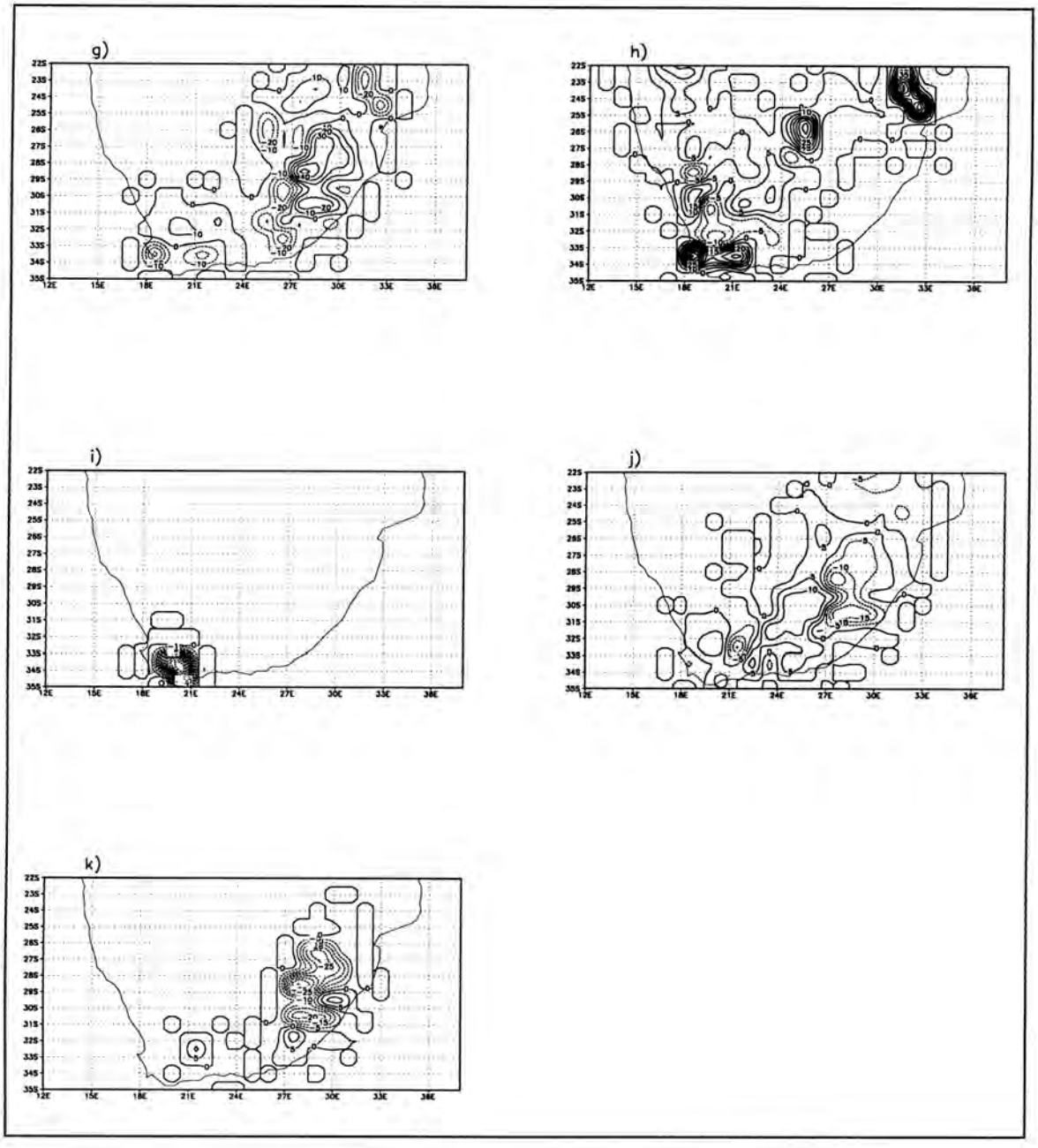

Figure 24 (continued): Vegetation class percentage cover anomalies (perturbation - observed) for g) Grassland, h) Dry or desert, i) Fynbos, j) Forbs, herbs, vines, epiphytes or ferns and k) Other (unclassified)

CHAPTER 4

VALIDATION OF THE AMIP RUN

CHAPTER 4

VALIDATION OF THE AMIP RUN

The first section in this chapter provides some background on the Atmospheric Model Intercomparison Project (AMIP), the primary aims of the project and the prescribed conditions under which the GENESIS AMIP configured run is conducted. The section which follows validates the AMIP configured run (hereafter referred to as the AMIP run) of the GENESIS GCM and compares the results of a number of variables with observed data. The importance of this is emphasised by the fact that in order to make comparisons between the present day and a doubled CO_2 scenario, it is necessary to have an accurate picture of the ability of the GCM to capture the present day situation.

4.1 The Atmospheric Model Intercomparison Project

Intercomparison of results from different atmospheric models is an essential component of modelling research and much of this comparison in the past has been in the context of numerical weather prediction (Gates, 1992a, 1992b). There has, until recently, been less of an effort from the climate modelling community. Therefore, the need for a systematic and comprehensive intercomparison of different climate models was realised (Gates, 1992). As a result of this, the Atmospheric Model Intercomparison Project (AMIP) was launched and soon became a priority of the Program for Climate Model Diagnosis and Intercomparison (PCMDI) (Gates, 1992a, 1992b).

AMIP involves an undertaking of systematic intercomparisons and validations of different GCMs on daily, seasonal and annual time scales, given realistic boundary conditions. Thus, it is necessary for models to simulate the same time period and under comparable conditions. The test period for AMIP runs that was chosen was 1979-1988, which therefore includes the major El Niño of 1982-1983 (Gates 1992a,

1992b). Global distributions of sea-ice and sea surface temperatures are prescribed in terms of a 2° square grid of monthly averages (Gates 1992a, 1992b). The land surface is not subjected to common specification although, as established earlier, the validation and intercomparison of these schemes is being undertaken as an associated project. Other elements such as surface elevation data, geophysical constants (e.g. gravity) have not been specified, although CO_2 concentration (345 ppm) and the solar constant (1365 Wm^{-2}) have been prescribed (Gates 1992a, 1992b).

4.2 Validation of model run with observed data

An AMIP run of the GENESIS GCM, using the EVE model vegetation option has been performed at the Pennsylvania State University. As part of this study, it was necessary to validate some of the fields of this run, using observed data. Without such a comparison, the validity of this study in the context of global climate change may be open to question. Therefore, in this regard, the GSFC observational data set for the window 16°S to 38°S and 12.5°E to 37.5°E has been extracted. This data set is on a 2° latitude by 2.5° longitude grid and extends from 3 March 1985 to 30 September 1993 (30 November in the case of precipitation).

For the purposes of this validation, the GSFC data set was composited into 1 year of monthly averages. The 10 year AMIP run of the GENESIS GCM was likewise composited into 1 summary year of monthly averages. Fields available from the GSFC observational data set, which are compared with the GENESIS AMIP run are as follows: sea level pressure, surface temperature, heights of the 500 hPa surface, surface specific humidity, specific humidity at the 500 hPa level and precipitation. The GENESIS AMIP run spans the single biggest El Niño event in history (1982-1983), which is not represented in the GSFC observational data set. However, it should be noted that despite the fact that the GSFC and GENESIS data sets are spanning different time periods, this is not problematic, as an exact match is not sought, but rather an evaluation of whether the GCM performs within the bounds of observation.

4.2.1 Sea level pressure

GSFC observed sea level pressure (SLP) for summer (figure 25 a)) reveals a pressure minimum of 1008 hPa over the west and a general pressure increase to the east and south of this pressure minimum. In winter (figure 25 b)) the pressure minimum (1007 hPa) is further north and extends into Namibia. Pressures over coastal regions tend to be higher.

The GENESIS summer SLP distribution (figure 26 a)) exhibits a similar pattern over the sub-continent and captures the minimum over the west quite successfully, although the minimum is offset slightly northwards. The pressure over the eastern regions is generally 5-10 hPa too high. However, values over the NE tend to a little lower (approximately 3 hPa). In winter (figure 26 b)), GENESIS predicts a pressure maximum of 1023 hPa over the interior and values are considerably higher than what is observed, although the pattern is reasonably comparable to the observed pattern.

It should be noted that SLP is perhaps not the best variable for comparison, since SLP values over the central plateau, which is at an altitude of 800m, are interpolated. The heights of the 500 hPa surface are perhaps more meaningful and will be examined and compared in section 4.2.3.

4.2.2 Surface temperature

The GSFC observational data set mean temperature distribution for summer (figure 27 a)) shows temperature maximums over the NW and western regions of the examination window (values are up to 301K) and over the Indian Ocean (298K). Temperature minimums are over the eastern interior and Atlantic Ocean. Temperatures over the sub-continent range between approximately 292K and 301K. In winter (figure 27 b)) the pattern of temperatures is somewhat similar, although the mean temperatures are considerably lower over the eastern and SW parts of the country.

The GENESIS AMIP run mean summer temperatures (figure 28 a)) show a more smoothed pattern (due to the coarser resolution) and the localised peak temperatures

displayed on figure 27 a) are not observed to the same extent (again, a function of resolution). Temperatures are, on average, comparable to the observed, and the range of values is similar. Temperatures over the sub-continent range between approximately 291K and 299K, which is comparable to the range of the observed. The winter distribution of mean temperature of the GENESIS AMIP (figure 28 b)) run exhibits a temperature minimum over the central interior (283K), increasing to the north. The pattern is similar to the observational data set, but the minimum is offset slightly to the west and the temperatures are generally too low.

4.2.3 Height of the 500 hPa surface

The height of the 500 hPa pressure level observed in the GSFC data set in summer (figure 29 a)), shows a pattern of increasing heights from the south, northwards and westwards. Minimum heights are 5820 geopotential metres (gpm) in the SW and maximum heights are 5885 gpm in the NW. The scenario for winter (figure 29 b)) is similar, but the height minimum is over the SE Indian Ocean (5680 gpm). Highest values (5860 gpm) are again over the northern part of the examination window.

The GENESIS AMIP run captures the pattern of the height of the 500 hPa pressure surface fairly successfully in summer (figure 30 a)). However, the degree of the gpm minimum in the SW is not as pronounced, and gpm values are not quite as high as observed. The winter pattern (figure 30 b)) is comparable to the observed, although the model generally predicts gpm values which are up to 100 gpm too low. The meridional pressure gradients in summer are not comparable, with the gradient for the GENESIS AMIP run being considerably higher. However, the meridional pressure gradient for winter is less dissimilar.

4.2.4 Surface specific humidity

GSFC observed surface specific humidity is displayed on figures 31 a) and 31 b) for summer and winter respectively. In summer the highest specific humidity values (16 - 17 $g.kg^{-1}$) are over the Indian Ocean. Specific humidity values over the central interior of the sub-continent are on average 11 - 14 $g.kg^{-1}$. In winter the specific humidity is

lowest (5 $g.kg^{-1}$) over the central interior and values increase northwards and southwards of this and over the Indian Ocean, where values are as high as 18 $g.kg^{-1}$.

The GENESIS AMIP run observed surface specific humidities for summer and winter are displayed on figures 32 a) and 32 b) respectively. The summer scenario captures the maximum observed over the extreme NE, but is approximately 1 - 2 $g.kg^{-1}$ too low. Values over the west are similarly too low (up to 5 $g.kg^{-1}$). In winter the specific humidity values are also too low. The pattern of low specific humidity values over the NW is a misrepresentation. As is the case for summer, specific humidity values in the model in winter are generally too low.

4.2.5 Specific humidity at the 500 hPa level

Specific humidity values at the 500 hPa level for the GSFC observational data set are displayed on figures 33 a) and 33 b) for summer and winter respectively. Values for summer are lowest over the ocean and highest over the central interior, and range between 0.9 $g.kg^{-1}$ and 1.7 $g.kg^{-1}$. The winter situation exhibits a general decrease in specific humidity values, with values over the central region being generally 0.35 $g.kg^{-1}$ and the adjacent oceans, 0.6 $g.kg^{-1}$.

The GENESIS summer scenario (figure 34 a)) displays the highest specific humidity over the NE (values of approximately 2 $g.kg^{-1}$) which is comparable with the GSFC observational data set. However, values are generally higher than observed over the entire domain. In winter (figure 34 b)) the specific humidity pattern is dissimilar to the GSFC data, and there is a specific humidity peak over the eastern interior which is not reflected in the observed data. However, the range of specific humidity values for this season is reasonably comparable.

4.2.6 Precipitation

Precipitation, as it has been established in chapter 3, is grossly overestimated in the GENESIS GCM, and this is one of the limitations of this particular GCM. The atmospheric dynamics in the model are therefore not capturing the observed precipitation successfully in this regard. From an examination of the observed (figures

35 a) and 35 b)) and the GENESIS model (figures 36 a) and 36 b)), it is clear that GENESIS vastly overpredicts precipitation in both seasons, and further highlights the need for downscaling of GCM atmospheric forcing.

4.2.7 Summary

It is evident from the above comparisons, that in many respects the GENESIS AMIP run is successfully representing the observed. However, there are some differences, which could not only be explained in terms of the model's inability to represent the atmospheric physics successfully, but also partially by the fact that the GENESIS GCM is operating on a coarser resolution than the GSFC observational data set (3.75° x 3.75° as opposed to 2° x 2.75°) and therefore the model cannot capture the more localised detail that the finer resolution observational data set displays.

Nevertheless, in analysing and interpreting the results of the perturbation, the GENESIS model is an acceptable representation of the observed.

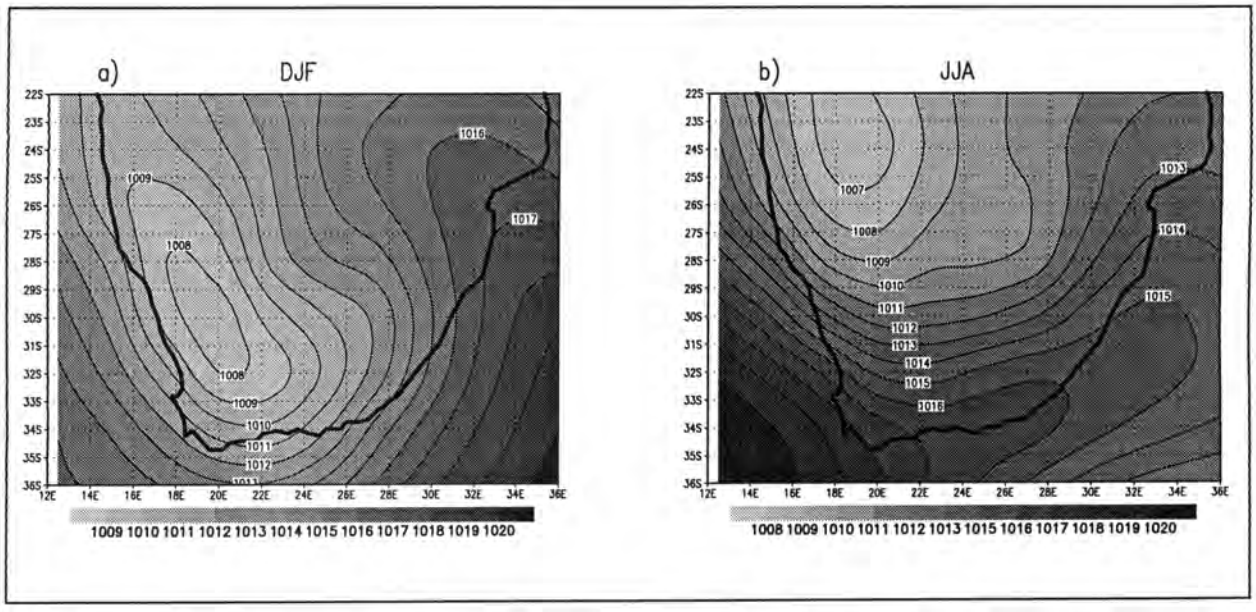

Figure 25: GSFC observed mean sea level pressure (hPa) for a) summer (DJF) and b) winter (JJA)

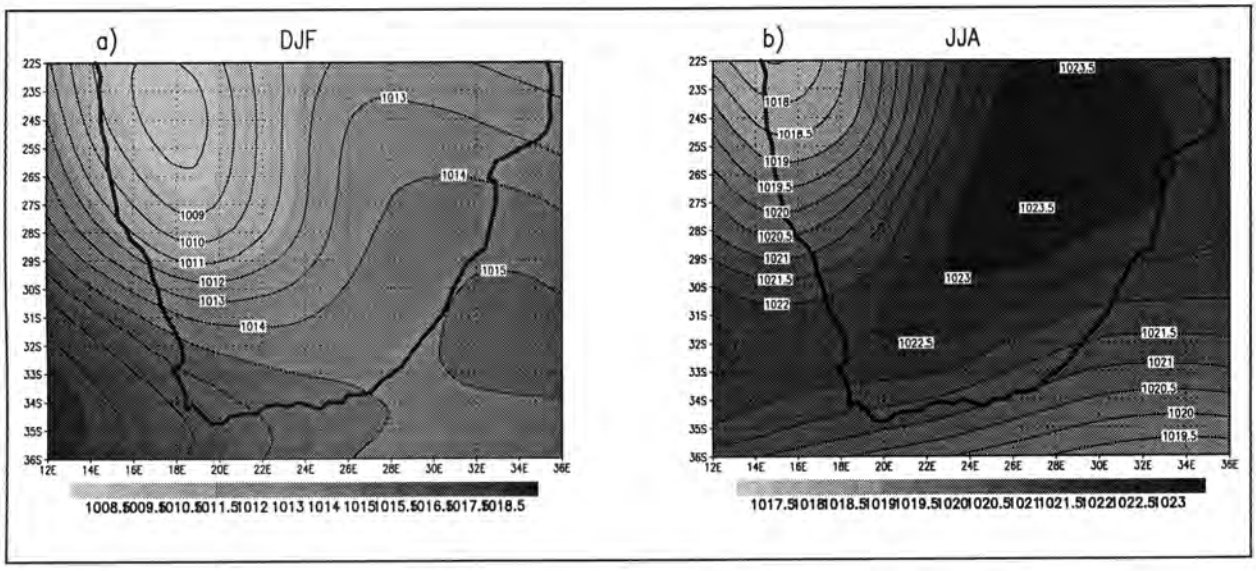

Figure 26: GENESIS 10 year AMIP run mean sea level pressure (hPa) for a) summer (DJF) and b) winter (JJA)

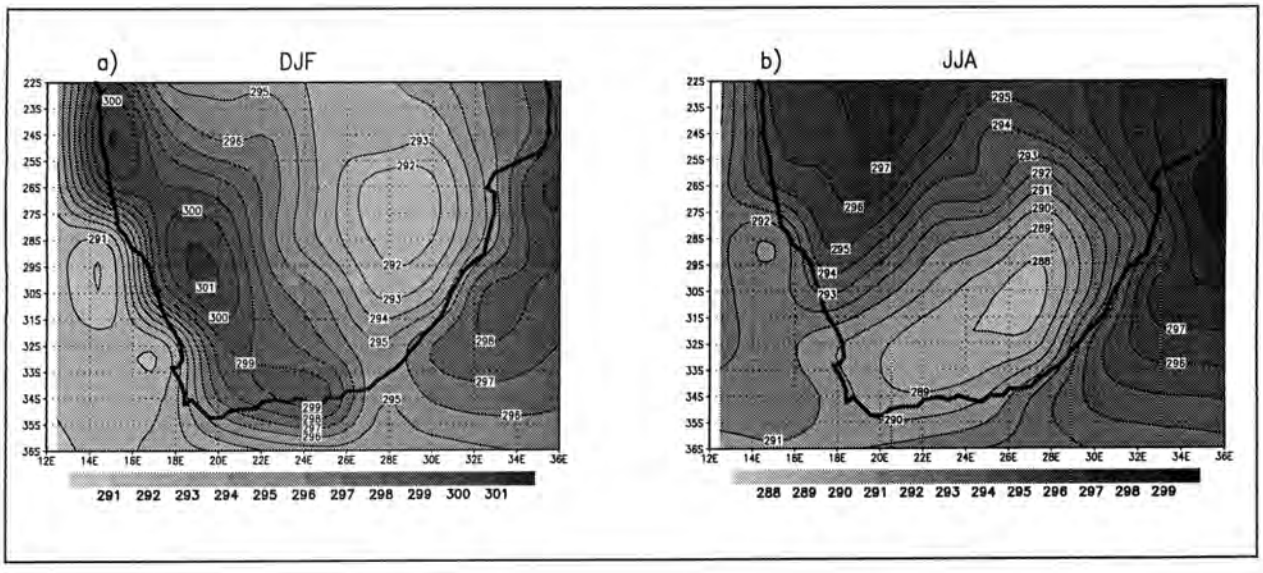

Figure 27: GSFC observed mean surface temperature distribution (K) for a) summer (DJF) and b) winter (JJA)

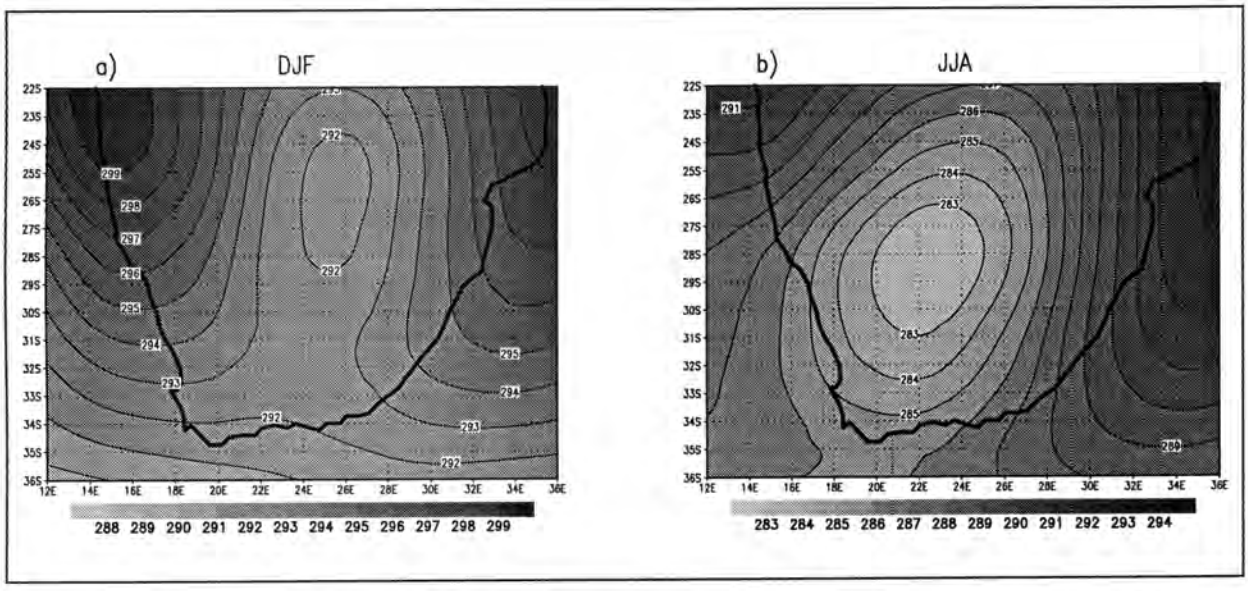

Figure 28: GENESIS 10 year AMIP run mean surface temperature distribution (K) for a) summer (DJF) and b) winter (JJA)

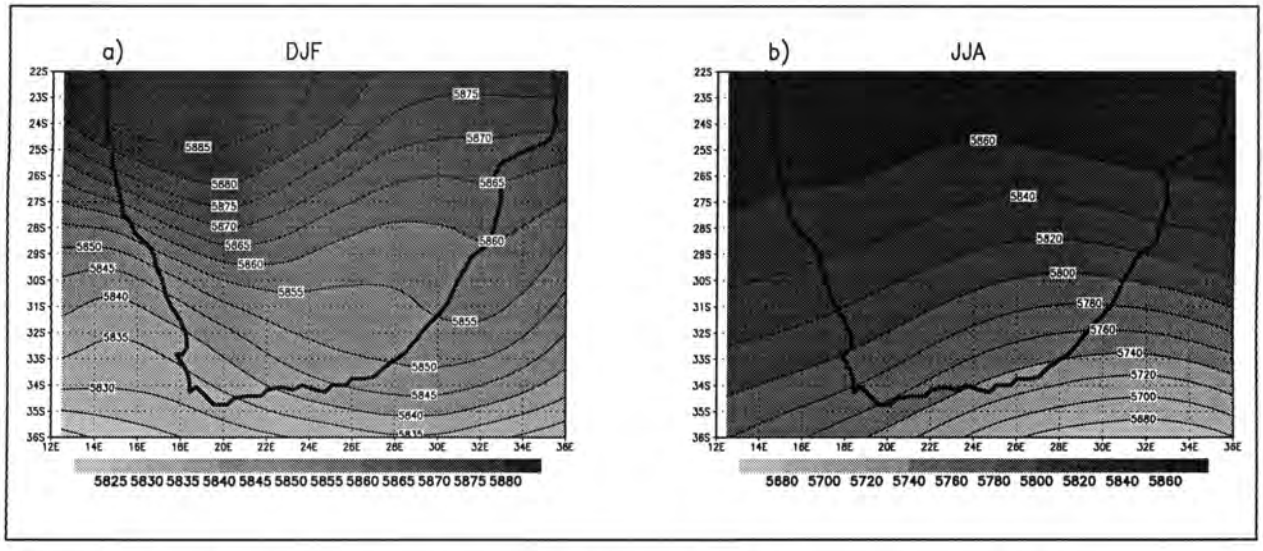

Figure 29: GSFC observed mean height of the 500 hPa surface (gpm) for a) summer (DJF) and b) winter (JJA)

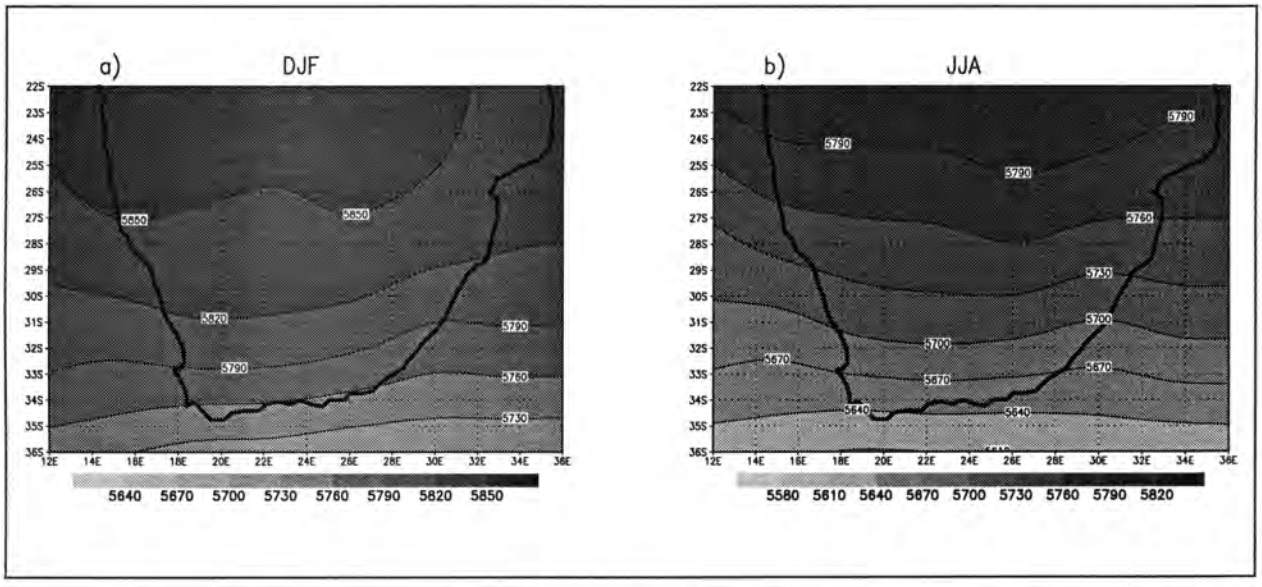

Figure 30: GENESIS 10 year AMIP run mean height of the 500 hPa surface (gpm) for a) summer (DJF) and b) winter (JJA)

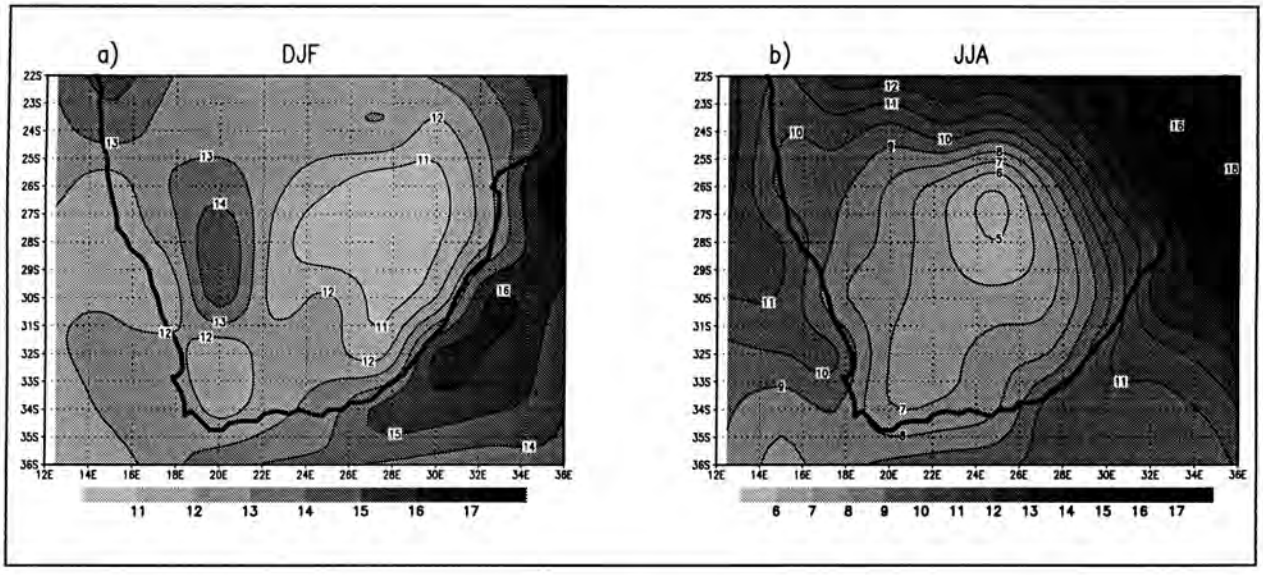

Figure 31: GSFC observed mean surface specific humidity ($g.kg^{-1}$) for a) summer (DJF) and b) winter (JJA)

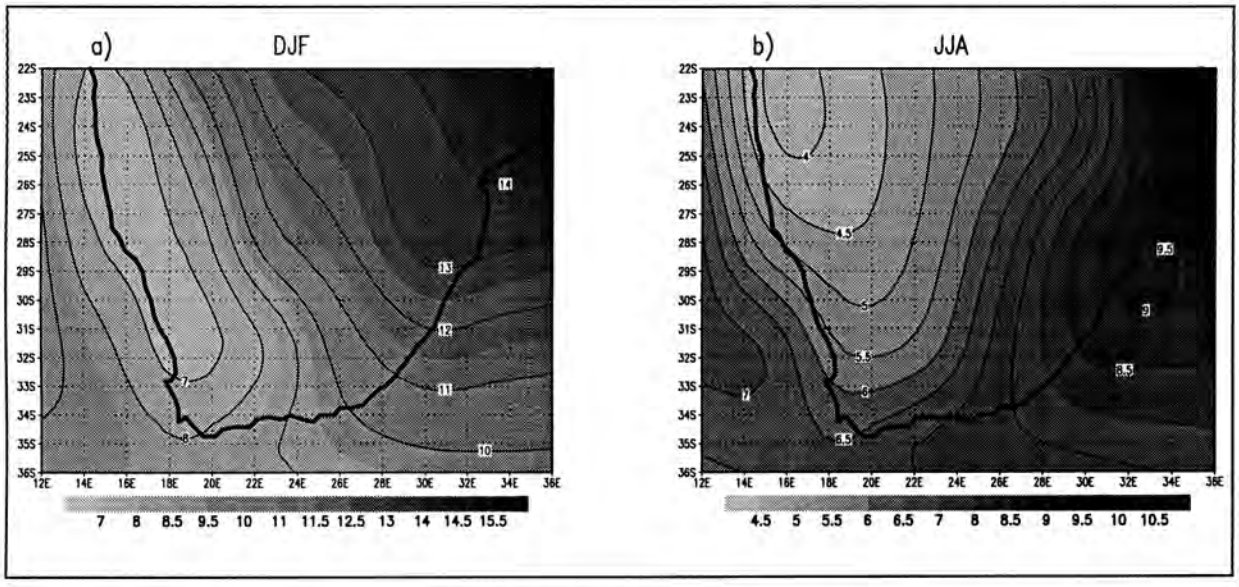

Figure 32: GENESIS 10 year AMIP run mean surface specific humidity ($g.kg^{-1}$) for a) summer (DJF) and b) winter (JJA)

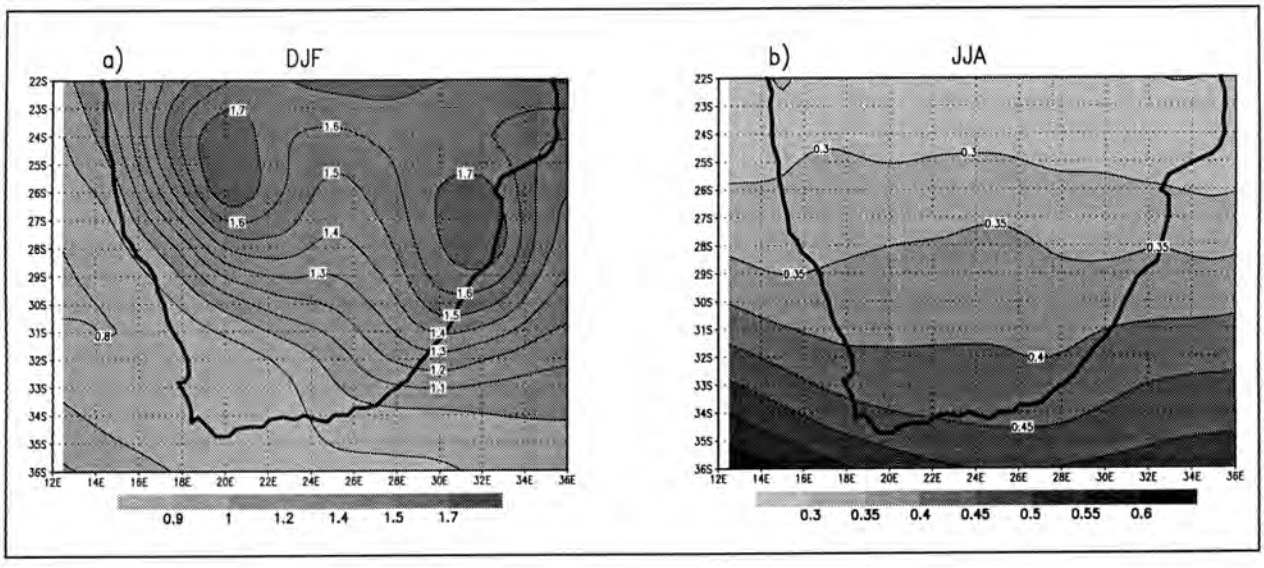

Figure 33: GSFC observed mean specific humidity ($g.kg^{-1}$) at the 500 hPa level for a) summer (DJF) and b) winter (JJA)

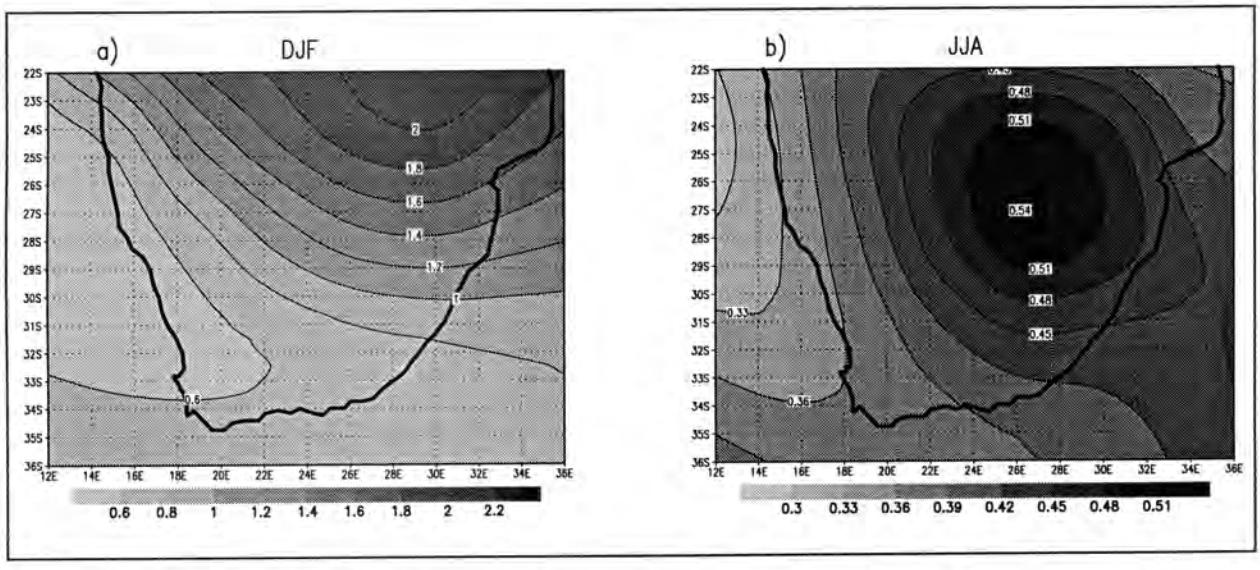

Figure 34: GENESIS 10 year AMIP run mean specific humidity ($g.kg^{-1}$) at the 500 hPa level for a) summer (DJF) and b) winter (JJA)

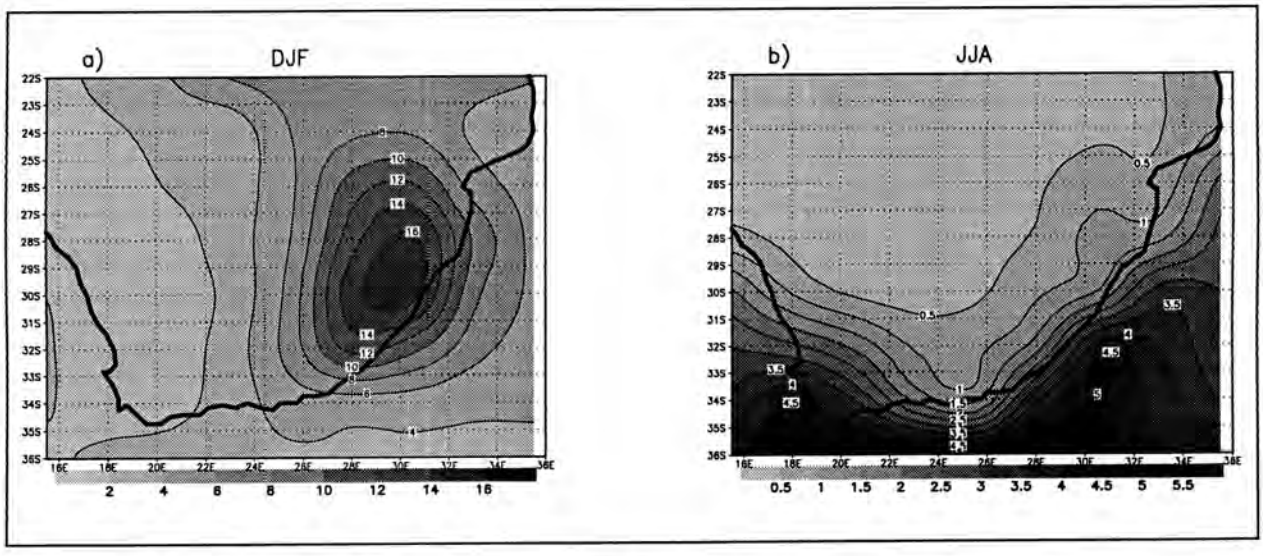

Figure 35: GSFC observed mean precipitation (cm/month) for a) summer (DJF) and b) winter (JJA)

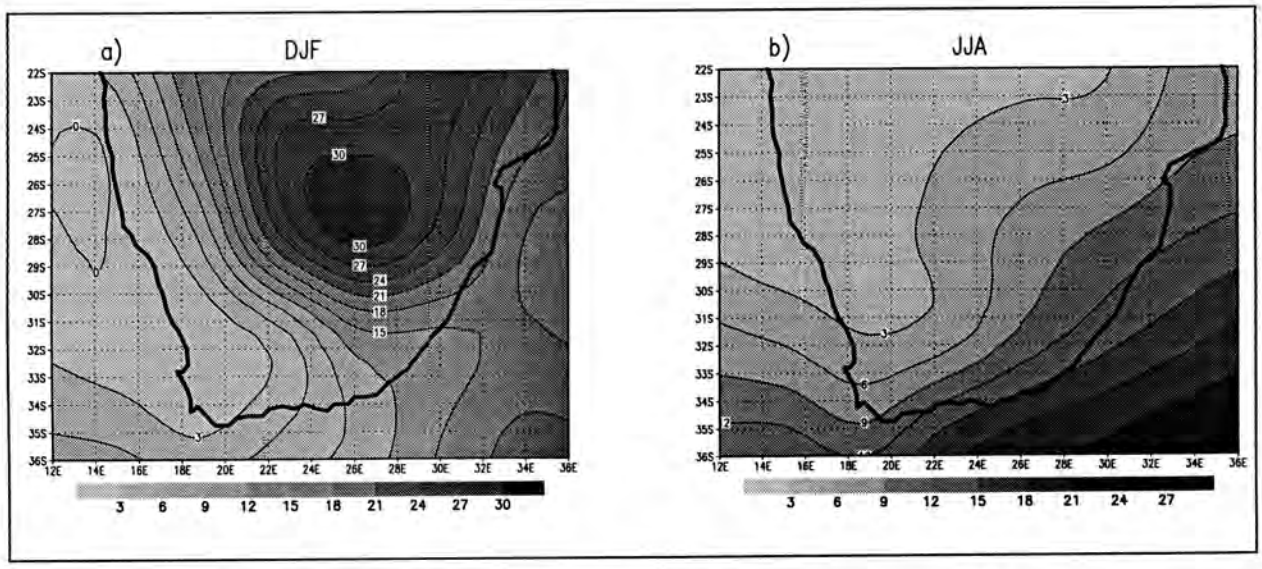

Figure 36: GENESIS 10 year AMIP run mean precipitation (cm/month) for a) summer (DJF) and b) winter (JJA)

CHAPTER 5

GENESIS GCM PERTURBATION RUNS

CHAPTER 5

GENESIS GCM PERTURBATION RUNS

The changes in vegetation as a result of CO_2 forcing, detailed in chapter 3, are now examined within the context of atmospheric sensitivity. This sensitivity to vegetation will be examined in terms of a number of variables (see table 4). These variables were selected as they are representative of both surface and upper level atmospheric features relevant to regional climates. Furthermore, changes evident in these variables as a result of the $2xCO_2$ induced vegetation scenario are informative with regards to atmospheric dynamics and climate impacts.

- Sea level pressure
- Height of the 500 hPa pressure surface
- Precipitation (stratiform and convective)
- Temperature (surface and 500 hPa levels)
- Specific humidity (surface and 500 hPa levels)
- U and V wind components
- Sensible and latent heat fluxes
- Horizontal divergence (1000 and 500 hPa levels)

Table 4: List of variables to be examined

In the sensitivity study, the year 1980 of the AMIP configured GENESIS GCM run was selected for implementation of the changes in vegetation induced by the CO_2 forcing. This year was selected as representative of some median state, and is notably not a strong El Niño year which would perhaps show a different atmospheric response

(and would nonetheless make a very interesting further study). A one-year simulation was deemed sufficient for the purposes of an initial investigation.

Three simulations of the same year were performed initially in order to ascertain whether the model responds to the internal stochastic precipitation parameterization. However, as it transpired, the random number generator in the model is initialised to the same value for identical run restarts, and hence the atmospheric fields produced by the 3 runs were identical.

When a run is restarted from a file, the initial conditions are truncated values of the full computer numerical resolution. Thus a restart would deviate with time compared to a run with no interruption in calculation. Therefore, as the 1980 perturbation run was generated from a restart file, an unchanged one year simulation of the 1980 AMIP configured run was also re-initiated in order to be consistent. The change from the original 1980 AMIP run to the restarted 1980 AMIP run was minimal, and an example of the similarity between the two is produced in figures 37 and 38.

The changes in the prescribed vegetation characteristics were incorporated into GENESIS through LSX, and subsequent to the perturbation runs, the selected atmospheric variables (table 4) were extracted. Considering this study was primarily concerned with seasonal or monthly time scales in South Africa, the data were composited into monthly averages. Monthly values for daily variance were also calculated in order to gauge how daily variance may have changed as a consequence of vegetation induced CO_2 forcing.

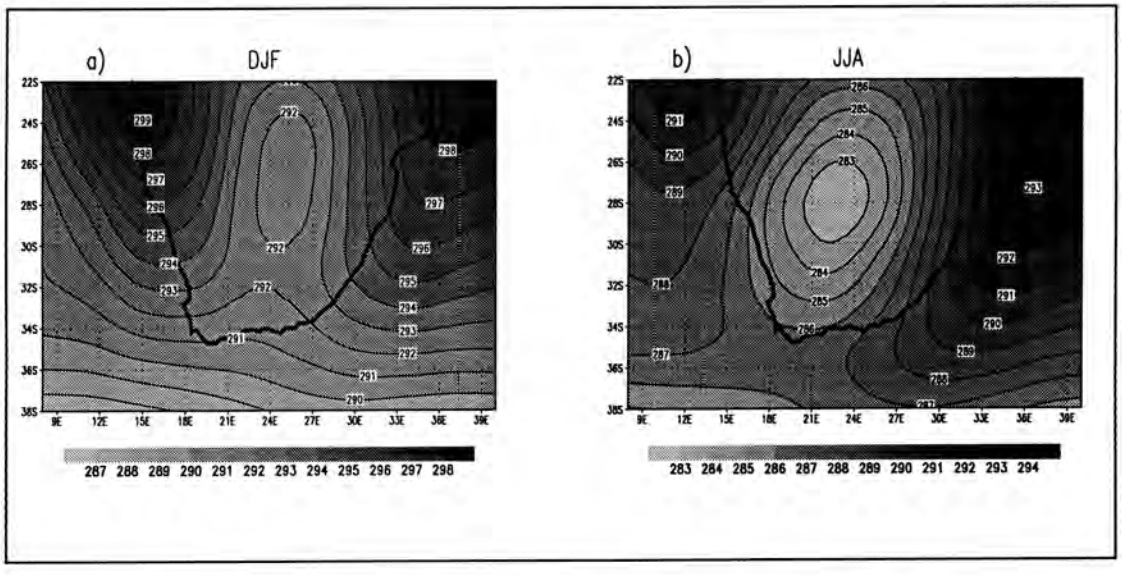

Figure 37: Original 1980 AMIP run temperature distribution (K) for a) summer (DJF) and b) winter (JJA)

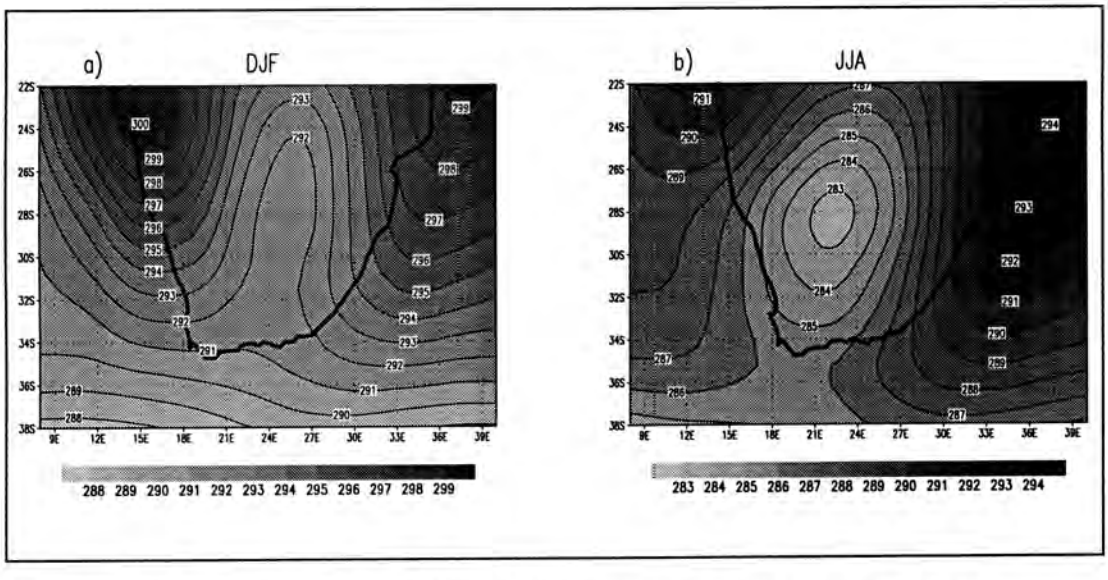

Figure 38: Restarted 1980 AMIP run temperature distribution (K) for a) summer (DJF) and b) winter (JJA)

5.1 Comparison of GENESIS AMIP run year 1980 with other years

Before analyses of the perturbation run are examined and discussed, it is necessary to compare briefly the AMIP year 1980 with other years of the AMIP run (i.e. 1979 and 1981-1988), thereby establishing how similar or different this year is with respect to other model years. This is achieved by comparing the means of a subset of the variables from table 4.

5.1.1 Sea level pressure

The AMIP 1980 simulation mean sea level pressure in January varies from approximately 1006 hPa in the NW to up to 1022 hPa in the SW. These variations are comparable to other years of the AMIP run in terms of the pattern. However, the intensity of the pressure maximum in the SW is not observed to the same extent in most model run years, except for 1983 (a strong El Niño year) and 1987. Nevertheless, most other years are only approximately 1 hPa lower over this region, except for 1985 where pressures are 1 - 3 hPa lower. Slightly higher pressures are observed over the east (near Durban) in 1979, 1983 and 1987. Other model years are more comparable to 1980 in the east.

In July, the pressure pattern is similar in all years and the 1980 run showed pressures varying from about 1017 hPa to 1029 hPa in the north and NE. This is comparable to other model years, which range typically between 1-2 hPa of this. In contrast, 1982 and 1983 display substantially lower pressures, which may be related to the fact that these two years showed strong El Niño signals.

5.1.2 Height of the 500 hPa surface

In the 1980 AMIP run year, mean heights of the 500 hPa surface vary from approximately 5580 gpm in the south to 5880 gpm in the north during summer. The pattern is similar in other years, but there is some variation in the heights of the 500 hPa surface between years. 1982, for example, has lower gpm values in the SE and higher gpm values in the north. Higher values in the north are also evident in 1987, but lower values are noticeable in the same region during 1979. The years 1985 and 1986 seem most similar to 1980.

The winter situation during 1980 shows a mean height range of the 500 hPa surface from 5550 gpm in the south to 5850 gpm in the north. The pattern in all years is again comparable, but 1980 seems to be capturing higher gpm values over the south. This is particularly the case with regard to the El Niño years of 1982 and 1983. In the north, values are similar for all years, but again 1980 seems to have slightly higher gpm values than most model years.

5.1.3 Surface temperature

Mean surface temperature during January 1980 ranges from approximately 285K to 302K, with two regions of temperature maximums in the NW and NE, and cooler temperatures extending southwards. This pattern is evident throughout the 10 year AMIP run. However, 1982 is warmer (about 0.5K - 1K) in the NW, and 1979 and 1984 cooler. 1986 and 1987 are warmer over the north, yet 1981 and 1983 are comparable.

July 1980 displays a similar temperature pattern to January, but temperatures are lower and range from 281K to 295K. The temperatures over the interior in 1980 do appear slightly warmer (up to 1K) than in some years (e.g. 1982, 1985 and 1987).

5.1.4 Surface specific humidity

Mean surface specific humidity for 1980 ranges from 5 $g.kg^{-1}$ to 16 $g.kg^{-1}$ in summer and from 3 $g.kg^{-1}$ to 12 $g.kg^{-1}$ in winter; values increase from the west to the NE. 1985 and 1987 are similar to 1980 in terms of the ranges in both seasons. In contrast, 1982 and 1983 display lower specific humidity values in the NE during January and over the west and NW during July. There is also a degree of variability of specific humidity over the west coast in summer, and 1980 falls somewhere in between this range.

5.1.5 Summary

In general 1980 appears to be a fairly average year, not exhibiting either a strong El Niño or La Niña signal. The years 1982 and 1983 appear to be the most different from the rest, which one would have anticipated, considering that these two years straddle an intense El Niño event. There are differences between 1980 and other years, but

these variations are not extensive or large in magnitude and this year is therefore a suitable one on which to perform anomaly runs.

5.2 The atmospheric sensitivity to vegetation changes

The first step in gaining an understanding of the atmospheric response to vegetation is to consider fairly simple mean and variance changes in various atmospheric variables such as precipitation, temperature, pressure and specific humidity. This, coupled with an examination of wind vector anomalies, divergence fields, and moisture and heat fluxes should enable an understanding of the first order impact by the vegetation. It should be noted that the changes identified here are based only on one year, and thus are not necessarily representative of the magnitude of the long term response.

Mean precipitation (convective and stratiform combined) for 1980 of the AMIP run and the perturbation anomaly (perturbation run - 1980 AMIP run) are displayed on figures 39 and 40. It is clear from the figures that in summer mean precipitation is at a maximum over the eastern half of the sub-continent, and the anomaly map shows a decrease in precipitation (approximately 10%) over the southern portion of this region. Winter precipitation anomalies are observed in the all year round and summer rainfall regimes, where there is a decrease of up to 30%. Winter rainfall over the Western Cape has likewise decreased, but by less (approximately 15%).

The observed temporal trend (H. Mulenga, pers. comm.) of summer precipitation over the last century (1905-1989) is displayed on figure 41, and an analysis of this observed temporal trend in conjunction with the AMIP and perturbation runs makes for an interesting comparison. It is evident from figure 41 that the observed trend in for a decrease in precipitation through the last century in two primary regions, namely, the NW and east. This trend of decreasing precipitation may be linked to the long term trend of desertification, noted by Acocks (1953), over large parts of the country.

It is apparent that the observed trend of decreasing precipitation in the SE is evident on the anomaly map, and this is therefore comparable with the observed trend over the

last century. However, the decreasing precipitation trend is not reflected in the NW on the anomaly map, which displays a precipitation increase in this region.

Observed standard deviation in summer rainfall from 1950-1989 is displayed on figure 42, and it is informative to compare this with the variance of precipitation in the GENESIS 1980 AMIP run and the perturbation anomaly. In the observed standard deviation of summer precipitation, two regions of high standard deviation (and therefore high variance) are distinguished -- in the SE and NW. In the AMIP run, the region of high summer variance of precipitation is evident over the SE, but not over the NW (see figure 43). The anomaly map of precipitation variance shows a variance decrease in the SE and central regions. The decrease in variance is therefore not supportive of the observed trend of increasing variance over time, which has been continuous over the last 40 years.

These differences could perhaps be explained by the fact that the anomaly maps are showing a response to the vegetation component of a possible climate change only and not to climate change *per se*. Furthermore, the observed trends and variance changes through the century may not necessarily be projected into a future climate.

Temperature changes are evident over the NW, where a decrease in mean temperatures is seen in both summer (0.6 - 1K) and winter (0.8 - 1K) (see figures 44 and 45). This could be related in part to the reduction in savanna and an increase in dry or desert classes. Dry or desert vegetation will have a higher albedo and therefore could account for surface temperatures being lower. There are also temperature increases (up to 0.4 K) in summer, but these are confined to the eastern regions. Temperature changes at the 500 hPa level are not significant.

An increase in surface specific humidity in summer in the NW is also apparent (figure 46 a) and 47 a)). The change is approximately 1.4 $g.kg^{-1}$ in this region and is quite significant considering the region only has typical values of 6-7 $g.kg^{-1}$. The effect in winter is negligible, despite an anomaly (0.7 $g.kg^{-1}$ decrease in a region with a typical

range of 8-9 $g.kg^{-1}$) in the east (figure 46 b) and 47 b)). This increase is likely to be linked partially to the increase in precipitation.

In addition to the mean surface specific humidity changes, there is furthermore a change in the surface specific humidity variance and an approximate 25% increase in variance in the NW and central eastern regions during summer (see figure 48 a) and 49 a)). The winter situation in the anomaly displays an increase in variance (up to 25%) as well, but the increase is confined more to the eastern region (figure 48 b) and 49 b)). The implication of these variance changes is a modification in conditions with more variation about the mean specific humidity than in 1980 of the AMIP run.

At the 500 hPa level, mean specific humidity changes in summer (figure 50 and 51) evident in the north (particularly the NE), where there is an increase of up to 10%. In winter, however, the mean over the summer rainfall area in the NE has decreased by about 25% in parts, as evidenced by figure 50 a) and 51 a), and indicates a decrease in the absolute amount of water in the atmosphere at this level. This is likely to be related in part to the changes in large scale circulation, such as changes in pressure and moisture fluxes. There is, in addition, more variability about the mean in winter (see figure 52).

There is a decrease by up to 9 gpm in the height of the 500 hPa pressure surface in the NE in winter (figure 54). In summer over the north (figure 53), there is a smaller increase of 4 gpm. Variance in winter is displayed on figure 55, and shows an increase by up to 25% in the SE and a decrease of approximately 20% in the NE. Sea level pressure changes are not large, but there is an increase in pressure over the interior in both summer and winter (figure 56 and 57). Thus, the implication is for a strengthening of the semi-permanent surface high pressure over the interior region and a weakening of the low pressure over the NW in both seasons.

The most useful means to use to explain and understand the changes as a result of vegetation changes is perhaps to examine how the wind and associated moisture and heat fluxes have changed, and how the patterns of horizontal divergence have altered.

Mean surface wind fluxes observed at the 1000 hPa level in summer show the general ESE winds (surface phenomena) over the east quite clearly (figure 58 a)) and it is interesting to note the changes in the anomaly (figure 59 a)), where winds have obtained a more southerly component. Over the southern regions, there is a shift of SW to westerly winds. Magnitudes of winds in summer have also changed and are lower over the Indian Ocean near Durban.

The winter situation shows an increase in the northerly component of the winds in the central interior (NW to WNW). Wind speeds have increased significantly over the SE Indian Ocean and extreme NE (figure 58 b) and 59 b)). These wind magnitude changes near the surface level may possibly be related to a decrease in surface friction (through a general increased aridity) and more notably the changes in the meridional temperature and pressure gradients (a strengthening of the high pressure and weakening of the low pressure over the interior in both seasons) observed.

Figures 60 and 61 display the mean 500 hPa level wind fields for summer and winter for the observed and anomaly. It is evident from these figures that there is a shift from winds with a more westerly component to winds with a more easterly component. This, coupled with what was observed at the 1000 hPa level, is indicative of a strengthening and southwards extension of the Hadley Cell, resulting in a southwards displacement of the westerly wind belt. The southwards extension of the Hadley Cell is an anticipated effect of global climate change and it is interesting to observe that vegetation changes are in support of this alteration as well. This could have implications for southern Africa, especially the winter rainfall regions with their associated frontal rainfall. These changes are in fact already noted in terms of precipitation decreases in the anomaly map over the Western Cape in winter as a function of the Hadley Cell changes. Wind direction magnitude changes in winter are more pronounced than in summer where changes are reasonably insignificant. The greatest change in magnitude of wind direction is apparent in the NW.

Observed and anomaly horizontal divergence fields for the 1000 hPa level are displayed on figures 62 and 63 respectively. It can be seen from the observed map,

that in summer there is predominantly surface convergence (important for convective rainfall) over the interior, and two small regions of divergence over the extreme SW and SE. In the anomaly map for summer, there is less convergence over the interior region, more convergence over the Indian Ocean east of Durban, more divergence in the SE and less divergence over the extreme SW. Thus, it appears that the surface convergence (and therefore positive vertical motion) required for uplift of moisture over the interior has reduced, and therefore the divergence fields support the observed decrease in precipitation over the majority of the summer rainfall region.

In winter, the observed pattern is one of surface divergence at the 1000 hPa level over most of the analysis window, except for a small region over the south and extreme NE. In the anomaly map, there appears to be an increase in divergence at this level over most of the region, but a decrease in divergence (i.e. a decreased tendency for positive vertical motion) over the NE. These observations are in support of the observed precipitation fields, since precipitation over much of the area has reduced, except over the NE, where the anomaly showed an increase in the tendency for vertical uplift necessary for the convective rainfall increase observed.

Horizontal divergence fields at the 500 hPa level for the observed and anomaly maps, are displayed on figures 64 and 65. In the observed, there is divergence over most of the region in summer, but with convergence over the SW. The winter pattern is also one of divergence, but with convergence over the central southern region extending northwards. The observed patterns are in support of the 1000 hPa level patterns, since upper level regions of divergence are above regions of horizontal convergence at the 1000 hPa level.

The anomaly maps indicate less divergence over the interior in summer, which, coupled with less convergence at the 1000 hPa level, reinforces the trend of less precipitation over much of the sub-continent during this season. In winter, there is less divergence (i.e. a tendency towards convergence) over the eastern interior, which is in agreement with the increased 1000 hPa level divergence. There is additionally

increased divergence over the Western Cape, which is again in agreement with surface increased divergence.

Latent heat fluxes can be implied by examining U and V wind vector components with an incorporation of specific humidity (i.e. Uq and Vq). At the near surface level (1000 hPa level), there is a decrease in the latent heat fluxes in summer (see figure 66 a) and 67 a)) over the SE Indian Ocean, implying that there is a decrease in moisture feeding in over the interior from this region. This could therefore further explain the decrease in precipitation over the adjacent land area, since less moisture is feeding in and therefore available for uplift.

In winter there is a decrease in near surface latent heat fluxes in the SW (contributing to the decrease in precipitation over the Western Cape). There is additionally an increase in the extreme NE (see figure 66 b) and 67 b)), related to the precipitation increase in this region. In the NW there is an increase in specific humidity at the surface level in summer, which is prevented from convective uplift allowing for redistribution at a higher level, through the intensification of the high pressure system at the 500 hPa level. Therefore, the 500 hPa level indicates less moisture coming in over the NW in summer, and more moisture is feeding out over the SE Indian Ocean (figure 68 a) and 69 a)). Thus, moisture available for convective uplift and rainfall over the interior has reduced. During winter there is a decrease in moisture availability over the entire region and this explains the decrease in precipitation at the surface over most of the sub-continent (figure 68 b) and 69 b)).

Sensible heat fluxes can be considered through examining U and V wind components in conjunction with temperature (i.e. Ut and Vt). Unfortunately sensible heat fluxes at the 1000 hPa level could not be assessed, because of the interpolation to below ground level. However, analysis at the 500 hPa level reveals some atmospheric signals which are shown on figures 70 and 71. Mean sensible heat fluxes in summer and winter at the 500 hPa level show a decrease over the north and an increase over the south. Thus, there are flux gains over the ocean, and a loss of heat over the interior (particularly the northern interior) at this level. This could therefore serve to explain the magnitude of

increases observed in mean temperatures at the surface over most of the interior, since strong vertical redistribution of heat does not seem to be apparent.

5.2.1 Summary and synthesis

As highlighted in chapter 3, there is a trend of westwards and upwards movement of lowland vegetation and eastwards and southwards movement of more dryland vegetation. Thus, the response of the former appears to be primarily to temperature changes and the latter to precipitation changes. The effect of these vegetation changes is complex and some signals of the effect of the changes on the atmosphere have been witnessed in the GENESIS GCM perturbation. One would anticipate a number of feedbacks into the climate system with a complex set of interactions between vegetation and the atmosphere. Not all of these changes could be interpreted directly, but some these have been fairly clearly understood. Furthermore, there are a host of variables and combinations of variables which could have been examined in terms of atmospheric sensitivity to surface changes, but a detailed examination of all of these changes is beyond the scope of the present study.

It should be noted that it is not only the spatially co-located vegetation changes that affect the atmosphere, but also changes in other regions. What has been related in this section (5.2) has been concerned with co-located vegetation primarily and therefore the implied broader impacts on atmospheric processes need to be further investigated. It is likely that in some regions where the changes in the atmosphere cannot be explained successfully by the localised vegetation changes, the response is most likely as a result of vegetation changes in other regions as well as other atmospheric changes in the climate system, since moisture and heat fluxes allow for redistribution.

The response to vegetation perturbations as a result of CO_2 forcing is most apparent in convective rainfall regions. Changes in the eastern half of the sub-continent, particularly the SE, were most pronounced during summer. Precipitation decreases as well as minor decreases in specific humidity were evident and are linked to the decrease in near surface (1000 hPa level) convergence and decreases in latent heat fluxes feeding in over the interior from the Indian Ocean. Thus, with less moisture

feeding in over the interior from the Indian Ocean, the available moisture for uplift is reduced. Furthermore, the decreased surface convergence and increased surface pressure inhibits vertical moisture fluxes between the surface and upper levels. Thus, moisture gain at higher levels is restricted and this impacts on precipitation amount at the surface.

Over the eastern regions (particularly the SE) during winter, there is a decrease in precipitation and a decrease in surface specific humidity, which is probably associated with the increase in the intensity of the surface high pressure.

Changes in the NW of the study domain are different from those in the eastern half of the country, but are again most pronounced during summer. Precipitation during summer in this region has increased and this compares favourably with the noticeable increase in specific humidity at the 500 hPa level. The weakening of the surface low over this region has allowed for a potential moisture gain at higher levels.

The changes described are most likely the impact of a number of atmospheric processes operating on a broader scale. The Hadley Cell extension evident from the wind field changes appears to be exerting a major influence and is affecting subsidence and vertical dynamics implied by the horizontal divergence fields at the near surface and upper levels. A general increase in surface pressure and a strengthening of the semi-permanent high over the interior relates well with the southwards extension of the Hadley Cell. The increased surface divergence in winter, and decreased convergence in summer is also linked to the Hadley Cell extension coupled with the associated increased sea level pressure.

Wind magnitude anomalies are exerting a broad influence on horizontal convergence and divergence patterns. At the near surface (1000 hPa) level in summer, the anomaly shows lower wind speeds over the Indian Ocean east of Durban. This therefore aids in explaining the increased convergence over this region. Near surface wind magnitude anomalies in winter indicate an increase in wind speed and this relates favourably with the increased divergence evident. The relationship between wind magnitudes and

convergence and divergence is not quite so marked over the interior, since the changes in wind speed are not as pronounced.

Midlatitude processes are also linked to the Hadley Cell extension and have exerted their influence further southwards. This could therefore explain the decrease in winter precipitation and latent heat fluxes over the Western Cape. The inference that a southwards shift of midlatitude processes is associated with a decrease in winter precipitation can be explained by the fact that with a southwards shift of the westerlies, fewer cold fronts are passing over the southern regions of the country.

Thus, while it is not only co-located vegetation which is having an impact on the atmosphere, there is the influence of the overall vegetation perturbations on atmospheric dynamics and processes over the entire region. These processes, as it has been highlighted, are interlinked and interconnected. Therefore the processes need to be understood as a change in dynamics as a whole rather than changes in individual atmospheric variables within the climate system.

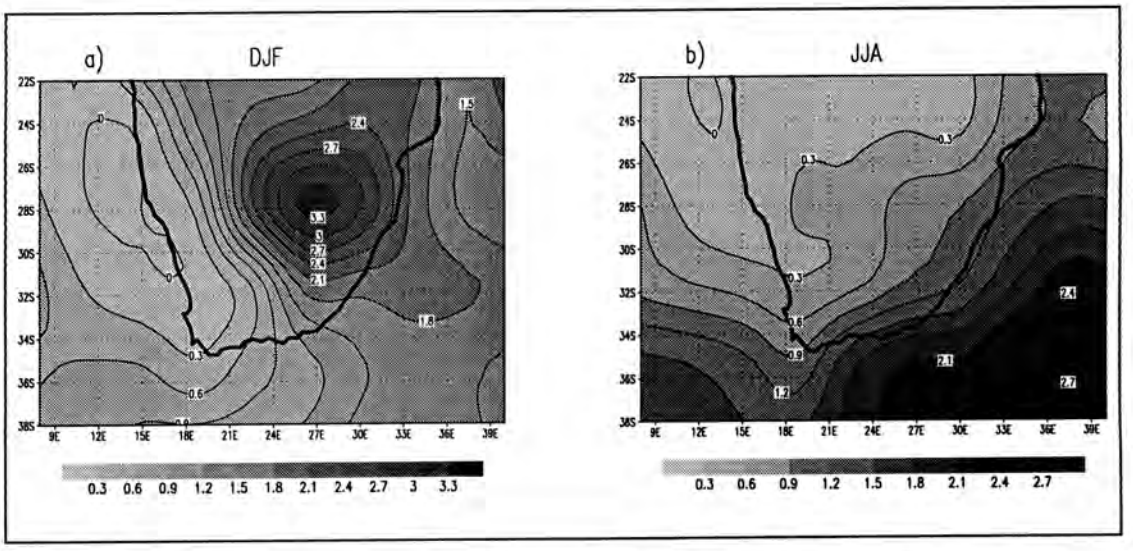

Figure 39: AMIP 1980 mean surface precipitation (mm/day) for a) summer (DJF) and b) winter (JJA)

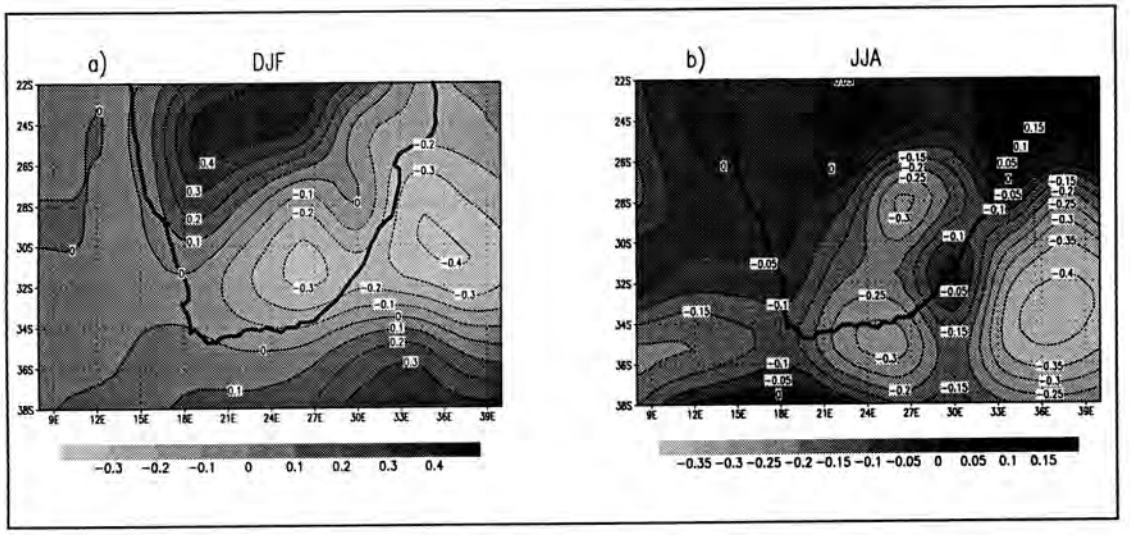

Figure 40: Mean surface precipitation anomaly (mm/day) (perturbation - 1980) for a) summer (DJF) and b) winter (JJA)

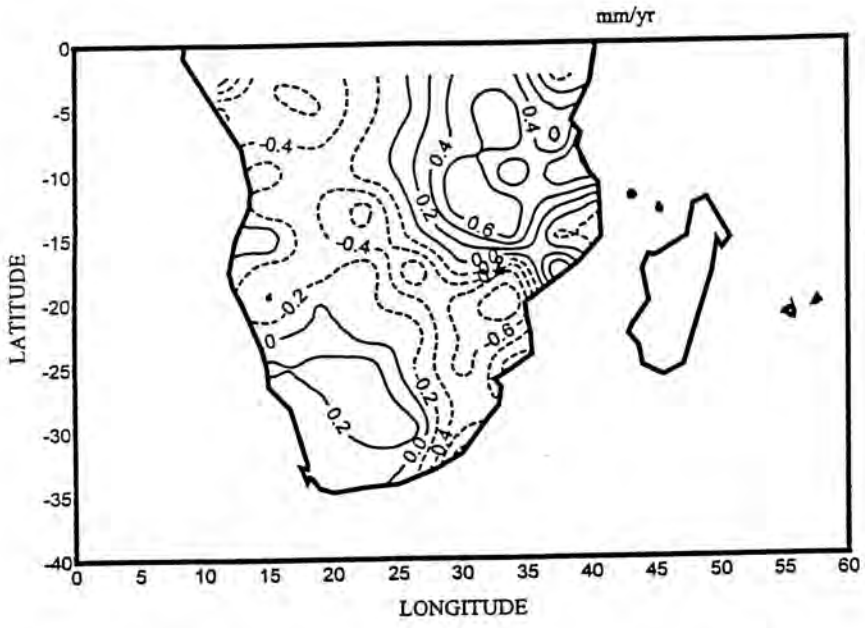

Figure 41: Observed summer (DJF) precipitation trend over southern Africa from 1905 - 1989 (H. Mulenga, pers. comm.)

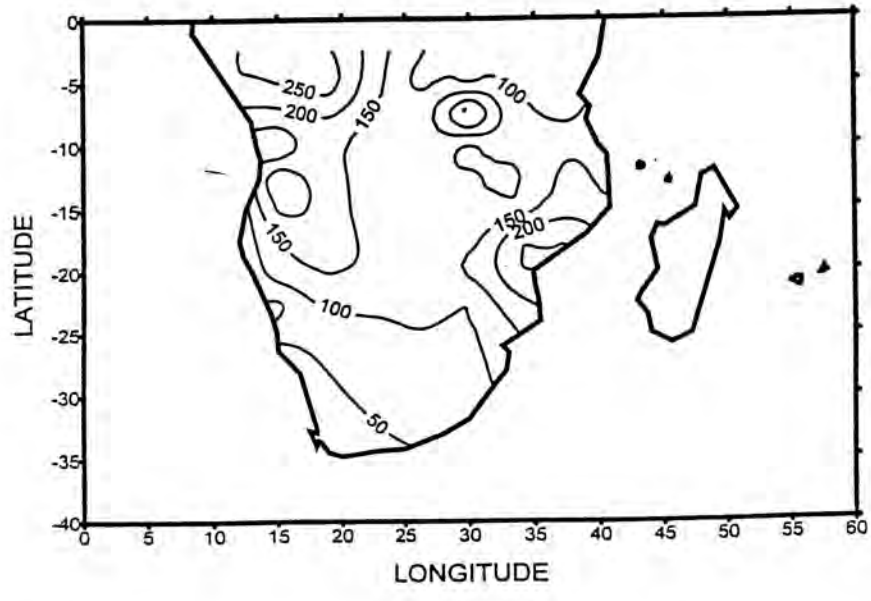

Figure 42: Standard deviation of summer (DJF) precipitation from 1950 - 1989 (H. Mulenga, pers. comm.)

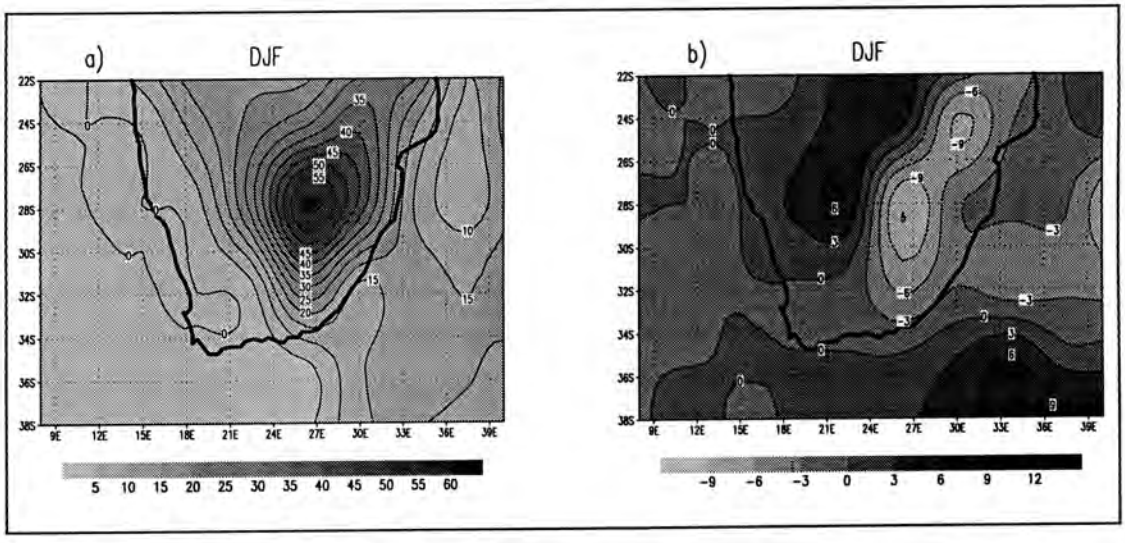

Figure 43: a) Mean variance of precipitation (mm/month)^2 for summer (DJF) and b) Mean variance of precipitation anomaly (mm/month)^2 (perturbation - 1980) for summer (DJF)

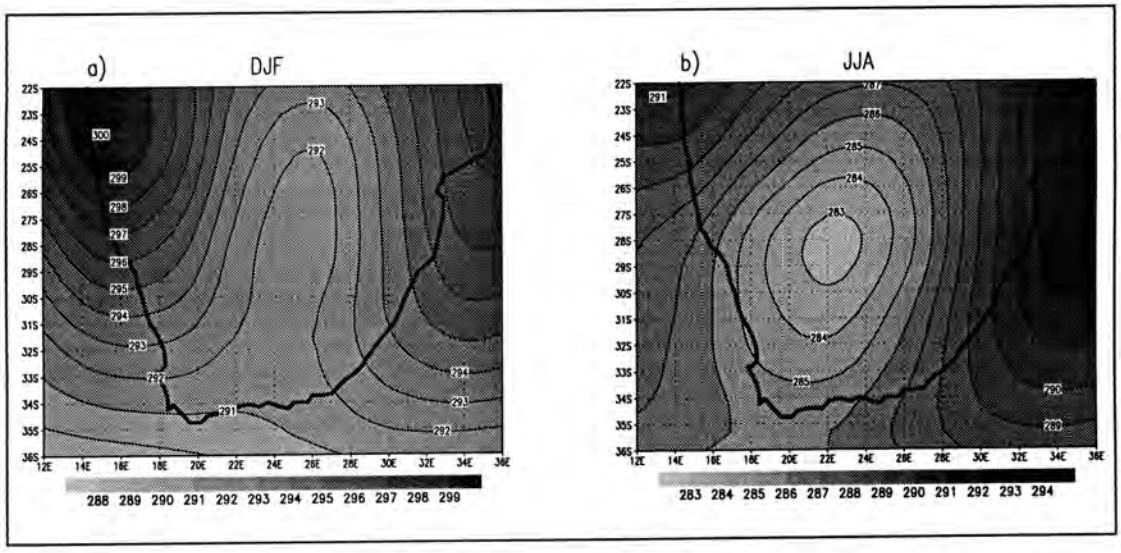

Figure 44: AMIP 1980 mean surface temperature (K) for a) summer (DJF) and b) winter (JJA)

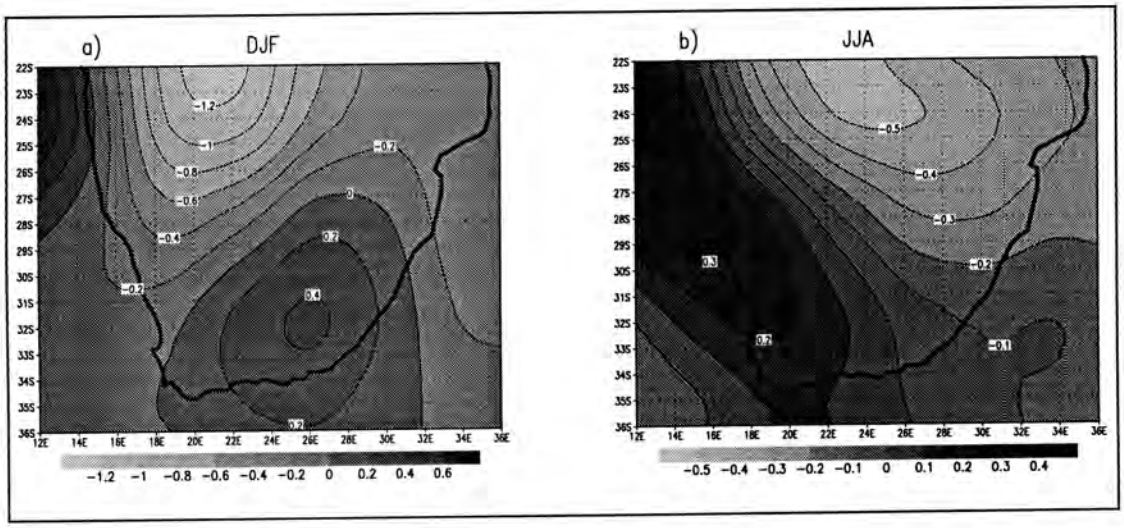

Figure 45: Mean surface temperature anomaly (K) (perturbation - 1980) for a) summer (DJF) and b) winter (JJA)

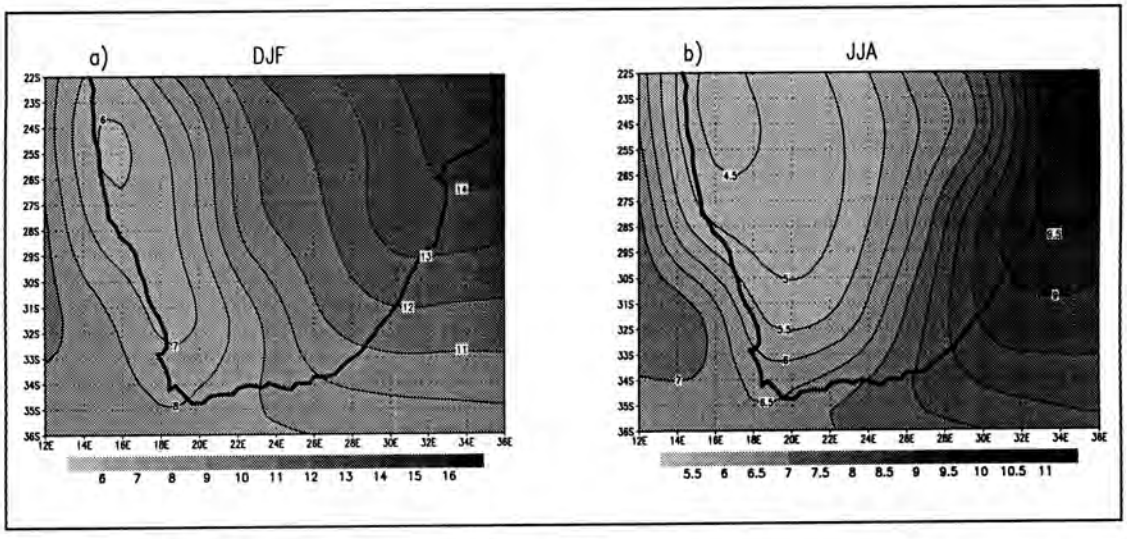

Figure 46: AMIP 1980 mean surface specific humidity ($g.kg^{-1}$) for a) summer (DJF) and b) winter (JJA)

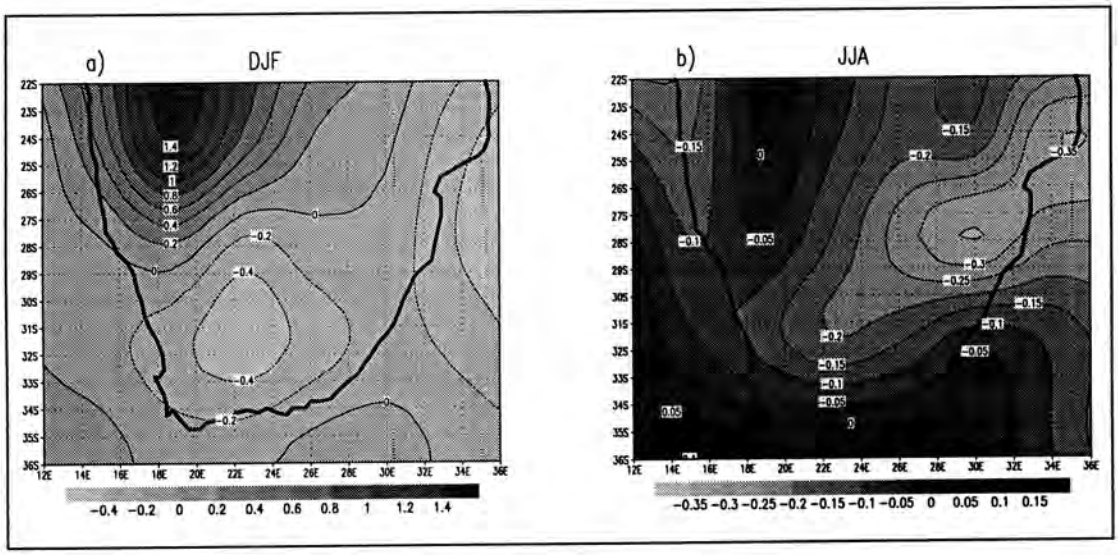

Figure 47: Mean surface specific humidity anomaly ($g.kg^{-1}$) (perturbation - 1980) for a) summer (DJF) and b) winter (JJA)

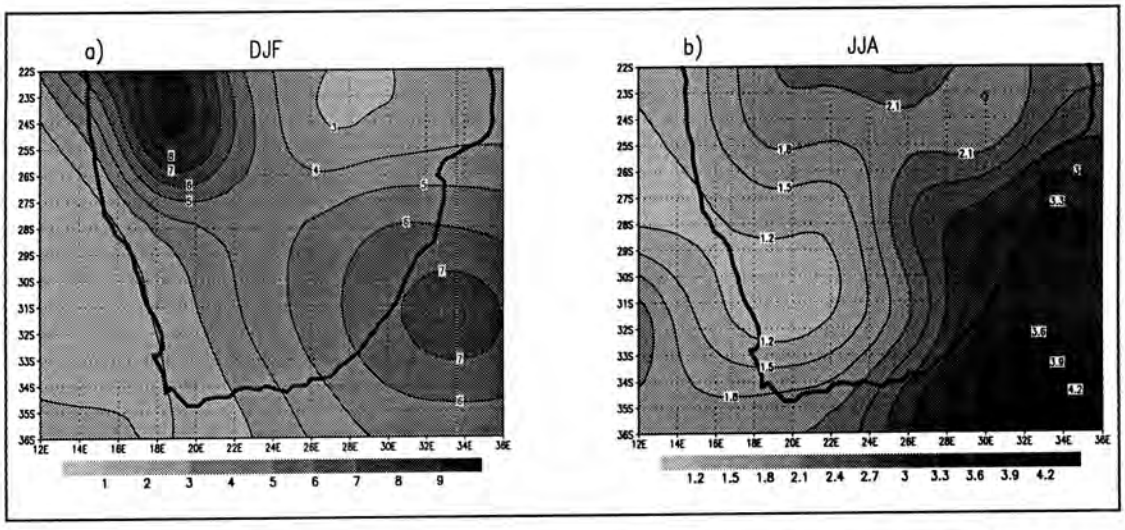

Figure 48: AMIP 1980 mean variance of surface specific humidity $(g.kg^{-1})^2$ for a) summer (DJF) and b) winter (JJA)

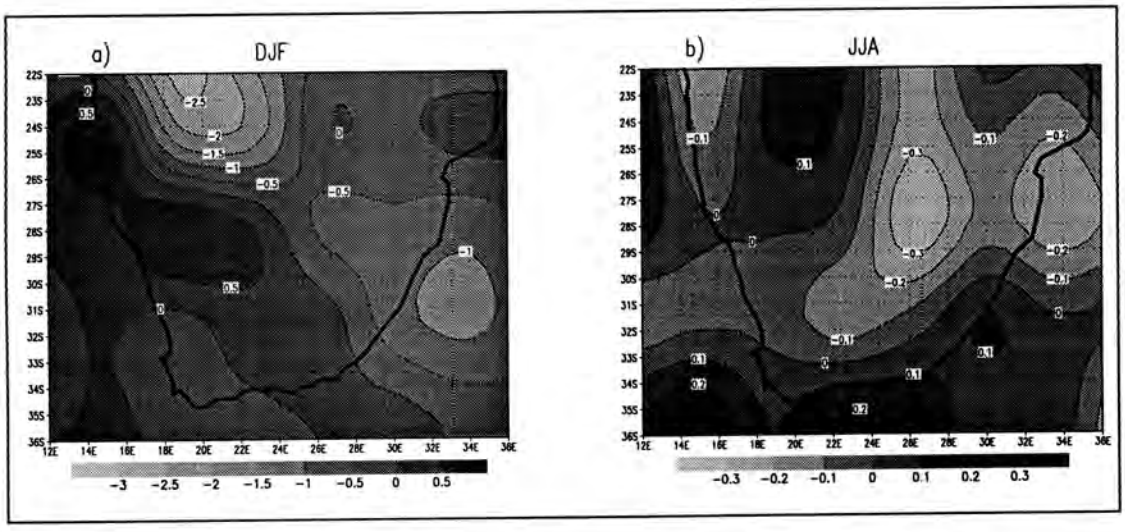

Figure 49: Mean variance of surface specific humidity anomaly $(g.kg^{-1})$ (perturbation - 1980) for a) summer (DJF) and b) winter (JJA)

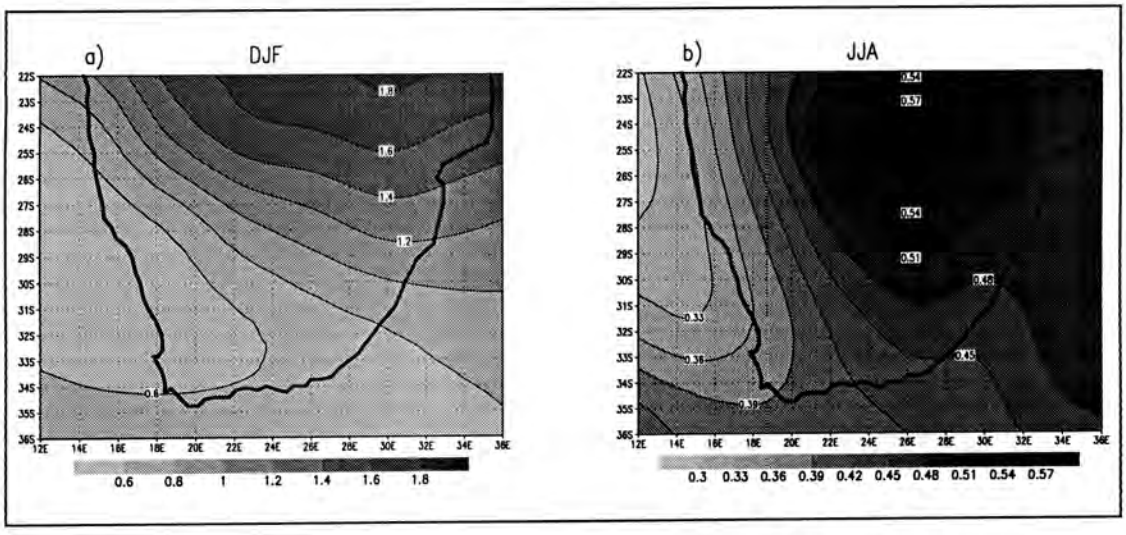

Figure 50: AMIP 1980 mean 500 hPa level specific humidity ($g.kg^{-1}$) for a) summer (DJF) and b) winter (JJA)

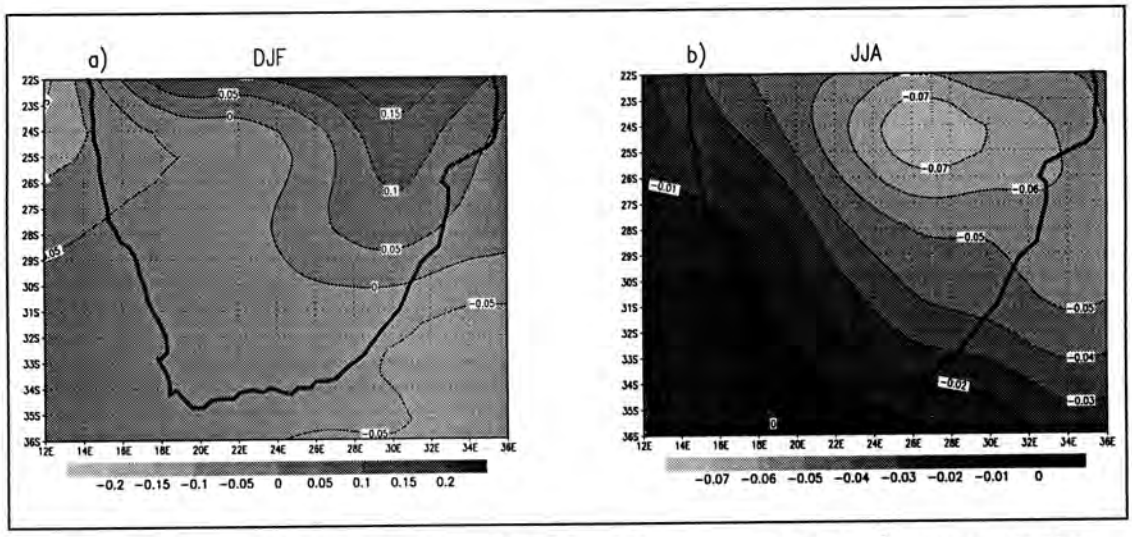

Figure 51: Mean 500 hPa level specific humidity anomaly ($g.kg^{-1}$) (perturbation - 1980) for a) summer (DJF) and b) winter (JJA)

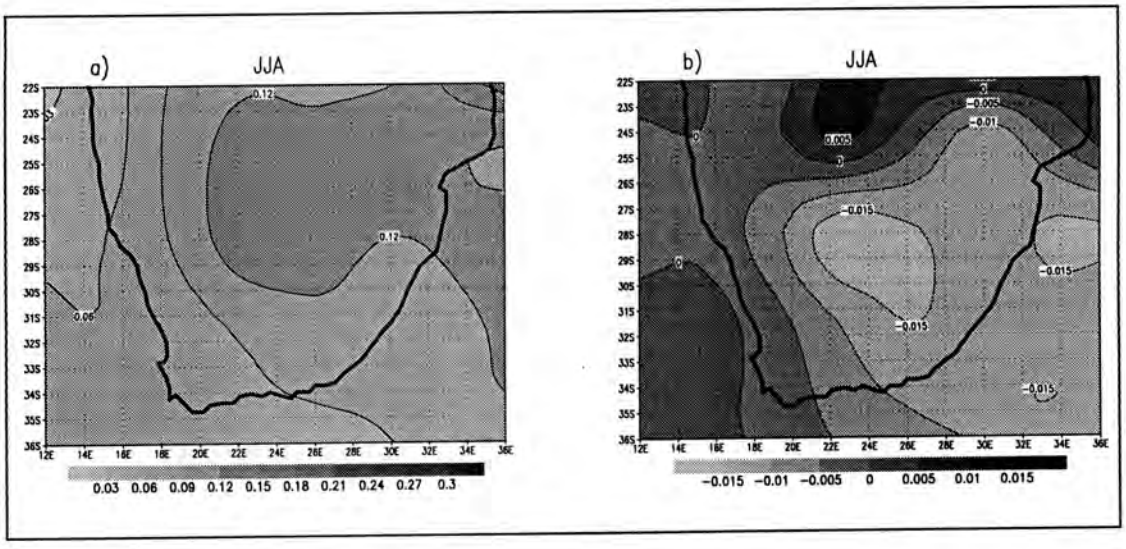

Figure 52: a) AMIP 1980 mean variance of the 500 hPa level specific humidity $(g.kg^{-1})^2$ for winter (JJA) and b) mean variance of specific humidity anomaly $(g.kg^{-1})^2$ (perturbation - 1980) at the 500 hPa level for winter (JJA)

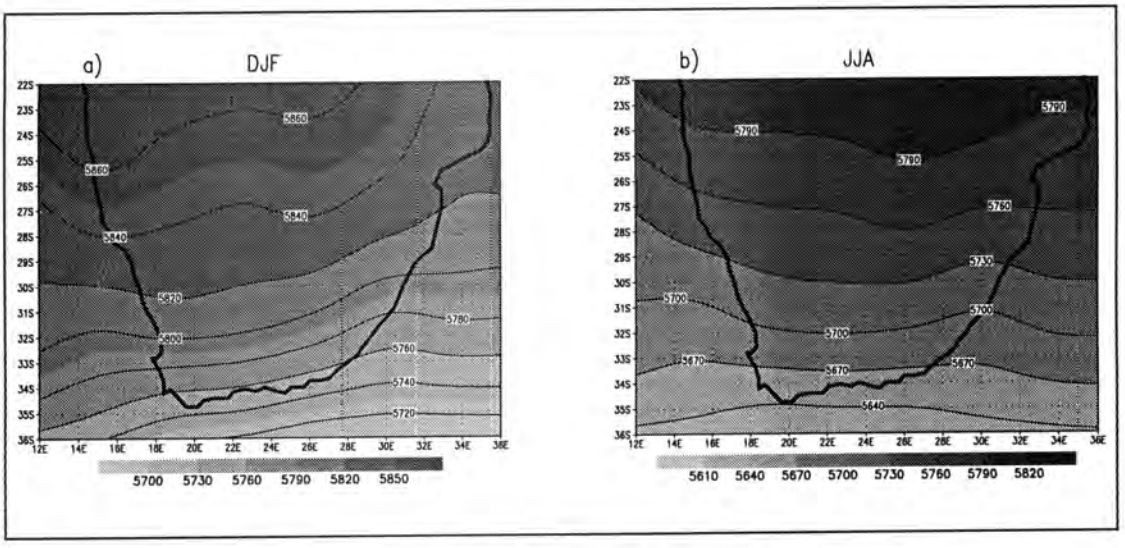

Figure 53: AMIP 1980 mean height of the 500 hPa surface (gpm) for a) summer (DJF) and b) winter (JJA)

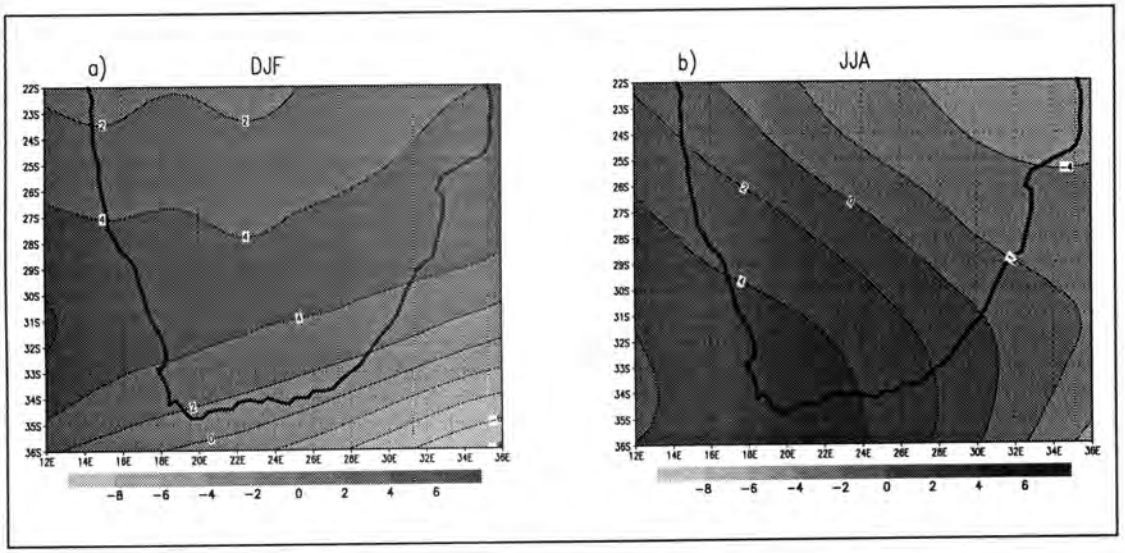

Figure 54: Mean height anomaly (perturbation - 1980) for the 500 hPa surface (gpm) for a) summer (DJF) and b) winter (JJA)

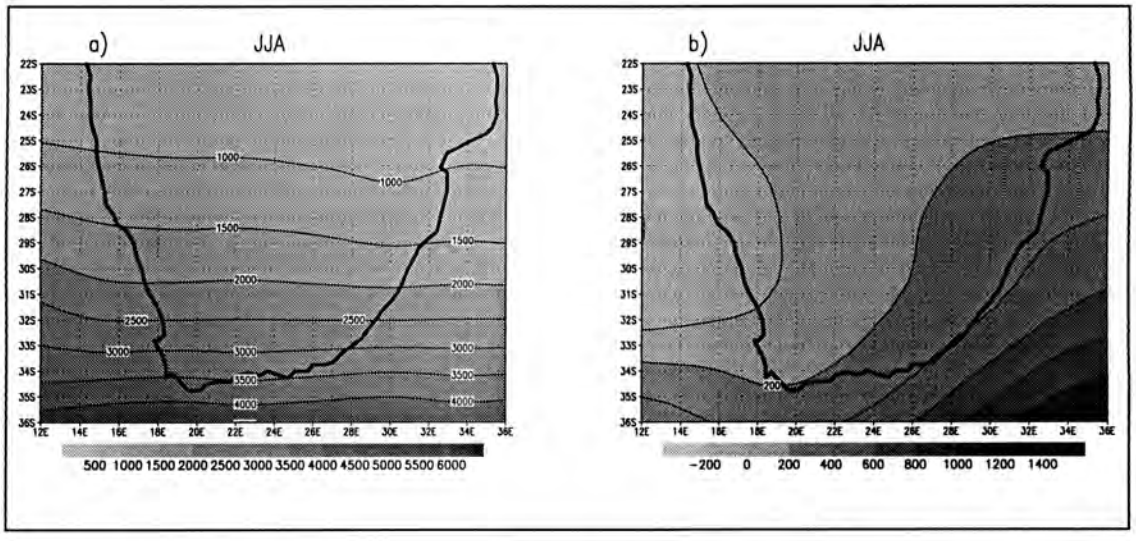

Figure 55: a) AMIP 1980 mean variance of the 500 hPa pressure surface (gpm)^2 in winter (JJA) and b) Mean variance of the anomaly (perturbation - 1980) for the 500 hPa pressure surface (gpm)^2 for winter (JJA)

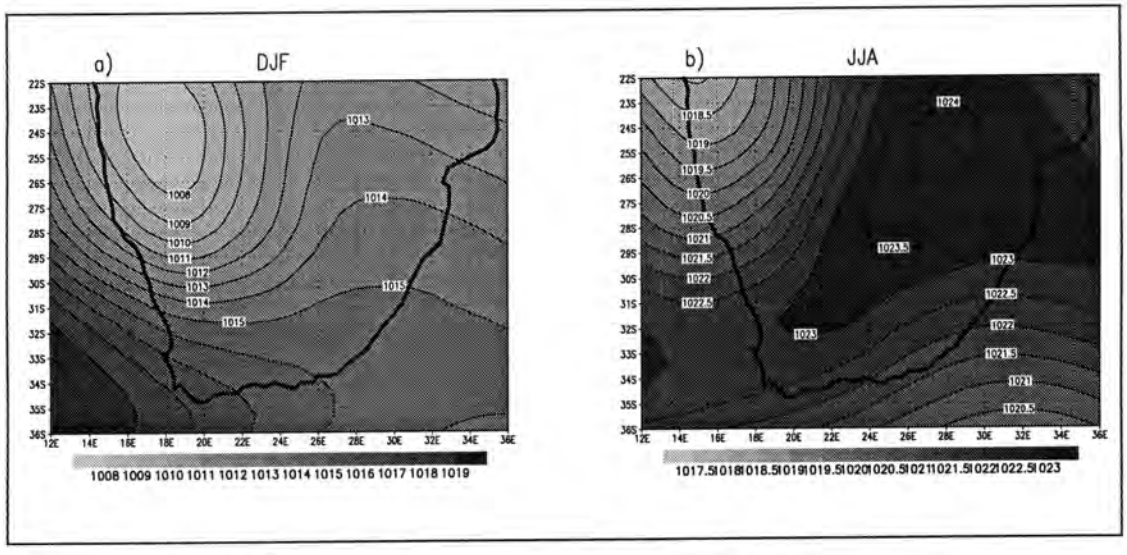

Figure 56: **AMIP 1980 mean sea level pressure (hPa) for a) summer (DJF) and b) winter (JJA)**

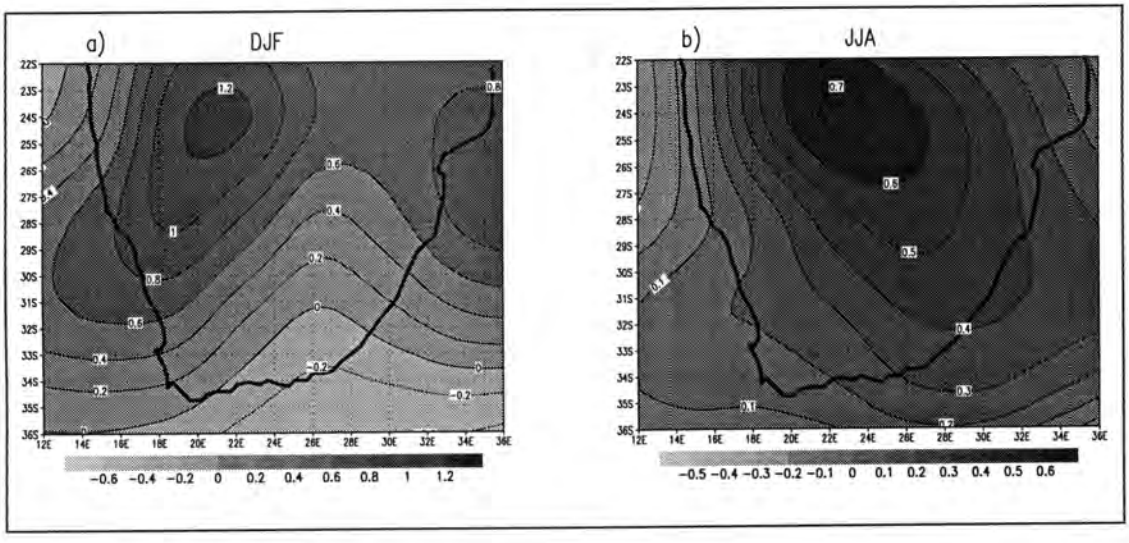

Figure 57: **Mean sea level pressure anomaly (hPa) (perturbation - 1980) for a) summer (DJF) and b) winter (JJA)**

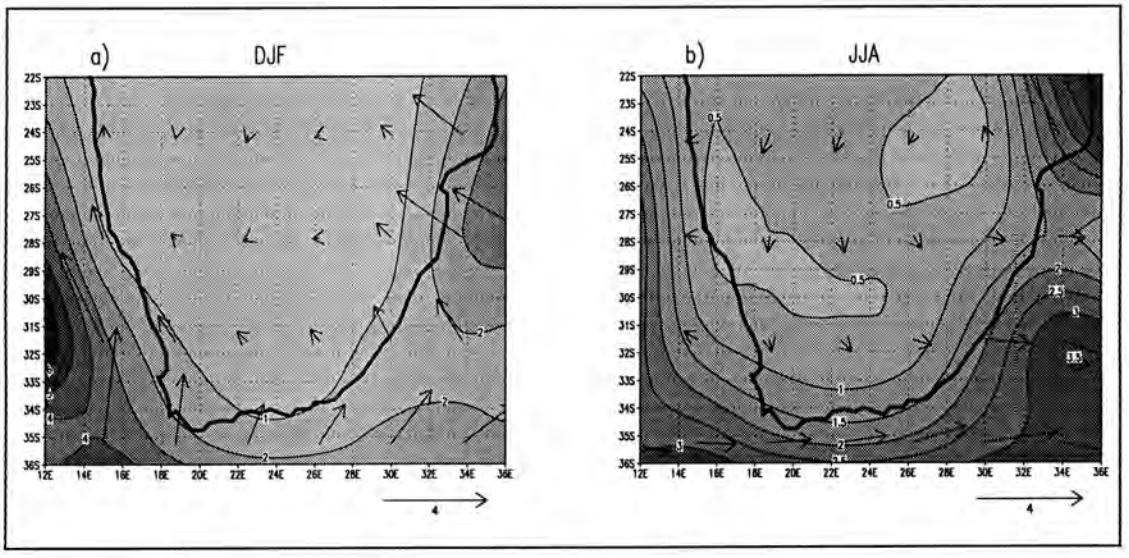

Figure 58: **AMIP 1980 mean wind direction and magnitude ($m.s^{-1}$) at the 1000 hPa level for a) summer (DJF) and b) winter (JJA)**

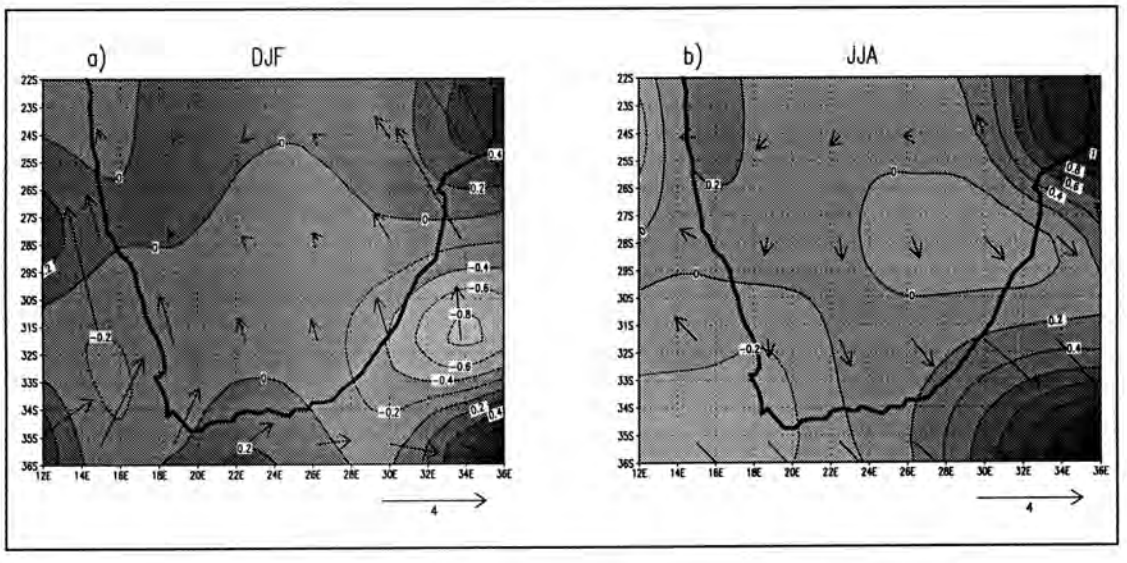

Figure 59: **Mean wind direction and magnitude anomaly ($m.s^{-1}$) (perturbation - 1980) at the 1000 hPa level for a) summer (DJF) and b) winter (JJA)**

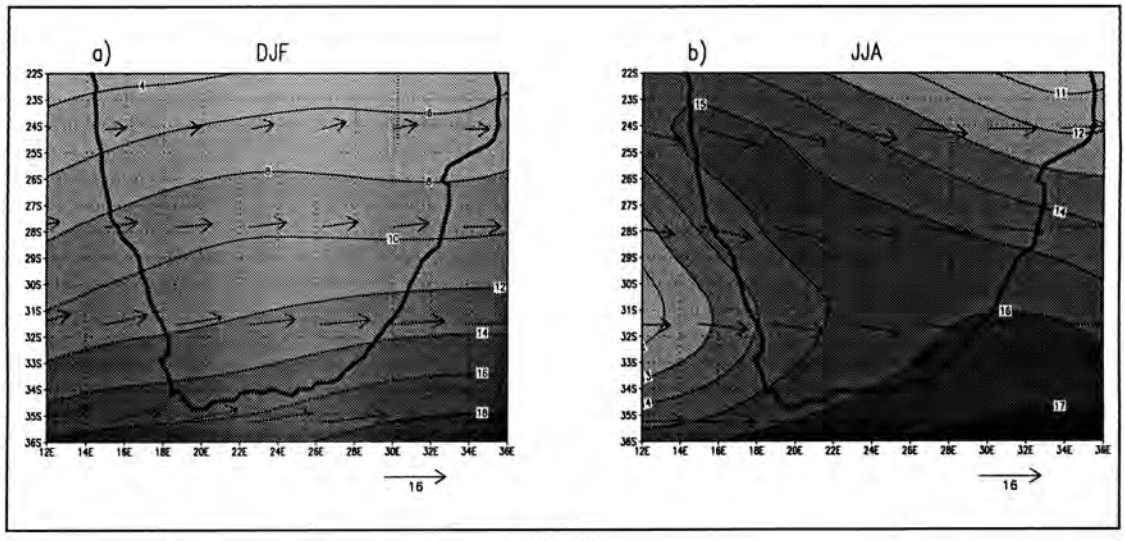

Figure 60: AMIP 1980 mean wind direction and magnitude ($m.s^{-1}$) at the 500 hPa level for a) summer (DJF) and b) winter (JJA)

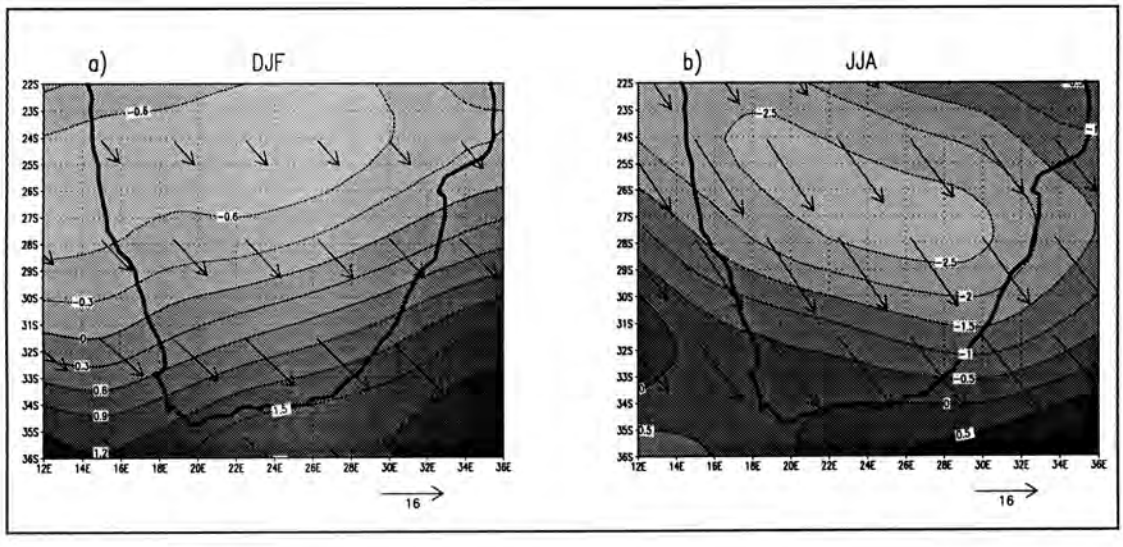

Figure 61: Mean wind direction and magnitude anomaly ($m.s^{-1}$) (perturbation - 1980) at the 500 hPa level for a) summer (DJF) and b) winter (JJA)

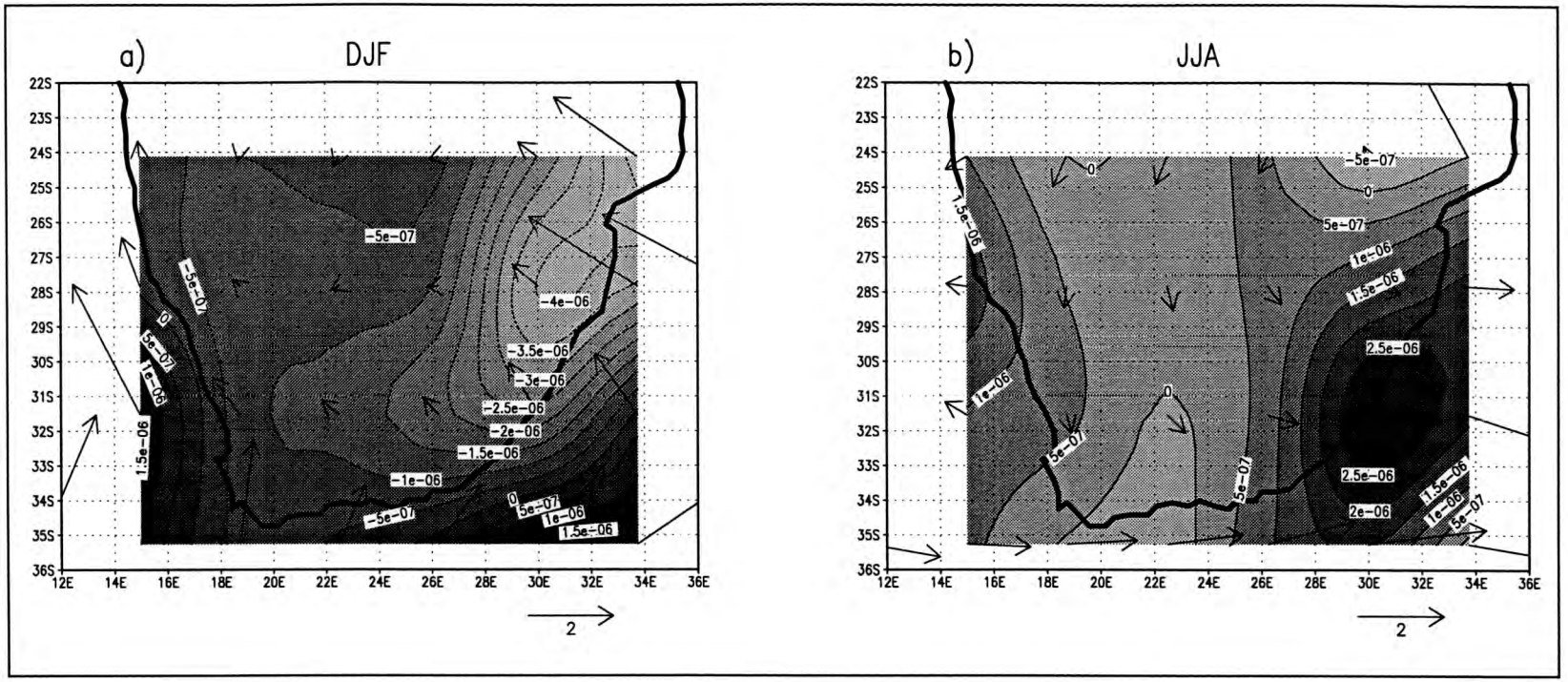

Figure 62: AMIP 1980 horizontal divergence at the 1000 hPa level for a) summer (DJF) and b) winter (JJA)

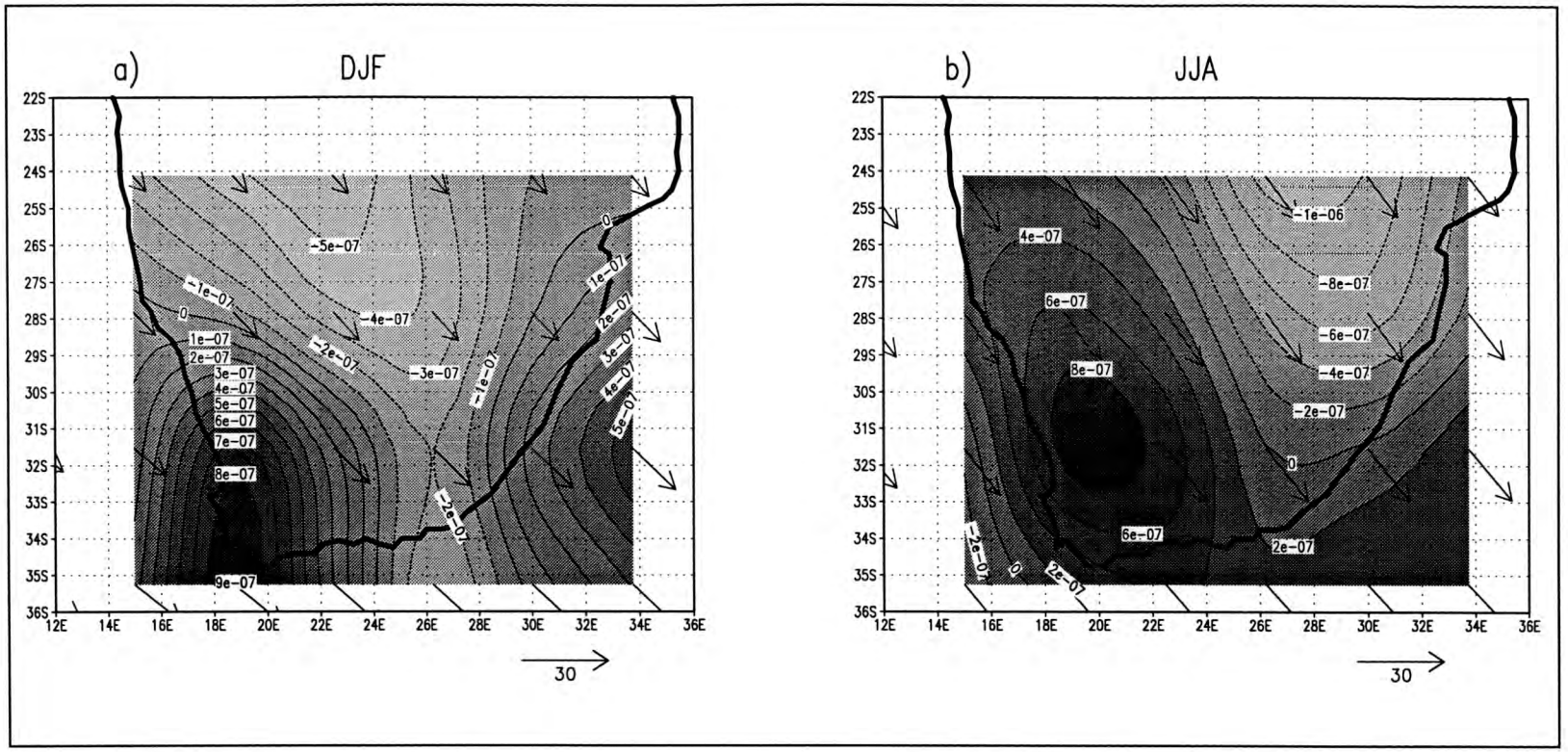

Figure 65: Horizontal divergence anomaly (perturbation - 1980) at the 500 hPa level for a) summer (DJF) and b) winter (JJA)

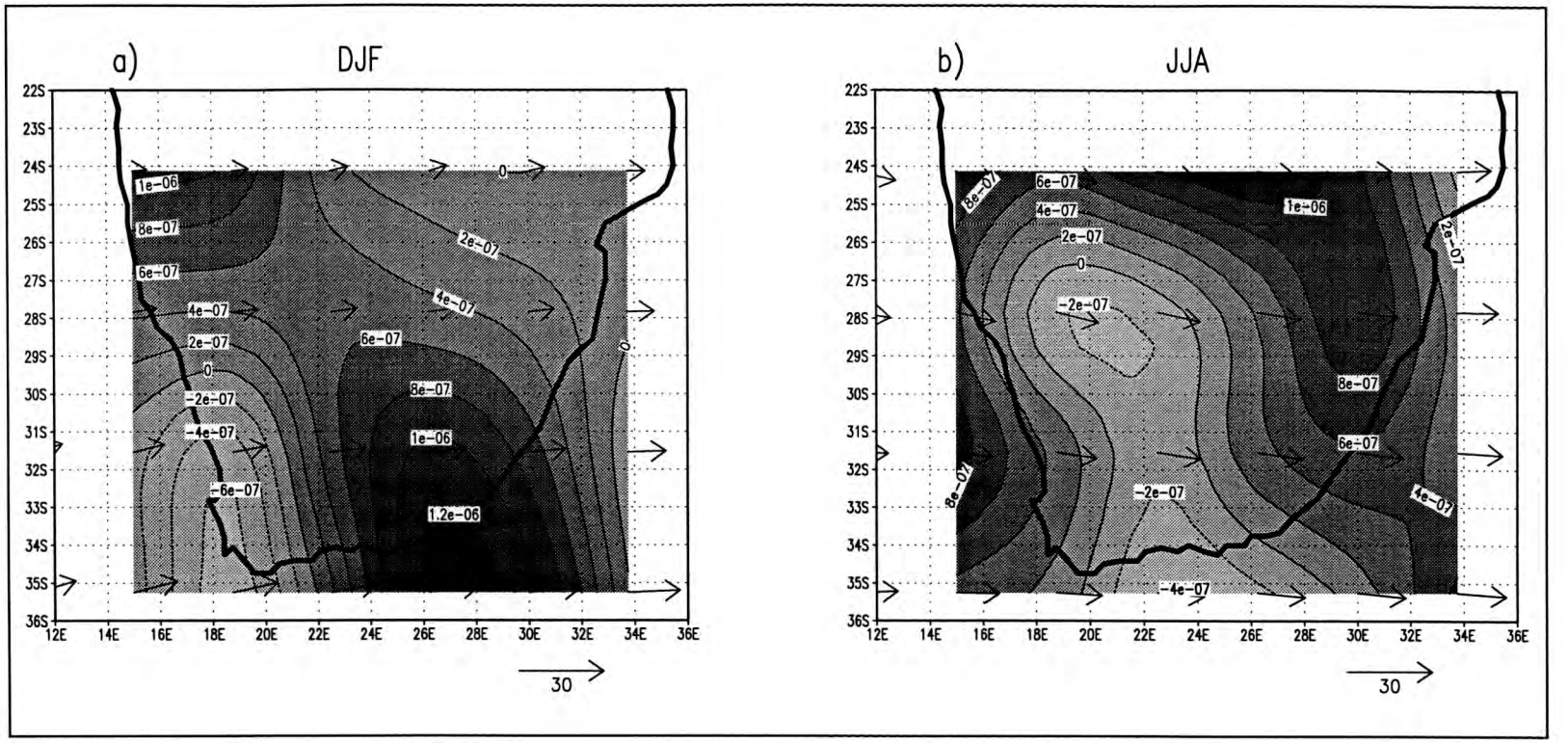

Figure 64: AMIP 1980 horizontal divergence at the 500 hPa level for a) summer (DJF) and b) winter (JJA)

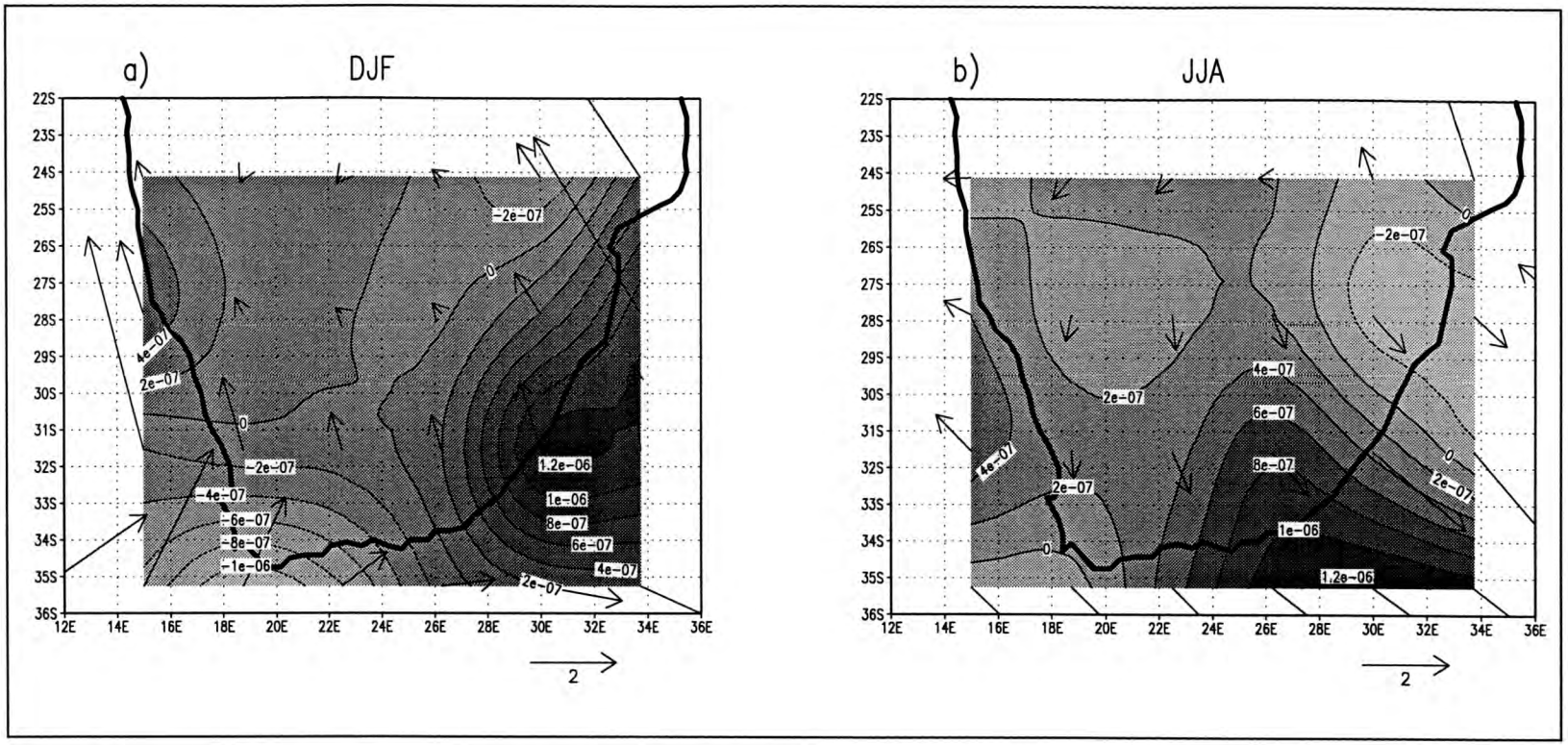

Figure 63: Horizontal divergence anomaly (perturbation - 1980) at the 1000 hPa level for a) summer (DJF) and b) winter (JJA)

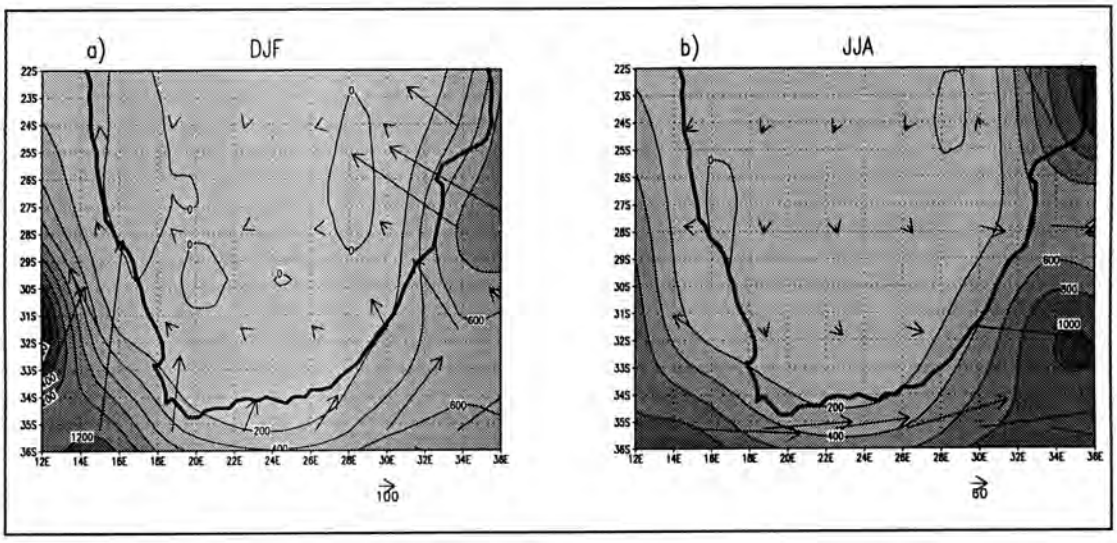

Figure 66: AMIP 1980 mean moisture fluxes ($m.s^{-1}.g.kg^{-1}$) at the 1000 hPa level for a) summer (DJF) and b) winter (JJA)

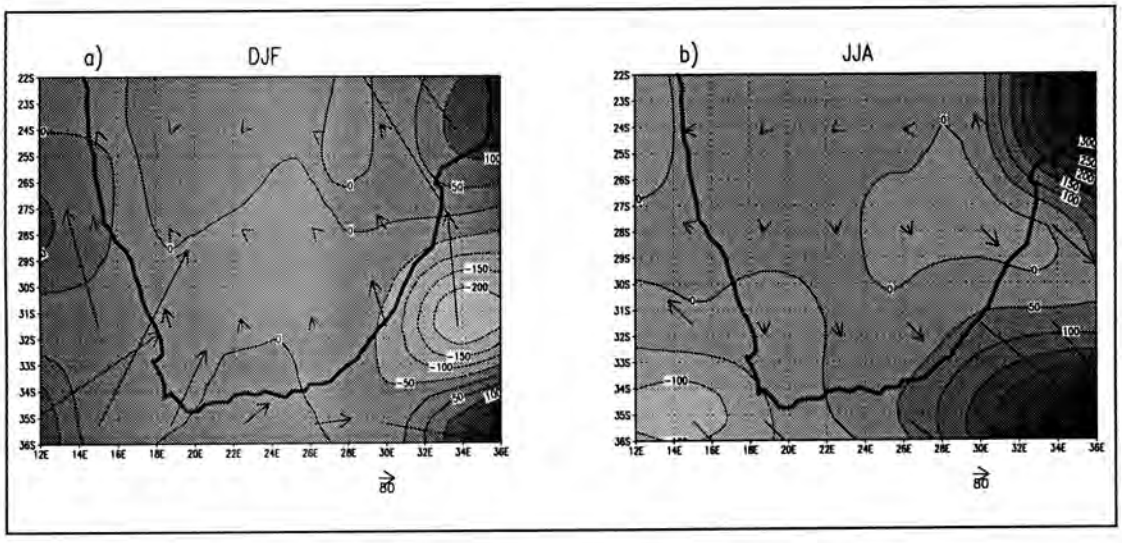

Figure 67: Mean moisture flux anomaly ($m.s^{-1}.g.kg^{-1}$) (perturbation - 1980) at the 1000 hPa level for a) summer (DJF) and b) winter (JJA)

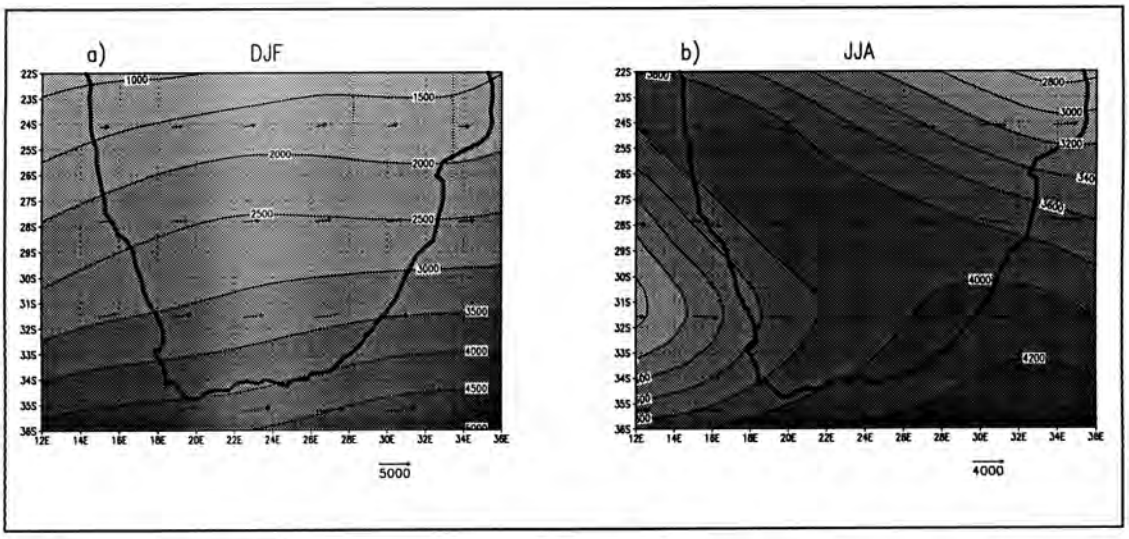

Figure 68: AMIP 1980 moisture fluxes ($m.s^{-1}.g.kg^{-1}$) at the 500 hPa level for a) summer (DJF) and b) winter (JJA)

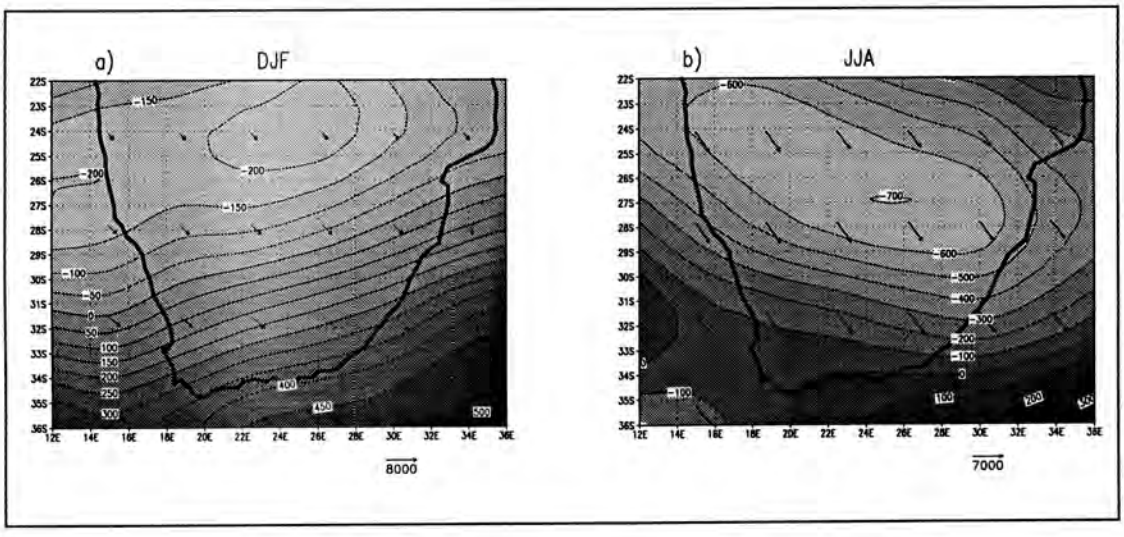

Figure 69: Moisture flux anomaly ($m.s^{-1}.g.kg^{-1}$) (perturbation - 1980) at the 500 hPa level for a) summer (DJF) and b) winter (JJA)

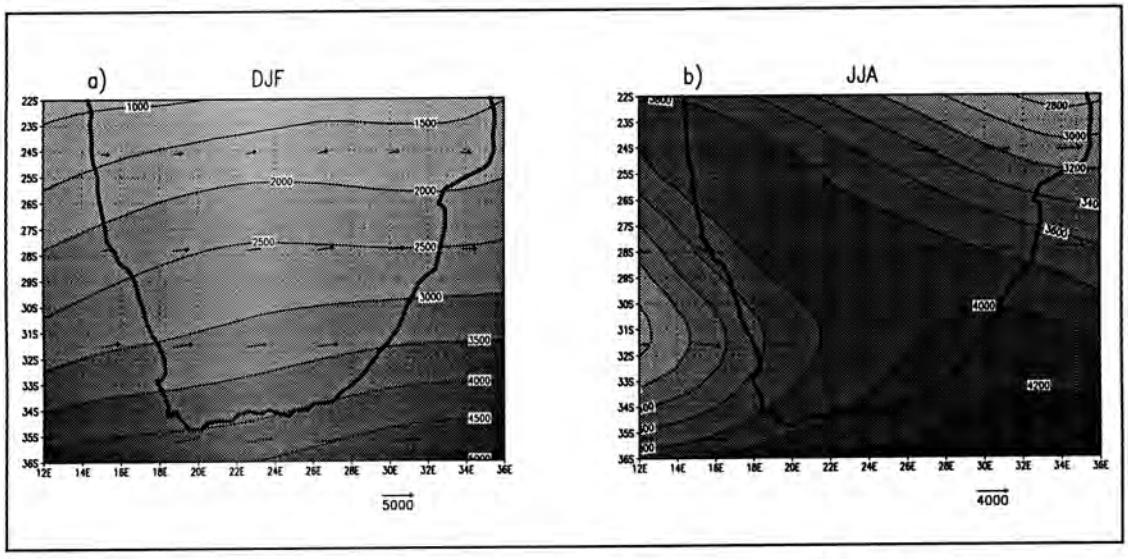

Figure 70: AMIP 1980 mean heat fluxes ($m.s^{-1}.K$) at the 500 hPa level for a) summer (DJF) and b) winter (JJA)

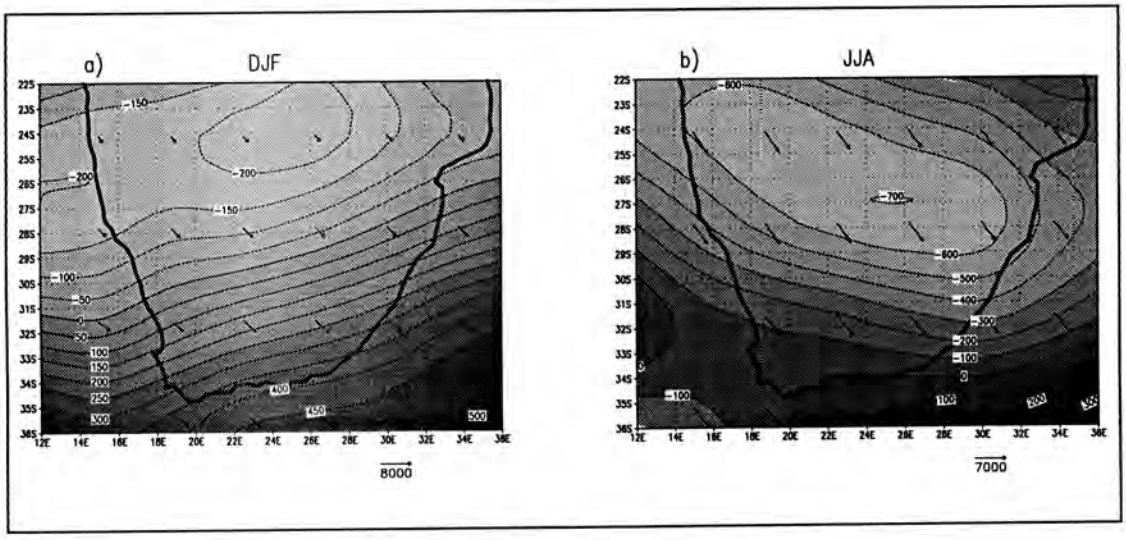

Figure 71: Mean heat flux anomaly ($m.s^{-1}.K$) (perturbation - 1980) at the 500 hPa level for a) summer (DJF) and b) winter (JJA)

CHAPTER 6

CONCLUSIONS AND RECOMMENDATIONS

CHAPTER 6

CONCLUSIONS AND RECOMMENDATIONS

This study has examined interactions between vegetation and the atmosphere over the South African region. The importance of this has been highlighted by the fact that vegetation characteristics affect sensible and latent heat fluxes which are important for the absorption of solar radiation and emission of infra-red radiation (Henderson-Sellers, 1990). The atmosphere-vegetation interactions have been examined through driving a vegetation model both in a stand-alone mode and incorporated within a general circulation model, and the study has been placed in the context of the portended global climate change. The initial sensitivity of the atmosphere to vegetation perturbations induced by CO_2 forcing has therefore been assessed.

The vegetation model driven in a stand-alone mode uses climatic variables of temperature, precipitation and relative humidity to predict a list of 110 life forms (which are subsequently summarised into a number of classes to aid interpretation) adapted to a particular climate. The model is driven using climatic variables taking into account CO_2 forcing, and the resultant vegetation changes were analysed. The vegetation was shown to have had a degree of sensitivity to these atmospheric variables, with larger vegetation classes such as dry or desert, savanna and grassland shifting their boundaries.

The dry or desert vegetation class was seen to decrease in percentage coverage in a few isolated regions. However, the most notable trend was a slight increase in the north, and an increase in the southwards and eastwards extent. Savanna vegetation displayed a decrease in vegetation in consequence to the increase in dry or desert vegetation in the NW, therefore confirming an encroachment by drier vegetation. Savanna has also increased in southwards and eastwards extent and appears to have invaded areas in the south which were formerly occupied by grassland. Grassland,

although exhibiting a decrease in percentage coverage in the central southern regions, did increase in percentage coverage east of this region, thus implying a vegetation shift.

The generalised response indicated a southwards and eastwards movement of more dryland vegetation and a westwards and upwards movement of lowland vegetation. Therefore, lowland vegetation is responding to temperature changes and dryland vegetation to precipitation changes. This is what one would expect from current climate change scenarios, and therefore the results are useful in demonstrating the ability of the vegetation model, and demonstrate their applicability in the context of atmospheric sensitivity studies rather than indicating what is already an anticipated quantity.

The GCM perturbations performed subsequently, taking into consideration vegetation changes induced by CO_2 forcing, confirmed that the atmosphere does respond to altered vegetation and emphasises that climate is sensitive to vegetation changes. This reinforces the need for better land surface parameterization schemes. The atmospheric response to vegetation changes was most apparent in the NW and SE of the study region, in areas subject to convective processes. Anomalies indicated a reduction in precipitation over the SE of the interior, related to less moisture feeding in over the interior from the SE Indian Ocean. This observation is supported by the horizontal divergence fields at the 1000 hPa and 500 hPa levels. Temperatures in the NW decreased in both summer and winter, and are possibly related to the increased aridity and associated albedo increases. Wind speed changes over the interior were also evident and could perhaps further support the notion of increased desertification, since higher wind speeds are possibly related to decreased surface stress. Changes in fluxes of sensible and latent heat were also observed, as well as changes in specific humidity and other variables. A southwards extension of the Hadley Cell was also apparent. It seems that much of the change in general could be ascribed to the general increase in aridity (and a movement towards plants adapted to drier conditions) over the sub-continent.

The results of this study should not be viewed purely in terms of the atmospheric response to vegetation over South Africa within a global climate change context, since they also aid in acquiring a greater understanding of the degree of sensitivity of the atmosphere to vegetation. Increased aridity, which is already a growing concern, has been shown to have effect on the atmosphere. Therefore, increased pressure placed on the land as a result of farming activities and the associated move towards aridification is likely to be having an impact on the climate at present. Furthermore, changes in local areas appear to manifest themselves in larger regional modifications, and thus local effects cannot be viewed in a local context only.

Despite the findings outlined above, attention must be drawn to some of the caveats of the present research and some recommendations for future studies of this nature need to be made.

6.1 Caveats

As with any study, there are invariably a number of limitations to which attention must be drawn, since the results of this study need to be assessed in the context of these constraints.

Firstly, EVE is a model and not observed vegetation *per se*, and therefore cannot capture the precision of the observed vegetation boundaries. Plants may well adapt to climate change (some plants are more productive under higher CO_2 conditions) with the constraints on each plant type altering, therefore implying that the limits of a life form based model may be artificial. Furthermore, this vegetation model does not account for burning or for vegetated areas presently covered by agricultural land as opposed to natural vegetation. Seasonal anthropogenic burning or inclusion of agricultural land would possibly result in a different response. The lack of these in EVE may be obscuring some of the resultant signals in the atmosphere, and could perhaps explain the inability to determine reasonable physical explanations for some of the changes. While there are a number of vegetation models which have been developed that operate on a finer scale than EVE, most of these models cannot be

incorporated easily into GCMs and therefore this study is constrained by the limits of the vegetation model.

There are also limitations which cannot be avoided, such as the precision of the data, which limits interpretability. Moreover, the resolution of the GCM prevents examination of some of the finer scale, more subtle changes. The inability of the GCM in capturing the observed atmospheric dynamics (for example, with respect to precipitation amount and pattern) is a further constraint. However, the model physics of the GENESIS GCM used (version 2.0a) are a substantial improvement over the prior version (version 1.02). Studies such as this thus serve to validate the ability of the GENESIS model, thereby providing feedback on the needs for improvements in future model versions.

6.2 Recommendations

A number of recommendations have emerged from this study, both in terms of improvements and possibilities for future research.

The AMIP model year 1980 was used in this study, but it is suggested that future model runs with vegetation perturbations be conducted using other years, such as strong El Niño or La Niña years. Therefore, the variability of the atmospheric response can be determined under differing climatic conditions. This would also place more statistical significance on the current findings.

It is furthermore recommended that some further analyses be undertaken using the data from the perturbation runs performed, in terms of different atmospheric levels (e.g. the 700 hPa level). A choice of variables had to be made in terms of limiting the scope of this research and an examination of other variables in conjunction with those analysed here would be optimal. In addition, it would be useful to examine not only the atmospheric output, but also the output of the land surface transfer model (e.g. surface fluxes).

It would be advisable to incorporate agricultural land and other land surface modifications (e.g. urban areas and their associated heat island effects) into a land surface model which could therefore better reflect the observed land use. Since fairly large portions of South Africa are used for agricultural or urban activities, it is not advisable to assume that the land is natural vegetation. Moreover, the signal in the atmosphere would possibly be different. In addition, it would be useful to examine vegetation response with regards to atmospheric sensitivity using alternative vegetation models.

In conjunction with an examination of vegetation classes, as presented in this research, it would be beneficial to investigate a finer level (i.e. the life form scale). Thus, an understanding of which life forms within a vegetation class are showing the most change, or are shifting their range of occurrence could be determined. It may well be a few life forms which are accounting for the changes witnessed in the model, as opposed to a general shift of all life forms in consequence to the CO_2 forcing.

It is suggested that the next step in the present research should involve the advancement of an understanding of the interactive sensitivity of the atmosphere and vegetation. This would not necessarily need to be achieved through the computationally intensive task of driving EVE interactively with the GENESIS GCM. An initial step could involve the incorporation of the changes in the atmospheric variables of precipitation, temperature and specific humidity (converted into relative humidity) back into driving EVE in a stand-alone mode. This step should prove to be the most beneficial in terms of the vegetation response, since it would be useful to examine how the perturbed vegetation responds to the new climate forcing. It has been suggested that the vegetation may alter less under these conditions (M. O'Callaghan, pers. comm.) and therefore the magnitude and direction of changes evident from this initial CO_2 forcing may not necessarily be justifiable. The perturbation in vegetation as a result of this could then in turn be incorporated back into running GENESIS. The atmospheric response to this would be interesting to examine, since the pseudo-interactivity may lend itself to different interpretations and observations.

It is hoped that more modelling based research of this nature will be conducted in future, as both general circulation models and land surface models improve. Studies of this nature using other GCMs, which show dissimilar skill in representing the observed in different regions could prove to be useful and complimentary and would enable a more substantial picture of the interactive response between the atmosphere and vegetation over the South African region to be obtained.

REFERENCES

Acocks, J.P.H. (1953). Veld Types of South Africa. *Memoirs of the Botanical Survey of South Africa,* No. 28.

Acocks, J.P.H. (1988). Veld Types of South Africa. *Memoirs of the Botanical Survey of South Africa,* No. 57.

Adamson, R.S. (1938). *The vegetation of South Africa.* British Empire Vegetation Committee, London.

Barron, E.J., Peterson, W.W., Pollard, D. and Thompson, S.L. (1993). Past climate and the role of ocean heat transport: model simulations for the Cretaceous. *Palaeoceanography*, 8, 785-798.

Bergengren. J.C. (1995). *Coupled GENESIS-EVE Experiments with 1x and 2x* CO_2. Second GENESIS User's Workshop, National Center for Atmospheric Research, Boulder, Colorado, 8-10 August.

Bergengren, J.C. and Thompson, S.L. (1997a). Modeling the Effects of Global Climate Change on Natural Vegetation I. The Equilibrium Vegetation Ecology Model. To be submitted to *Global and Planetary Change.*

Bergengren, J.C. and Thompson, S.L. (1997b). Modeling the Effects of Global Climate Change on Natural Vegetation II. The Equilibrium Vegetation Ecology Model and the Sensitivity of the Terrestrial Biosphere to Climate Change. To be submitted to *Global and Planetary Change.*

Bonan, G.B., Pollard, D. and Thompson, S.L. (1992). Effects of boreal forest vegetation on global climate. *Nature*, 359, 716-718.

Box, E.O. (1981a). *Macroclimate and Plant Forms: An Introduction to Predictive Modeling in Phytogeography.* Dr W. Junk Publishers, The Hague, Netherlands, 258pp.

Box, E.O. (1981b). Predicting Physiognomic Vegetation Types with Climate Variables. *Vegetatio*, 45, 127-139.

Camillo, P.J., Gurney, R.J. and Schmugge, T.J. (1983). A soil and atmospheric boundary layer model for evapotranspiration and soil moisture studies. *Water Resources Research,* 2, 729-738.

Carter, T.R., Parry, M.L., Harasawa, H. and Nishioka, S. (1994). *IPCC Technical Guidelines for Assessing Climate Change Impacts and Adaptions.* IPCC Special Report to Working Group II of IPCC, 59pp.

Cowling, R.M. and Richarson, D. (1997*). Vegetation of Southern Africa.* Cambridge University Press (in press).

Crowley, T.J. and Baum, S.K. (1994). General circulation model study of late Carboniferous interglacial climates. *Palaeoclimates*, 1, 3-21.

Currie, R.G. (1993). Luni-solar 18.6 and 10-11 year solar cycle signals in South African rainfall. *International Journal of Climatology*, 13, 237-256.

Dickinson, R.E. (1984). *Modelling evapotranspiration for Three-Dimensional Global Climate Models. Climate Processes and Climate Sensitivity*, in Hansen, J.E. and Takahashi, T. (eds.). *Geophysical Monographs of the American Geophysical Union*, 29, 58-72.

Dickinson, R.E., Henderson-Sellers, A., Kennedy, P.J. and Wilson, M.F. (1986). Biosphere-atmosphere transfer scheme (BATS) for NCAR Community Climate Model. *NCAR Technical Note NCAR/TN-275+STR*, National Center for Atmospheric Research, Boulder, Colorado.

Dickinson, R.E., Errico, R.M., Giorgi, F. and Bates, G.T. (1989). A Regional Climate Model for the Western United States. *Climatic Change*, 15, 383-422.

Dickinson, R.E., Henderson-Sellers, A., Kennedy, P.J. and Giorgi, F. (1992). Biosphere-Atmosphere Transfer Scheme (BATS), Version 1e as Coupled to the NCAR Community Climate Model. *NCAR Technical Note.*

Donlin, M and Child, J (1992). Is neural computing the key to artificial intelligence? *Computer Design*, 31, 87-104.

Dorman, J.L and Sellers, P.J. (1989). A Global Climatology of Albedo, Roughness Length and Stomatal Resistance for Atmospheric General Circulation Models as Represented by the Simple Biosphere Model (SiB). *Journal of Applied Meteorology*, 28, 833-855.

Ellery, W.N., Scholes, R.J. and Mentis, M.T. (1991). An initial approach to predicting the sensitivity of the South African grassland biome to climate change. *South African Journal of Science*, 87, 499-503.

Feder, T. (1996). Attacks on IPCC Report Heat Controversy Over Global Warming. *Physics Today*, August 1996, 55-57.

Foley, J.A., Kutzbach, J.E., Coe, M.T. and Levis, S. (1994). Feedbacks between climate and boreal forests during the Holocene epoch. *Nature*, 371, 52-54.

Franchito, S.H. and Rao, V.B. (1992). Climatic change due to land surface alterations. *Climatic Change*, 22, 1-34.

Gates, W.L. (1992a). AMIP: The Atmospheric Model Intercomparison Project. *Bulletin of the American Meteorological Society*, 73(12), 1962-1970.

Gates, W.L. (1992b). AMIP: The Atmospheric Model Intercomparison Project. *Program for Climate Model Diagnosis and Intercomparison (PCMDI),* Report no. 7.

Giorgi, F. (1990). Sensitivity of wintertime precipitation and soil hydrology simulation over the western United States to Lower Boundary Specifications. *Atmosphere Ocean*, 28(1), 1-23.

Giorgi, F. and Bates, G.T. (1989). The climatological skill of a regional model over complex terrain. *Monthly Weather Review*, 117, 2325-2347.

Hansen, J., Johnson, D., Lacis, A., Lebedeff, S., Lee, P., Rind, D. and Russell, G. (1981). Climate Impacts of Increasing Atmospheric Carbon Dioxide. *Science*, 213 (4511), 975-966.

Henderson-Sellers, A. and Gornitz, V. (1984). Possible climatic impacts of land cover transformations, with particular emphasis on tropical deforestation. *Climatic Change*, 6, 231-256.

Henderson-Sellers, A. (1987). Effects of change in land-use on climate in the humid tropics, In Dickinson, R.E. (ed.), *The Geophysiology of Amazonia*. John Wiley and Sons, New York, 463-493.

Henderson-Sellers, A. and McGuffie, K. (1987). *A Climate Modelling Primer*. John Wiley and Sons, Suffolk, 217pp.

Henderson-Sellers, A. (1990). Predicting Generalized Ecosystem Groups with the NCAR CCM: First Steps Towards an Interactive Biosphere. *Journal of Climate*, 3, 917-940.

Henderson-Sellers, A., Yang, Z.-L. and Dickinson, R.E. (1993a). The Project for Intercomparison of Land-Surface Parameterization Schemes. *Bulletin of the American Meteorological Society*, 74(7), 1335-1349.

Henderson-Sellers, A. (1993b). Continental Vegetation as a Dynamic Component of a Global Climate Model: A Preliminary Assessment. *Climatic Change*, 23, 337-377.

Henderson-Sellers, A., Pitman, A.J., Love, P.K., Irannejad, P and Chen, T.H. (1995). The Project for Intercomparison of Land Surface Parameterization Schemes (PILPS): Phases 2 and 3. *Bulletin of the American Meteorological Society*, 76(4), 489-503.

Hewitson, B.C. and Crane, R.G. (1994). *In Neural Nets: Applications in Geography*, eds. B.C. Hewitson and R.G. Crane, chapter 1, pp. 1-9, Kluwer, Dordrecht.

Hewitson, B.C. (1995). A methodology for developing regional climate change scenarios from General Circulation Models. *Final Report for the Water Research Commission.*

Hewitson, B.C. (1996). Analysis of regional precipitation impacts from GCM derived regional climate change scenarios. *Interim Progress Report for the Water Research Commission*, 13pp.

Hewitson, B.C. and Crane, R.G. (1996). Climate Downscaling: Techniques and Application. *Climate Research*, 7, 85-95.

Hudson, D.A. (1997). Southern African Climate Change Simulated by the GENESIS GCM. *South African Journal of Science* (accepted).

Hudson, D.A. and Hewitson, B.C. (1997). Midlatitude Cyclones South of Africa in the GENESIS GCM. *International Journal of Climatology*, 17(5), 459-473.

Huntley, B and Webb, T. (1988). *Vegetation History*. Kluwer, Dortrecht. (In: Prentice, I.C., Cramer, W., Harrison, S.P., Leemans, R., Monserad, R.A. and Solomon, A.M.; 1992: A global biome model based on plant physiology and dominance, soil properties and climate. *Journal of Biogeography*, 19, 117-134.)

Hurrel, J.W. and van Loon, H. (1994). A modulation of the atmospheric annual cycle in the Southern Hemisphere. *Tellus*, 325-338.

Ingram, W.J., Wilson, C.A. and Mitchell, J.F.B. (1989). Modeling climate change: An assessment of sea ice and surface albedo feedbacks. *Journal of Geophysical Research*, 94, 8609-8622.

Intergovernmental Panel on Climate Change (IPCC) (1995). *Summary for Policymakers of the Contribution of Working Group 1 to the IPCC Second Assessment Report, 1995*.

Kumar, A., Leetmaa, A. and Ji, M. (1994). Simulations of Atmospheric Variability Induced by Sea Surface Temperatures and Implications for Global Warming. *Science*, 266, 632-637.

Key, J.R. (1994). In *Neural Nets: Applications in Geography*, eds. B.C. Hewitson and R.G. Crane, chapter 8, pp. 145-179, Kluwer, Dordrecht.

Kuchler, A.W. (1983). World Map of Natural Vegetation. *Goode's World Atlas*, 16th edition, Rand McNally.

Leemans, R. and Cramer, W.P. (1990). *The IIASA Database for Mean Monthly Values of Temperature, Precipitation and Cloudiness of a Global Terrestrial Grid.* WP-41, International Institute of Applied Systems Analyses, Laxenburg Working Paper, IIASA, Laxenburg, Austria. 60pp.

Legates, D.R. and Willmott, C.J. (1990a). Mean Seasonal and Spatial Variability in Global Surface Air Temperature. *Theoretical and Applied Climatology*, 41, 11-21.

Legates, D.R. and Willmott, C.J. (1990b). Mean Seasonal and Spatial Variability in Gauge-Corrected Global Precipitation. *International Journal of Climatology*, 10, 111-127.

Mahfouf, J.-F., Manzi, A.O., Noilhan, J., Giordani, H. and Déqué, M. (1995). The Land Surface Scheme ISBA within the Météo-France Climate Model ARPEGE. Part 1: Implementation and Preliminary Results. *Journal of Climate*, 8 (8), 2039-2057.

Mason, S.J. and Lindesay, J.A. (1993). A note on the modulations of Southern Oscillations - Southern African rainfall associations with the Quasi-biennial oscillation. *Journal of Geophysical Research*, 8847-8850.

Matthews, E. (1985). Atlas of Archived Vegetation, Land-Use and Seasonal Albedo Data Sets. *NASA Technical Memo*, 86096.

McCumber, M.C. and Pielke, R.A. (1981). Simulation of the effects of surface fluxes of heat and moisture in a mesoscale numerical model. *Journal of Geophysical Research*, 86, 9929-9938.

McGinnis, D.L. (1994). In *Neural Nets: Applications in Geography*, eds. B.C. Hewitson and R.G. Crane, chapter 5, pp. 79-99, Kluwer, Dordrecht.

Midgley, G.F. and O'Callaghan, M. (1993). *Review of likely impacts of climate change on South African flora and vegetation.* Report Prepared for the southern African Nature Foundation, 23pp.

Miller, G.H. and de Vernal, A. (1992). Will greenhouse warming lead to Northern Hemisphere ice-sheet growth? *Nature*, 355, 244-246.

Mitchell, J.F.B. and Lupton, G. (1984). A 4 x CO_2 integration with prescribed changes in sea surface temperatures. *Progress in Biometeorology*, 3, 353-374.

Noilhan, J. and Planton, S. (1989). A Simple Parameterization of Land Surface Processes for Meteorological Models. *Monthly Weather Review*, 117, 536-549.

Ojima, D.S., Kittel, T.G.F., Rosswall, T. and Walker, B.H. (1991). Critical Issues for Understanding Global Change Effects on Terrestrial Ecosystems. *Ecological Applications*, 1(3), 316-325.

Olson, J.S., Watts, J.A. and Allison, L.J.P. (1983). Carbon in Live Vegetation of Major World Ecosystems. *DOE/NBB Report no. TR004*, Oak Ridge National Laboratory, Oak Ridge.

Palmer, C. (1996). *Formulas for humidity calculations* (USA Today Weather). http://www.usatoday.com:80/weather/whumcalc.htm

Peixoto, J.P. and Oort, A.H. (1992). *Physics of Climate.* American Institute of Physics, New York, 520pp.

Pentz, J.A. (1945). An agro-ecological survey of Natal. *Department of Agriculture Forestry Bulletin No. 250.*

Phillips, T. (1996). *AMIP Diagnostic Subprojects: Further Information.* http://www-pcmdi.llnl.gov/phillips/AMIPspinfo.html#SP12

Phillips, N.A. (1956). The general circulation of the atmosphere: A numerical experiment. *Quarterly Journal of the Royal Meteorological Society*, 82, 123-164.

Pitman, A.J., Yang, Z.-L., Cogley, J.G. and Henderson-Sellers, A. (1991). Description of Bare Essentials of Surface Transfer for the Bureau of Meteorology Research Centre AGCM. *BMRC Research Report*, 32, Melbourne.

Pole Evans, I.B. (1936). A vegetation map of South Africa. *Memoirs of the Botanical Survey of South Africa No. 14.*

Pollard, D. and Schulz, M. (1994). A model for the potential locations of Triassic evaporite basins driven by paleoclimate GCM simulations. *Global and Planetary Change*, 9, 233-249.

Pollard, D. and Thompson, S.L. (1994). Sea-ice dynamics and CO_2 sensitivity in a global climate change model. *Atmosphere-Ocean*, 32, 449-467.

Pollard, D. and Thompson, S.L. (1995a). A Global Climate Model (GENESIS) with a Land-Surface Transfer Scheme (LSX). Part 1: Present Climate Simulation. *Journal of Climate*, 8(4), 732-761.

Pollard, D. and Thompson, S.L. (1995b). Use of a Land-Surface-Transfer Scheme (LSX) in a Global Climate Model: The Response to Doubling Stomatal Resistance. *Global and Planetary Change*, 10, 129-161.

Pollard, D. and Thompson, S.L. (1995c). *Users' Guide to the GENESIS Global Climate Model Version 2.0*. Interdisciplinary Climate Systems Section, Climate and Global Dynamics Division, National Center for Atmospheric Research, Boulder, Colorado.

Prentice, I.C. (1992). Climate Change and long-term vegetation dynamics. In: *Vegetation Dynamics theory* (ed. by D.C. Glenn-Lewin, R.A. Peet and T.T. Veblen). Chapman and Hall.

Prentice, I.C., Cramer, W., Harrison, S.P., Leemans, R., Monserad, R.A. and Solomon, A.M. (1992). A global biome model based on plant physiology and dominance, soil properties and climate. *Journal of Biogeography*, 19, 117-134.

Preston-Whyte, R.A. and Tyson, P.D. (1988). *The Atmosphere and Weather of Southern Africa*. Oxford University Press, Cape Town, 374pp.

Reader's Digest Association South Africa. (1984). *Reader's Digest Illustrated Atlas of southern Africa*. Government Printer, South Africa.

Release Notes for GENESIS 2.0, 26 July 1995.

Rind, D. (1987). The Doubled CO_2 Climate: Impact of the Sea Surface Temperature Gradient. *Journal of the Atmospheric Sciences*, 44(21), 3235-3268.

Rind, D., Healy, R., Parkinson, C. and Martinson, D. (1995). The Role of Sea Ice in 2 x CO_2 Climate Model Sensitivity. Part 1: The Total Influence of Sea Ice Thickness and Extent. *Journal of Climate*, 8, 449-463.

Rutherford, M.C. and Westfall, R.H. (1986). Biomes of southern Africa - An Objective Categorization. *Memoirs of the Botanical Survey of South Africa No. 54*, Botanical Research Institute, Department of Water Supply, South Africa. 98pp.

Sato, N., Sellers, P.J., Randall, D.A., Schneider, E.K., Shukla, J., Kinter III, J.L., Hou, Y-.T. and Albertazzi, E. (1989). Effects of Implementing the Simple Biosphere Model in a General Circulation Model. *Journal of the Atmospheric Sciences*, 46(18), 2757-2782.

Schutz, C. and Gates, W. L. (1971). *Global Climatic Data for Surface, 800mb, 400mb: January*. The Rand Corporation, R-913-ARPA.

Schutz, C. and Gates, W. L. (1972). *Global Climatic Data for Surface, 800mb, 400mb: July*. The Rand Corporation, R-913-ARPA.

Schutz, C. and Gates, W. L. (1973). *Global Climatic Data for Surface, 800mb, 400mb: April*. The Rand Corporation, R-913-ARPA.

Schutz, C. and Gates, W. L. (1974). *Global Climatic Data for Surface, 800mb, 400mb: October*. The Rand Corporation, R-913-ARPA.

Sellers, P.J., Mintz, Y., Sud, Y.C. and Dalcher, A. (1986). A Simple Biosphere Model (SiB) Using Point Micrometeorological and Biophysical Data. *Journal of Applied Meteorology*, 26, 622-651.

Sellers, P.J., Randall, D.A., Collatz, G.J., Berry, J.A., Field, C.B., Dazlich, D.A., Zhang, C., Collelo, G.D. and Bounoua, L. (1996a). A Revised Land Surface Parameterization (SiB2) for Atmospheric GCMs, Part 1: Model Formulation. *Journal of Climate*, 9, 676-705.

Sellers, P.J., Los, S.O., Tucker, C.J., Justice, C.O., Dazlich, D.A., Collatz, G.J., Randall, D.A. (1996b). A Revised Land Surface Parameterization (SiB2) for Atmospheric GCMs. Part 2: The Generation of Global Fields of Terrestrial Biophysical Parameters from Satellite Data. *Journal of Climate*, 9, 706-737.

Simmon, R. (1997). *The Goddard DAAC*. http://daac.gsfc.nasa.gov/

Slingo, A. and Slingo, J.M. (1991). Response of the National Center for Atmospheric Research Community Climate Model to improvements in the representations of clouds. *Journal of Geophysical Research*, 96, 15341-15357.

Smith, R.N.B. (1990). A scheme for predicting layer clouds and their water content in a general circulation model. *Quarterly Journal of the Royal Meteorological Society*, 99, 56-72.

Thompson, S.L. and Pollard, D. (1995). A Global Climate Model (GENESIS) with a Land-Surface Transfer Scheme (LSX). Part II: CO_2 Sensitivity. *Journal of Climate*, 8, 1104-1121.

Thompson, S.L. and Pollard, D. (1997). Greenland and Antarctic Mass Balances for Present and Doubled CO_2 from the GENESIS Version 2 Global Climate Model. *Journal of Climate* (in press).

Tyson, P.D. (1987). *Climatic Change and Variability in Southern Africa.* Oxford University Press, Cape Town, 219pp.

Wasserman, P.D. (1989). *Neural Computing Theory and Practice.* Van Nostrand Reinhold, New York.

Verseghy, D.L. (1991). CLASS: A Canadian Land Surface Scheme for GCMs, I. Soil Model. *International Journal of Climatology*, 11, 111-133.

Verseghy, D.L. (1993). CLASS - A Canadian Land Surface Scheme for GCMs. II: Vegetation Model and Coupled Runs. *International Journal of Climatology*, 13, 347-370.

Wilson, M.F. and Henderson-Sellers, A. (1985). A Global Archive of Land Cover and Soil Data for Use in General Circulation Climate Models. *Journal of Climatology*, 5, 119-143.

Xue, Y., Sellers, P.J., Kinter, J.L. and Shukla, J. (1991). A Simplified Biosphere Model for Global Climate Studies. *Journal of Climate*, 4, 345-364.

Yang, Z.-L. (1992). *Land-surface Processes in 3-Dimensional Climate Models.* Unpublished PhD thesis, School of Earth Sciences, Macquarie University, Sydney.

Yang, Z.-L. (1995). Investigating Impacts of Anomalous Land-Surface Conditions on Australian Climate with an Advanced Land-Surface Model Coupled to the BMRC GCM. *International Journal of Climatology*, 15, 137-174.

APPENDIX A

List of 110 life forms

1. Equatorial Rainforest Broadleaf Trees
2. Equatorial-Montane Rainforest Broadleaf Trees
3. Tropical Evergreen Microphyll-Broadleaf Trees
4. Tropical-Monsoon Evergreen Broadleaf Trees
5. Tropical Evergreen Sclerophyll-Broadleaf Trees
6. Mediterranean Evergreen Broadleaf Trees
7. Warm-Temperate-Mesic Evergreen Broadleaf Trees
8. Warm-Temperate Evergreen Broadleaf Trees
9. Tropical-Monsoon Raingreen Broadleaf Trees
10. Tropical-Montane Raingreen Broadleaf Trees
11. Tropical-Xeric Raingreen Broadleaf Trees
12. Equatorial-Xeric Raingreen Broadleaf Trees
13. Western-Temperate Summergreen Broadleaf Trees
14. Eastern-Temperate Summergreen Broadleaf Trees
15. Eastern-Temp-Xeric Summergreen Broadleaf Trees
16. Cool-Temp/Boreal Summergreen Broadleaf Trees
17. Tropical Evergreen Linearleaf Trees
18. Tropical-Xeric Evergreen Needleleaf Trees
19. Mediterranean Evergreen Needleleaf Trees
20. Heliophilic Evergreen Needleleaf Trees
21. Warm-Temp-Montane Evergreen Needleleaf Trees
22. Temperate-Mesic Evergreen Needleleaf Trees
23. Western-Temperate Evergreen Needleleaf Trees
24. Eastern-Temperate Evergreen Needleleaf Trees
25. Cool-Temp/Boreal Evergreen Needleleaf Trees
26. Cool-Temp/Boreal Summergreen Needleleaf Trees
27. Hydrophilic Summergreen Needleleaf Trees

28. Tropical Evergreen Broadleaf Small-Trees
29. Warm-Temperate Evergreen Broadleaf Small-Trees
30. Cool-Maritime Evergreen Broadleaf Small-Trees
31. Tropical Raingreen Broadleaf Small-Trees
32. Temperate Summergreen Broadleaf Small-Trees
33. Temperate Evergreen Needleleaf Small-Trees
34. Tropical Evergreen Broadleaf Dwarf-Trees
35. Tropical-Montane Evergreen Dwarf-Trees
36. Temp-Montane/Boreal Needleleaf Dwarf-Trees
37. Palmiform Rosette-Trees
38. Palmiform Small-Rosette-Trees
39. Fern Small-Rosette-Trees
40. Tropical-Montane Small-Rosette-Trees
41. Xeric Small-Rosette-Trees
42. Raingreen Broadleaf Arborescent-Shrubs
43. Evergreen Broadleaf Arborescent-Shrubs
44. Summergreen Broadleaf Arborescent-Shrubs
45. Xeric Leafless Arborescent-Shrubs
46. Tropical Evergreen Broadleaf Shrubs
47. Hot-Desert Evergreen Broadleaf Shrubs
48. Desert Evergreen Leaf-Succulent Shrubs
49. Mediterranean Evergreen Broadleaf Shrubs
50. Mesic-Montane Evergreen Broadleaf Shrubs
51. Warm-Temperate Evergreen Broadleaf Shrubs
52. Cool-Temperate-Xeric Evergreen Shrubs
53. Temperate Summergreen Broadleaf Shrubs
54. Cool-Temp/Boreal Summergreen Broadleaf Shrubs
55. Temperate-Xeric Summergreen Broadleaf Shrubs
56. Mediterranean Summergreen Broadleaf Shrubs
57. Mediterranean Evergreen Needleleaf Shrubs
58. Evergreen Needleleaf Shrubs
59. Xeric Dwarf-Shrubs

60. Mediterranean Dwarf-Shrubs
61. Cool-Maritime Evergreen Dwarf-Shrubs
62. Cool-Temp/Boreal Evergreen Dwarf-Shrubs
63. Tundra Evergreen Dwarf-Shrubs
64. Tundra Summergreen Dwarf-Shrubs
65. Cool-Maritime/Tropical-Alpine Cushion-Shrubs
66. Xeric Cushion-Shrubs
67. Mesic Palmiform Rosette-Shrubs
68. Xeric Rosette-Shrubs
69. Arborescent Stem-Succulents
70. Branched Stem-Succulents
71. Unbranched Stem-Succulents
72. Arborescent Grasses
73. Tall-Cane Grasses
74. Sclerophyllous Grasses
75. Tall Grasses
76. Short-Sward Graminoids
77. Short-Bunch Graminoids
78. Desert Short-Bunch Graminoids
79. Temperate Tall Tussock-Graminoids
80. Temperate Short Tussock-Graminoids
81. Tropical-Montane Short Tussock-Graminoids
82. Cool-Maritime Short Tussock-Graminoids
83. Tundra Short Tussock-Graminoids
84. Tropical Evergreen Forbs
85. Temperate Evergreen Forbs
86. Succulent Forbs
87. Raingreen Forbs
88. Summergreen Forbs
89. Desert Ephemeral Herbs
90. Tropical-Alpine Raingreen Herbs
91. Tundra Summergreen Herbs

92. Desert Cushion-Herbs
93. Tropical-Montane Cushion-Herbs
94. Tundra Summergreen Cushion-Herbs
95. Tropical Liana Evergreen Vines
96. Evergreen Vines
97. Raingreen Vines
98. Summergreen Vines
99. Tropical Broadleaf Epiphytes
100. Broadleaf Epiphytes
101. Narrowleaf Epiphytes
102. Evergreen Ferns
103. Summergreen Ferns
104. Mesic Peat-Forming Bryophytes
105. Mesic Bryophytes
106. Epiphytic Bryophytes
107. Mesic Lichens
108. Boreal Lichens
109. Desert Cryptogams
110. Polar Cryptogams